

Characterization of Cerebral Blood Flow in Older Adults: A Potential Early Biomarker  
for Alzheimer's Disease

Cecily Gwinn Swinford

Submitted to the faculty of the University Graduate School  
in partial fulfillment of the requirements  
for the degree  
Doctor of Philosophy  
in the Program of Medical Neuroscience,  
Indiana University

April 2022

Accepted by the Graduate Faculty of Indiana University, in partial fulfillment of the requirements for the degree of Doctor of Philosophy.

Doctoral Committee

---

Shannon L. Risacher, Ph.D., Chair

---

Andrew J. Saykin, Psy.D.

January 14, 2022

---

Liana G. Apostolova, M.D.

---

Yu-Chien Wu, M.D., Ph.D.

---

Sujuan Gao, Ph.D.

© 2022

Cecily Gwinn Swinford

## DEDICATION

This work is dedicated to my parents Danny and Jodi Swinford, my sister Claudia Swinford, and my grandmothers Jewel Gwinn Arnold and Cecil Livonia Abner, for all of their love, encouragement, and support.

## ACKNOWLEDGEMENT

I would like to thank my mentors, Dr. Andrew Saykin and Dr. Shannon Risacher, for their genuine encouragement and support and for having confidence in my work. Thank you for helping me along each step of the way. I would also like to thank my committee members, Dr. Liana Apostolova, Dr. Yu-Chien Wu, and Dr. Sujuan Gao, for all of their thoughtful guidance throughout the duration of this project.

I am grateful to my parents, Danny and Jodi, my sister Claudia, my grandparents, aunts, uncles, cousins, friends, and teachers and mentors over the years who have believed in me and have instilled in me that I can do anything I set my mind to.

Finally, I would like to thank the participants of the Indiana Alzheimer's Disease Research Center who have selflessly and bravely dedicated their time and effort to help create a future without Alzheimer's disease. Without them, none of this work could have been completed.

Cecily Gwinn Swinford

CHARACTERIZATION OF CEREBRAL BLOOD FLOW IN OLDER ADULTS: A  
POTENTIAL EARLY BIOMARKER FOR ALZHEIMER'S DISEASE

Over 5 million older adults have Alzheimer's disease (AD) in the US, and this number is projected to double by 2050. Clinical trials of potential pharmacological treatments for AD have largely shown that once cognitive decline has occurred, targeting AD pathology in the brain does not improve cognition. Therefore, it is likely that the most effective treatments for AD will need to be administered before cognitive symptoms occur, necessitating a biomarker for the early, preclinical stages of AD. Cerebral blood flow (CBF) is a promising early biomarker for AD. CBF is decreased in individuals with AD compared to their normally aging counterparts, and it has been shown that CBF is altered in mild cognitive impairment (MCI) and earlier stages and may occur prior to amyloid or tau aggregation. In addition, CBF can be measured using arterial spin labeled (ASL) MRI, a noninvasive imaging technique that can be safely repeated over time to track prognosis or treatment efficacy. The complex temporal and spatial patterns of altered CBF over the course of AD, as well as the relationships between CBF and AD-specific and -nonspecific factors, will be critical to elucidate in order for CBF to be an effective early biomarker of AD. Here, we begin to characterize the relationships between CBF and risk factors, pathologies, and symptoms of AD. Chapter 1 is a systematic review of published literature that compares CBF in individuals with AD and MCI to CBF in cognitively normal (CN) controls and assesses the relationship between CBF and cognitive function. Chapter 2 reports our original research assessing the relationships between CBF, hypertension, and race/ethnicity in older adults without dementia from the

the Indiana Alzheimer's Disease Research Center (IADRC) and Alzheimer's Disease Neuroimaging Initiative (ADNI). Chapter 3 reports our original research assessing the relationships between CBF and amyloid beta and tau aggregation measured with PET, as well as whether hypertension or *APOEε4* positivity affects these relationships, in older adults without dementia from the IADRC. Chapter 4 reports our original research assessing the relationship between the spatial distribution of tau and subjective memory concerns.

Shannon L. Risacher, Ph.D., Chair

Andrew J. Saykin, Psy.D.

Liana G. Apostolova, M.D.

Yu-Chien Wu, M.D., Ph.D.

Sujuan Gao, Ph.D.

## TABLE OF CONTENTS

List of Tables .....	ix
List of Figures .....	x
List of Abbreviations .....	xii
Chapter 1: Altered Cerebral Blood Flow in Older Adults with Alzheimer’s Disease:	
A Systematic Review .....	1
1.1 Introduction.....	1
1.2 Methods.....	6
1.3 Results.....	11
1.4 Discussion.....	17
Chapter 2: Regional Cerebral Blood Flow is Related to Hypertensive Status and Self- Identified Race .....	58
2.1 Introduction .....	58
2.2 Methods.....	61
2.3 Results.....	65
2.4 Discussion.....	66
Chapter 3: Amyloid and Tau Pathology are Associated with Cerebral Blood Flow in Nondemented Older Adults with and without Genetic and Vascular Risk Factors: .....	82
3.1 Introduction .....	82
3.2 Methods.....	85
3.3 Results.....	90
3.4 Discussion.....	93
Chapter 4: Memory Concerns in the Early Alzheimer’s Disease Prodrome: Regional Association with Tau Deposition.....	111
4.1 Introduction .....	111
4.2 Methods.....	115
4.3 Results.....	118
4.4 Discussion.....	122
Chapter 5: Implications of Findings and Future Directions.....	145
References.....	152
Curriculum Vitae	

## LIST OF TABLES

Table 1. Characteristics of included articles .....	22
Table 2. Risk of bias assessment scores for included articles.....	31
Table 3. CBF in CN and AD individuals in each paper.....	34
Table 4. CBF in CN and MCI individuals in each paper.....	43
Table 5. Relationships between CBF and cognition in each paper.....	45
Table 6. Syntheses of CBF in AD compared to CN by brain region.....	55
Table 7. Demographic and Clinical Variables in the IMAS sample.....	73
Table 8. Demographic and Clinical Variables in the ADNI sample.....	73
Table 9. Correlations between ROI-based CBF and hypertension status in IMAS.....	73
Table 10. Correlations between voxel-wise CBF and hypertension status in IMAS.....	74
Table 11. Correlations between ROI-based CBF and self-identified race in IMAS.....	75
Table 12. Decreased voxel-wise CBF in self-identified African Americans in IMAS .....	75
Table 13. Decreased voxel-wise CBF in self-identified African Americans in ADNI .....	75
Table 14. Increased voxel-wise CBF in self-identified African Americans in IMAS .....	76
Table 15. Increased voxel-wise CBF in self-identified African Americans in ADNI.....	77
Table 16. Correlations between cluster CBF and MoCA delayed memory sub-score in IMAS and ADNI.....	79
Table 17. Demographic and clinical variables by diagnostic group.....	100
Table 18. Correlation of age and hypertension status with lobar CBF.....	100
Table 19. Negative correlations between voxel-wise CBF and MTL tau SUVR.....	101
Table 20. Amyloid positivity by hypertension status interaction effect on voxel-wise CBF .....	103
Table 21. Hypertension main effect on voxel-wise CBF.....	107
Table 22. Demographic and clinical variables of full sample by diagnostic group.....	128
Table 23. Demographic and clinical variables of amyloid-positive subset by diagnostic group.....	128
Table 24. Positive correlations between self-ECog memory scores and voxel-wise tau aggregation in the full sample.....	133
Table 25. Positive correlations between informant ECog memory scores and voxel-wise tau aggregation in the full sample .....	136
Table 26. Positive correlations between self-ECog memory scores and voxel-wise tau aggregation in the amyloid-positive subset.....	140
Table 27. Positive correlations between informant ECog memory scores and voxel-wise tau aggregation in the amyloid-positive subset .....	141

## LIST OF FIGURES

Figure 1. PRISMA flow chart of articles identified, assessed for eligibility, and included in systematic review.....	21
Figure 2. Effect sizes and 95% confidence intervals of frontal lobe CBF in AD relative to CN.....	47
Figure 3. Effect sizes and 95% confidence intervals of parietal lobe CBF in AD relative to CN.....	47
Figure 4. Effect sizes and 95% confidence intervals of temporal lobe CBF in AD relative to CN.....	48
Figure 5. Effect sizes and 95% confidence intervals of temporoparietal CBF in AD relative to CN.....	48
Figure 6. Effect sizes and 95% confidence intervals of occipital lobe CBF in AD relative to CN.....	49
Figure 7. Effect sizes and 95% confidence intervals of posterior cingulate CBF in AD relative to CN.....	49
Figure 8. Effect sizes and 95% confidence intervals of hippocampal CBF in AD relative to CN.....	50
Figure 9. Effect sizes and 95% confidence intervals of thalamic CBF in AD relative to CN.....	50
Figure 10. Effect sizes and 95% confidence intervals of frontal lobe CBF in MCI relative to CN.....	51
Figure 11. Effect sizes and 95% confidence intervals of parietal lobe CBF in MCI relative to CN.....	51
Figure 12. Effect sizes and 95% confidence intervals of temporal lobe CBF in MCI relative to CN.....	52
Figure 13. Effect sizes and 95% confidence intervals of temporoparietal CBF in MCI relative to CN.....	52
Figure 14. Effect sizes and 95% confidence intervals of posterior cingulate CBF in MCI relative to CN.....	53
Figure 15. Effect sizes and 95% confidence intervals of hippocampal CBF in MCI relative to CN.....	53
Figure 16. Effect sizes and 95% confidence intervals of thalamic CBF in MCI relative to CN.....	54
Figure 17. Visualization of correlations between voxel-wise CBF and hypertension status in IMAS.....	74
Figure 18. Visualizations of decreased voxel-wise CBF in self-identified African Americans in IMAS (A) and ADNI (B).....	76
Figure 19. Visualizations of increased voxel-wise CBF in self-identified African Americans in IMAS (A) and ADNI (B).....	77
Figure 20. Visualization of voxel-wise beta values in correlations of CBF and self-identified race in IMAS and ADNI.....	78
Figure 21. Scatterplots of correlations between fusiform CBF and MoCA delayed memory sub-score in IMAS (A), ADNI (B), and combined samples (C).....	80
Figure 22. Negative correlations between voxel-wise CBF and age (A) and hypertension status (B).....	101

Figure 23. Scatterplot of negative correlations between voxel-wise CBF and MTL tau SUVR.....	102
Figure 24. Visualization of negative correlations between voxel-wise CBF and MTL tau SUVR.....	102
Figure 25. Visualization of negative correlations between voxel-wise CBF and global cortical Centiloid.....	103
Figure 26. Global cortical Centiloid by hypertension status interaction effect on visual motor and supramarginal CBF .....	104
Figure 27. Global cortical Centiloid by hypertension status interaction effect on fusiform CBF .....	105
Figure 28. Global cortical Centiloid by hypertension status interaction effect on visual association and secondary visual CBF .....	106
Figure 29. Visualization of amyloid positivity by hypertension status effect on voxel-wise CBF .....	106
Figure 30. Visualization of amyloid positivity main effect on voxel-wise CBF .....	107
Figure 31. Visualization of hypertension main effect on voxel-wise CBF.....	108
Figure 32. Visualization of amyloid positivity by <i>APOE</i> $\epsilon$ 4 positivity effect on voxel-wise CBF .....	109
Figure 33. Visualization of MTL tau positivity by hypertension status effect on voxel-wise CBF .....	109
Figure 34. Visualization of MTL tau positivity by <i>APOE</i> $\epsilon$ 4 positivity effect on voxel-wise CBF .....	110
Figure 35. Relationships between self and informant memory concerns with frontal and parietal tau in the full sample .....	129
Figure 36. Relationships between self and informant memory concerns with frontal and parietal tau in the amyloid-positive subset.....	131
Figure 37. Memory concern source by tau location interaction in the full sample (A) and in the amyloid-positive subset (B) .....	133
Figure 38. Visualization of positive correlations between self-ECog (A&C) and informant (B&D) ECog scores with voxel-wise tau aggregation in the full sample (A&B) and the amyloid-positive subset (C&D) .....	144

## LIST OF ABBREVIATIONS

$^{11}\text{C}$	carbon-11
$^{123}\text{I}$	iodine-123
$^{123}\text{I-IMP}$	<i>N</i> -isopropyl-( $^{123}\text{I}$ )- <i>p</i> -iodoamphetamine
$^{15}\text{O}$	oxygen-15
$^{18}\text{F}$	fluorine-18
$^{99\text{m}}\text{Tc}$	technetium-99m
$^{99\text{m}}\text{Tc-ECD}$	technetium-99m ethyl cysteinate dimer
$^{99\text{m}}\text{Tc-HMPAO}$	technetium-99m hexamethylpropylene amine oxide
AA	African American
AChEI	acetylcholinesterase inhibitor
AD	Alzheimer's disease
ADNI	Alzheimer's Disease Neuroimaging Initiative
ANCOVA	analysis of covariance
ANOVA	analysis of variance
<i>APOE</i>	apolipoprotein E
ASL	arterial spin label
AV-1451	$^{18}\text{F}$ -flortaucipir
CAMCOG	Cambridge Cognition Examination
CAMDEX	Cambridge Mental Disorders of the Elderly Examination
CASL	continuous arterial spin label
CBF	cerebral blood flow
CCI-20	20-item Cognitive Change Index

CCI	Cognitive Change Index
CCSE	Cognitive Capacity Screening Examination
CDT	Clock Drawing Test
CN	cognitively normal
CSF	cerebrospinal fluid
CT	computed tomography
DSM-III	Diagnostic and Statistical Manual of Mental Disorders, 3 <sup>rd</sup> Edition
DSM-III-R	Diagnostic and Statistical Manual of Mental Disorders, 3 <sup>rd</sup> Edition, Revised
DSM-IV	Diagnostic and Statistical Manual of Mental Disorders, 4 <sup>th</sup> Edition
DSM-IV-R	Diagnostic and Statistical Manual of Mental Disorders, 4 <sup>th</sup> Edition, Revised
ECog	Measurement of Everyday Cognition
EEG	electroencephalogram
EMCI	early mild cognitive impairment
FOV	field of view
FEW	family-wise error rate
FWHM	full width at half maximum
GDS	Geriatric Depression Scale
HT	hypertension
IADRC	Indiana Alzheimer's Disease Research Center
IBM	International Business Machines

IBM SPSS 25	International Business Machines Statistical Package for the Social Sciences 25
ICD-10	International Classification of Diseases, Tenth Revision
IMAS	Indiana Memory and Aging Study
LM-delayed	Logical Memory - Delayed
LONI	Laboratory of NeuroImaging
MCI	mild cognitive impairment
mCT	molecular computed tomography
MMSE	Mini-Mental State Exam
MMSQ	Mini-Mental State Questionnaire
MNI	Montreal Neurological Institute
MoCA	Montreal Cognitive Assessment
MPRAGE	magnetization prepared – rapid gradient echo
MRI	magnetic resonance imaging
MTL	medial temporal lobe
NIA	National Institute on Aging
NINCDS-ADRDA	National Institute of Neurological and Communicative Disorders and Stroke and the Alzheimer’s Disease and Related Disorders Association
PASL	pulsed arterial spin label
pCASL	pseudo-continuous arterial spin label
PET	positron emission tomography
PiB	Pittsburgh Compound-B

QUIPS II	quantitative imaging of perfusion using a single subtraction, second version
ROI	region of interest
ROS	reactive oxygen species
SCD	subjective cognitive decline
SMC	significant memory concern
SPECT	single-photon emission computerized tomography
SPET	single-photon emission tomography
SPM12	Statistical Parametric Mapping, version 12
SPM8	Statistical Parametric Mapping, version 8
SUVR	standardized uptake value ratio
T1	longitudinal relaxation time
TE	time to echo
TMT-B	Trail Making Test Part B
TR	repetition time
WA	white American

# Chapter 1: Altered Cerebral Blood Flow in Older Adults with Alzheimer's Disease: A Systematic Review

## 1.1 Introduction

Alzheimer's disease (AD) is the leading cause of dementia, accounting for 60-80% of dementia cases.<sup>1</sup> Both the prevalence and mortality rate of AD are increasing in the U.S. and globally, and there are no current treatments that can stop or reverse the progressive loss of cognitive function caused by AD.<sup>1</sup> AD is characterized by the presence of aberrant aggregations of amyloid beta and tau proteins in the brain. Clinical trials of treatments targeting pathologic forms of these proteins have successfully reduced them but have been unable to stop the progression of cognitive decline.<sup>2</sup> The National Institute on Aging (NIA) has issued the goal to "prevent and effectively treat Alzheimer's disease by 2025." In order to effectively treat AD, a preventative treatment, administered before irreversible neuronal damage has occurred, may be necessary.<sup>2</sup> This would require the identification of older adults who are most likely to develop AD in the future. To do this, an effective early biomarker for AD is needed.<sup>3,4</sup> The disease process of AD can begin decades before cognitive decline is apparent and can manifest in preclinical stages of AD, including mild cognitive impairment (MCI), which can last for years before a clinical diagnosis of dementia.<sup>5,6</sup> MCI is a stage of decreased cognitive functioning as measured on objective cognitive tests accompanied by the preserved ability to achieve day-to-day activities.<sup>5</sup> Subjective cognitive decline (SCD), during which individuals still perform in the normal range on objective cognitive tests but report a subjective decline from their normal cognitive state, has been described as an even earlier stage in the course of AD.<sup>7,8</sup> An effective early biomarker for AD that can lead to preventative

treatment for AD must be able to distinguish individuals with SCD and MCI from normally aging individuals and from older adults experiencing cognitive changes due to other reasons, such as depression.<sup>9</sup> Therefore, biomarkers for preclinical AD will be necessary in order for treatments to be administered during the earliest disease stages, which may increase treatment efficacy.

Cerebral blood flow (CBF) is a potential early biomarker for AD. CBF is the rate at which blood reaches the brain and is typically measured in mL of blood per 100 grams of tissue per minute. The brain receives a disproportionately large amount of the body's blood supply relative to its size and is very sensitive to changes in blood pressure. The brain has unique mechanisms for keeping blood flow constant; if blood pressure increases, the vessels constrict and if blood pressure decreases, the vessels dilate.<sup>10</sup> This is the opposite of how blood vessels react to changes in blood pressure in most areas of the body and explains why hypertension and other cardiovascular risk factors, paired with age, which causes blood vessels in the brain to become more rigid, lead to a hyper-constricted cerebral vasculature and ultimately chronically reduced CBF.<sup>11</sup> Although the longstanding amyloid cascade hypothesis of AD posits that amyloid beta and its aggregation ultimately lead to the disease processes and outcomes in AD,<sup>12</sup> the more recently suggested two-hit hypothesis states that cerebrovascular dysfunction and amyloid beta pathology culminate to initiate and propagate AD.<sup>13</sup> CBF is globally decreased in patients with AD compared to age-matched non-demented counterparts. It has been shown that CBF is altered in individuals with preclinical AD as well, and that patterns of altered CBF are correlated with disease severity and progression from one diagnostic stage to the next.<sup>14</sup>

CBF has been studied in the context of AD and other dementias for several decades and has been measured by a variety of neuroimaging methods over time. The first measurements of CBF in humans were made in 1948 using the inhalation of nitrous oxide and quantification of the inert gas in venous blood.<sup>15</sup> In the 1960s, the use of radioactive tracers including krypton-85 and xenon-133 allowed for the measurement of regional as well as global CBF.<sup>16,17</sup> Over time, methods improved to allow for better precision of measurement. The development of positron emission tomography (PET) soon led to the use of positron-emitting tracers, particularly oxygen-15, for CBF measurement.<sup>18</sup> Dynamic contrast enhanced magnetic resonance imaging (DCE MRI) was developed around the same time as PET and utilized gadolinium-based contrast agents that had magnetic properties to trace and quantify CBF without the need for radioactive tracers.<sup>19,20</sup>

The most common methods of the studies included in this review are single-photon emission computerized tomography (SPECT) and the more recently developed arterial spin labeled (ASL) MRI. SPECT requires the blood to be labeled with an injection of a radioactive tracer, such as iodine-123 or technetium-99m. As the tracer undergoes radioactive decay, gamma rays are emitted and detected by a gamma camera. These detections are then reconstructed into a 3D image that depicts where in the brain the tracer (and thus blood) traveled during the imaging period.<sup>21</sup> ASL MRI, on the other hand, is completely noninvasive. MR imaging works by detecting the magnetic alignment of water molecules (specifically, of hydrogen atoms) in the body. In ASL MRI, blood is labeled as it flows into the brain by inverting the magnetization of the water molecules in the blood, and then an image is constructed from the magnetic signals detected in the

brain. When compared to an MR image taken without magnetically labeling the blood, the difference between the labeled and unlabeled images corresponds to the amount of blood that flowed into the brain during the imaging period of the labeled scan.<sup>22</sup> ASL MRI can therefore be safely and comfortably used at multiple time points to monitor changes in CBF over the course of disease or treatment, because it does not require the injection of a radioactive tracer.

In order for altered CBF to be a viable early biomarker for AD, we need to better understand how CBF changes throughout the progression of AD, including in preclinical and prodromal stages. It is also critical that the roles of other AD-related pathologies (amyloid beta, tau, gray matter atrophy, white matter lesions), AD risk factors (apolipoprotein E (*APOE*)  $\epsilon$ 4 genotype, diabetes, hypertension, and other types of cardiovascular disease), and demographic factors (age, sex, race/ethnicity, education, environmental risk factors) are taken into consideration when measuring CBF. These may affect or be affected by altered CBF, and all of these factors likely interact with each other to initiate and propagate the disease state.

The purpose of this review is to consolidate the literature comparing CBF in older adults with MCI or AD to those that are cognitively normal (CN). Patterns of altered CBF will be summarized using results from several brain regions. Results will also be summarized for the relationship between cognitive exam scores and CBF in older adults. The aim is to compile and synthesize the results of the existing literature concerning altered CBF in AD. This is important because various methods of imaging and CBF measurement have been used over the years; standardization of results will help to clarify whether previous findings are consistent. We also aim to summarize the methods used in

the various studies, for example whether potentially confounding factors are included. A recently published review<sup>23</sup> covers the same topic with a broader scope. It includes studies that measured CBF velocity, and it does not exclude articles based on the age of participants with AD. However, Zhang et al<sup>23</sup> does not include papers that report voxel-wise results in the form of z or t scores. The current review employs an age cutoff for the AD participants included because early onset AD, diagnosed before age 65, may be a different variant of AD; early onset AD patients tend to decline more rapidly and are more likely to have cognitive declines in areas other than memory as the initial symptoms. Therefore, we excluded papers where the mean age of AD participants minus two standard deviations (SDs) is less than 60, meaning that 95% of the individuals studied in each paper are at least 60 years old. This defines the overall included AD population as mostly late onset. We also included papers that report voxel-wise results to assess their consistency with papers that report regional CBF values.

The objective of this review is to assess the cumulative evidence of altered CBF in older adults with MCI and AD in multiple brain regions and of the relationship between CBF and cognitive exam scores in these individuals. We also aim to assess the consistency of findings across papers that use a variety of imaging, processing, and analytic methods. The main question in this review is a case-control observational research question in which the condition is MCI or AD and the variable of interest is defined as altered CBF. However, the direction of causality is not defined, and the question is more one of correlation between diagnosis and CBF. In reality, it is likely that AD pathologies and altered CBF exacerbate one another and have a cyclical relationship, and it is not clear which of the two is present first or whether both arise simultaneously

from a common cause. These questions may be answered in the future with the help of large longitudinal studies of CBF over the course of AD. As we describe later, this will be necessary in order to fully characterize CBF as an early biomarker for AD.

## 1.2 Methods

This systematic review includes all studies in which resting CBF is either compared between different diagnostic groups (CN, MCI, AD) or correlated with cognitive exam scores within or across diagnostic groups. Further, only studies in which the age of AD patients is at minimum 60 years old within two SDs from the mean are included. If there was not an SD listed for age of participants with AD, that paper was not eligible unless the minimum age was at least 60. Both observational studies and clinical trials that measured CBF at rest prior to treatment are included, as well as both cross-sectional and longitudinal designs. We chose to use a cutoff for participant age so that a majority of the AD patients would be near the age of 65 and likely to have the late-onset variant of AD. Early onset AD tends to progress more rapidly and is more likely to present with cognitive deficits other than memory difficulties in the early stages. This group should be studied separately when it comes to early biomarkers. Only manuscripts which were written in English were included. All manuscripts are published as original research papers or brief reports; conference abstracts were not included. There were no restrictions on the year of publication or on the method of CBF measurement, so long as the methodology was appropriate. Studies that were ineligible either did not measure CBF at rest or did not use resting CBF as an outcome measure in multiple diagnostic groups and/or in comparison with cognitive test scores.

PubMed was searched on March 23, 2021, through the National Library of Medicine and with access via Indiana University School of Medicine. 1197 potential articles resulted from a PubMed search of “brain-blood supply” and “Alzheimer’s disease.” We did not specify article type or language in the initial PubMed search in order to be inclusive of all possibly relevant articles. The search terms were chosen from PubMed MeSH terms that broadly encompassed the intended key topics of CBF and Alzheimer’s disease.

Due to the observational nature of the research question, the PICO method was not used. Unlike an intervention and outcome, CBF and AD diagnosis and/or severity do not have a known direction of causation. Therefore, the design used was a case-control observational research question in which the condition was AD or MCI and the variable of interest was altered CBF. However, we did not require that CBF measurement take place prior to MCI or AD diagnosis; it was decided to view AD and altered CBF as mutually propagating, as it is unknown whether AD pathology or altered CBF occurs first, and it has been shown that each can exacerbate the other.

For the main synthesis, we describe increase or decrease in CBF between cases of AD and controls in several brain regions. Altered CBF in MCI relative to controls and correlations between CBF and cognitive test scores are described as well, for articles which include these analyses. For papers that present relevant data only in the form of a graph, we extracted quantitative data using WebPlotDigitizer version 4.5 ([automeris.io/WebPlotDigitizer/](http://automeris.io/WebPlotDigitizer/)). For articles that had a high potential of duplicate or overlapping participant samples, the article with the higher quality rating (less risk for bias) was chosen.

The information recorded for each article were: author(s), article title, year of publication, place of the study, number of participants, diagnostic groups, criteria by which diagnoses were defined, method used to measure and quantify CBF, ages of participants, whether the paper is included in the synthesis, and which outcomes were reported. Additional, irrelevant methods and outcomes are not reported. To organize this information, we used a matrix from University of Maryland Research Guides ([lib.guides.umd.edu/SR/steps](http://lib.guides.umd.edu/SR/steps)).

To assess the risk of bias and the quality of each article, we used the NIH Quality Assessment of Case-Control Studies. The items on this tool were: clearly stated objective, clearly specified and defined population, sample size justification, use of same population for cases and controls, use of same inclusion and exclusion criteria for cases and controls, clearly defined and differentiated cases, random selection of sample from eligible individuals, use of concurrent controls, confirmation that exposure occurred prior to the condition, clearly defined and reliable measures of exposure/risk, blinded assessment of exposure/risk with regard to case/control, and use of matching or addition of confounding variables to statistical models. Overall judgments were “poor,” “fair,” or “good.” These decisions were made according to the guidance included in the tool, where it is explained that lack of some criteria correspond to “fatal flaws” while others do not much affect the overall quality of the paper. CBF was considered the “exposure,” and because the direction of causation between AD and altered CBF is outside the scope of this review, it was not relevant whether the exposure occurred prior to the condition. Therefore, this question was marked as “not applicable” and not used in the overall bias rating. Other items on the rating tool that were not used were: sample size justification, random

selection of sample from eligible individuals, and use of concurrent controls, because these items were all either not present or not reported in all or nearly all papers assessed. In addition, blind assessment of the CBF was not applicable for many of the papers, because the CBF was measured by fully automated methods. This item was considered for those papers in which hand-drawn regions of interest were used.

For each relevant paper, we reported mean and SD of CBF in each brain region for each diagnostic group. For articles that used voxel-wise measurement of CBF and reported the z or t scores of peak voxels, these scores, along with cluster sizes and p values are reported. For papers that measured the correlation between CBF and cognitive test scores, r and p values are reported. For papers with mean and SD regional CBF values, effect sizes were calculated, and syntheses were presented for multiple brain regions for that compared CBF between AD and CN. To measure effect size of the difference in CBF between CN and AD and between CN and MCI for papers that reported regional CBF values, we used Hedge's g, which is Cohen's d adjusted for small sample sizes, as well as the 95% confidence interval for Cohen's d. These effect size measures were chosen because CBF is a continuous measure that is dependent on the scanning and processing methods, so standardized measures were necessary. Effect size was calculated for the difference in CBF between MCI/AD and control groups in the following brain regions: frontal, temporal, parietal, temporoparietal, occipital, posterior cingulate, hippocampus, and thalamus. These regions were chosen because they were the most frequently used across all papers. Thresholds were not employed for the effect sizes; we assessed synthesized results by reporting the average, median, and range of effect size scores in each synthesis. Overall, we stated whether there were consistent or inconsistent

results for regional CBF change in participants with AD relative to CN across papers. For all results reported with Hedge's  $g$ , this value and the 95% confidence interval are presented in graphs, organized by brain region and by whether CN is compared to MCI or AD.

A meta-analysis was not done. Heterogeneity is discussed where there is inconsistency in findings across papers, but statistical analyses regarding heterogeneity were not completed. Sensitivity analyses were also not completed. The scope of this paper is to compile and present the findings in the literature and to discuss overall patterns of results. Reporting bias is taken into account, and certainty ratings for each synthesis are presented in the summary of findings table. The scope of this review only includes relevant articles from PubMed that are published, in English, and fully accessible through the Indiana University School of Medicine student credentials. Grey literature was not included. Negative findings were included whenever they were reported, but not all papers reported findings for every brain region. For the certainty assessment, we used the GRADE tool from the Cochrane handbook. Scores are "very low," "low," "moderate," and "high." Since this tool is designed for randomized clinical trials, it instructs the assessor to begin with "moderate" for observational or case-control studies. We rated each synthesis according to the rest of the GRADE criteria but did not strictly begin at "moderate" for each paper because, by design, most of the papers were not clinical trials.

### 1.3 Results

Of 1197 potential articles resulting from a PubMed search of “brain-blood supply” and “Alzheimer’s disease”, 185 were retained for further assessment, and 1012 were excluded. Of those excluded, 352 were reviews, editorials, commentaries, case studies, and other types of articles that did not match the eligibility criteria. 325 did not use resting CBF as an outcome measure, and 157 used animal models or cell cultures rather than human participants. Finally, 94 did not include participants with various diagnoses or levels of cognitive functioning, and full access was not available for 84 articles. Of the 185 retained, 29 articles were ultimately chosen for inclusion in this review, and 156 were excluded. Of these, 97 sampled AD patients who were too young or whose ages were not adequately defined, 25 did not use resting CBF as an outcome, 17 did not compare CBF between diagnostic groups or correlate it with cognitive function, 5 included participants with potentially confounding conditions, 3 were out of scope, 2 included patients with AD who were on psychotropic medication, and 7 were likely to have used the same participant groups as other articles included in this review. The process of choosing relevant articles is presented in Figure 1.

The papers considered “out of scope” include Iturria-Medina et al,<sup>24</sup> in which the authors create a 4D multifactorial causal model of AD; Moretti,<sup>25</sup> which focuses on and groups participants by alpha power ratio on EEG; and Vogel et al,<sup>26</sup> which measures and compares the heterogeneity of CBF rather than a measure of CBF itself. Papers that include patients and/or controls with other illnesses are: Jagust et al<sup>27</sup> (half of the AD patients have early onset AD), Dougall et al<sup>28</sup> (some controls have major depression), Starkstein et al<sup>29</sup> (some controls have dizziness), Cho et al<sup>30</sup> (controls have headaches or

syncope), and De Reuck et al<sup>31</sup> (the dementia group includes Pick's disease and Creutzfeldt-Jakob, and the nondemented group includes stroke and encephalopathy). The papers with potentially overlapping samples were: Hanyu et al<sup>32</sup> (with Hanyu et al<sup>33</sup>), Haji et al<sup>34</sup> (with Kimura et al<sup>35</sup>), Brown et al<sup>36</sup> (with Brown et al<sup>37</sup>), Colloby et al<sup>38</sup> (with Firbank et al<sup>39</sup>), Kawamura et al<sup>40</sup> and Mortel et al<sup>41</sup> (with Obara et al<sup>42</sup>) and Pearlson et al<sup>43</sup> (with Harris et al<sup>44</sup>).

Papers included in this review are listed and characterized in Table 1. They include: Alegret et al,<sup>45</sup> Benoit et al,<sup>46</sup> Brown et al,<sup>37</sup> Claus et al,<sup>47</sup> Dai et al,<sup>48</sup> Ding et al,<sup>49</sup> Encinas et al,<sup>50</sup> Firbank et al,<sup>39</sup> Hanyu et al,<sup>33</sup> Hanyu et al,<sup>51</sup> Harris et al,<sup>44</sup> Iizuka and Kameyama,<sup>52</sup> Jagust et al,<sup>53</sup> Johnson et al,<sup>54</sup> Kimura et al,<sup>35</sup> Lacalle-Aurioles et al,<sup>55</sup> Lee et al,<sup>56</sup> Mubrin et al,<sup>57</sup> Nagahama et al,<sup>58</sup> Obara et al,<sup>42</sup> Sase et al,<sup>59</sup> Schuff et al,<sup>60</sup> Shimizu et al,<sup>61</sup> Sundstrom et al,<sup>62</sup> Takahashi et al,<sup>63</sup> Tateno et al,<sup>64</sup> van de Haar et al,<sup>65</sup> Yew and Nation,<sup>66</sup> and Yoshida et al.<sup>67</sup> The table provides the following information for each included article: author, title, year of publication, location of the study (or study authors if this is unclear), sample size by diagnostic group, criteria used to define diagnostic groups, type of scan used to measure CBF, ages of participants in each diagnostic group, whether the paper was included in the syntheses, and whether outcomes included CBF in AD vs. CN, CBF in MCI vs. CN, and/or the correlation between CBF and cognitive test scores. Notes are included to clarify special circumstances for individual papers where necessary. Of the 29 papers, 19 measure CBF using SPECT, 6 using ASL MRI, and 4 using other methods. Publication dates range from 1987 to 2017.

Table 2 reports the component scores and overall quality rating on the risk of bias assessment for each paper. Justification for each score is given in the "Overall Quality

Rating and Notes” column. Of the 29 papers, 9 were rated as “good,” 13 were rated as “fair,” and 7 were rated as “poor.” All but one of the papers rated “poor” differed from those rated “good” and “fair” by the lack of reported cognitive test scores for the CN group, without which it is not clear that the CN group is free of cognitive decline. Sundstrom et al<sup>62</sup> was rated as “poor” because the CN group was younger than the AD group, and age was not used as a covariate in the analyses.

Tables 3, 4, and 5 report the results of interest for each study. Table 3 reports the comparison of CBF in CN and AD groups (notes clarify which papers include MCI in one of these groups or compare MCI to AD), Table 4 reports the comparison of CBF between CN and MCI groups, and Table 5 presents correlations between CBF and cognitive exam scores. In Tables 3 and 4, regional CBF data is given as mean (SD) for each group. For regional CBF in these tables and further analyses, values for left and right regions were averaged, with SDs pooled; this was also done across smaller brain regions within those of interest. When bilateral averaging was done, or when only one hemisphere was included in a given paper, this is clarified in the “Notes” column. For voxel-wise results, cluster size (k), p value, and z or t value are reported, and the specific region where the peak voxel is located is given in the “Notes” column. For all effect sizes, a positive value represents a decrease in CBF in patients relative to CN, as this was how the results were reported in nearly all of the papers. The “Notes” column also mentions if the data were extracted from a graph rather than reported numerically in the paper. Papers with qualitative results are included in this table as well, for completeness. These papers all used quantitative or semi-quantitative methods to measure CBF; papers that assessed CBF simply by visual inspection were not eligible to be included in this

review. Table 5 reports  $r$  and  $p$  values for the correlation of regional CBF and cognitive test scores, where available, with details in the “Notes” column.

Overall, most of the papers reported relatively decreased CBF in AD in all brain regions we included. Relatively increased CBF in AD was reported more rarely, and only in the frontal and temporal lobes, hippocampus, and thalamus. There were fewer papers that assessed CBF in MCI compared to CN, but relatively decreased CBF in MCI was reported in all regions except for the thalamus, and relatively increased CBF in MCI was reported in the frontal and temporal lobes, hippocampus, and thalamus.

Specifically, decreased CBF in AD was reported in the frontal lobe in 18 papers, in the parietal lobe in 20 papers, in the temporal lobe in 19 papers, in temporoparietal regions in 10 papers, in the occipital lobe in 9 papers, in the posterior cingulate in 9 papers, in the hippocampus in 3 papers, and in the thalamus in 5 papers. Relative increases in CBF in AD were reported in the frontal lobe in 3 papers, in the temporal lobe in one paper, in the hippocampus in one paper, and in the thalamus in two papers. Relative decreases in CBF in MCI were reported in the frontal lobe in one paper, in the parietal lobe in one paper, in the temporal lobe in three papers, in the temporoparietal region in one paper, in the occipital lobe in one paper, in the posterior cingulate in three papers, and in the hippocampus in one paper. Relative increases in CBF in MCI were reported in the parietal lobe in two papers, in the temporal lobe in one paper, in the hippocampus in one paper, and in the thalamus in one paper. These results include reports of altered CBF that were not statistically significant in the original papers.

Of the papers that assessed the relationship between cognitive test scores and CBF, a majority of them reported a positive correlation, but there were also reports of

negative correlations and of no correlation. Specifically, regional CBF was reported to be positively correlated with cognitive function in 9 papers. The cognitive tests used in these papers include the Mini Mental State Examination (MMSE), 15- Objects Test, 15 item Boston Naming Test, Poppelreuter test, Cognitive Capacity Screening Examination (CCSE), Cambridge Cognition Examination (CAMCOG; language, praxis, and abstraction sub-scores), Mini Mental State Questionnaire (MMSQ), Trail Making Test Part B (TMT-B), and the Clock Drawing Test (CDT). Regional CBF is negatively correlated with scores on TMT-B in one paper. One paper reported no correlation between global CBF and revised CAMCOG scores when other independent variables were in the model and another paper reported no correlation between regional CBF and the memory sub-score of the CAMCOG. One paper reported no correlation between regional CBF and the California Verbal Learning Test or Self-Ordering Test. Additionally, two papers reported both positive and negative correlations between cognitive test scores and CBF in distinct brain regions. Details for each set of results from each paper are given in the final columns of the tables.

Figures 2-16 graphically present the Hedge's  $g$  score and 95% confidence interval of Cohen's  $d$  for the difference in CBF between AD and CN (Figures 2-9) and between MCI and CN (Figures 10 -16) for each brain region. As in the tables, positive effects denote a decrease in CBF in MCI/AD relative to CN. Alegret et al<sup>45</sup> reports regional CBF as mean (SD) of eigenvariates from voxel-wise comparisons, which are not directly comparable to the other results but are included in these graphs for completeness.

Table 6 is a Summary of Findings table for the syntheses of results. Results are presented for CBF in CN vs. AD in papers that reported regional CBF values as mean

(SD). Seventeen papers were included. Alegret et al<sup>45</sup> was not included. Encinas et al<sup>50</sup> was also not included because there was no CN group in that study. Table 6 reports combined sample size, number of studies included, authors of included studies, mean, median, and range of Hedge's *g* scores, certainty, and comments for syntheses of CBF in AD relative to controls in each brain region. The region with the greatest mean and median Hedge's *g* (greatest decrease in CBF in AD compared to CN) is the temporoparietal, followed by the posterior cingulate. All regions had positive mean and median Hedge's *g* scores (denoting decreased CBF in AD compared to CN). Regions with at least one paper that reported an increase in CBF in AD compared to CN were frontal lobe, temporal lobe, and the hippocampus.

Reporting bias was assessed by rating the completeness of each paper in the syntheses. All eligible papers, those that reported mean and SD CBF values for AD and CN, were included, except for Alegret et al<sup>45</sup> due to the mean and SD coming from voxel-wise eigenvariates. Of the included papers, Firbank et al<sup>39</sup> was missing CBF data from the thalamus for one CN participant, and Schuff et al<sup>60</sup> did not analyze or report occipital CBF data because too few voxels were present after selecting only "pure" gray or white matter voxels. Otherwise, results were fully reported in all papers. Papers were included in regional syntheses if they reported CBF values for relevant subregions, some of which we combined for an average value within the synthesis region. This review only includes published articles from PubMed that were in English and fully accessible. These restrictions contribute to a moderate level of reporting bias, but reporting bias is likely not increased from other sources or for other reasons.

Certainty of syntheses was rated based on cumulative risk of bias scores of the constituent papers; if the weighted average risk of bias score (based on sample size) was less than “fair,” the overall certainty was lowered. Certainty was also lowered due to inconsistency (scores were higher if all results were in the same direction), and indirectness and/or imprecision (including papers where we combined subregions’ values, subgroups, or where we extracted data from graphs). Large effect sizes, evidence of dose-response relationships (MCI values intermediate between CN and AD values), and confounding factors that would have likely resulted in an effect of the opposite direction were considered as reasons to raise or maintain the certainty score. Justifications for the certainty score are included in detail in Table 6 for each synthesis.

#### 1.4 Discussion

In this systematic review, we compiled findings of altered CBF in MCI/AD from previously published literature. There were consistent reports of decreased CBF in AD compared to CN in parietal, temporoparietal, occipital, and posterior cingulate regions. Frontal, temporal, hippocampal, and thalamic regions each had either increases in CBF in AD or no differences reported in at least one paper. Interestingly, thalamic CBF in AD was relatively decreased in all five papers that reported regional CBF and was relatively increased in the two papers that reported voxel-wise results. Across regions, 93% of the results reported decreased CBF in AD compared to CN. For CBF in MCI compared to CN, the results were more mixed. Only five papers reported regional or voxel-wise comparisons in CBF between CN and MCI, but of the 16 regional results, 5 (31%) of them reported increased CBF in MCI compared to CN. While the higher percentage of

results reporting an increase in CBF in MCI could be due to the low number of papers comparing CBF between MCI and CN, it has been suggested that increased CBF in MCI could be a compensatory response to early AD pathology, in which increased blood flow is necessary in order to function at a normal level. In Zhang et al,<sup>23</sup> the authors concluded that decreased CBF begins in posterior cingulate, temporoparietal, and thalamic regions during MCI, and that decreased CBF becomes more widespread in AD. We did find some evidence of decreased CBF in MCI, and MCI values were intermediate between CN and AD in the same paper.<sup>45,48</sup> Like Zhang et al,<sup>23</sup> we found quite consistent findings of positive correlations between regional CBF and cognitive functioning, which supports the idea that decreased CBF is associated with cognitive impairment in AD. It will be necessary for future studies to elucidate whether transient increases in CBF during MCI are characteristic of this stage of disease or if this only occurs in a particular subset of individuals with MCI.

Another finding from this review is that only a few papers comparing CBF between diagnostic stages included potentially confounding variables in the analyses. Nearly all of the papers used diagnostic groups that did not differ by age, so this was largely accounted for. Sundstrom et al<sup>62</sup> reported that the CN group was younger than the AD group. The only paper that did not report adequate information about group age was Mubrin et al<sup>57</sup>. Neither of these papers were included in the syntheses presented in the Summary of Findings Table. Aside from age, three papers included sex as a covariate, and one paper each included presence of hypertension, white matter lesion volume, presence of the *APOE*  $\epsilon 4$  allele, body mass index, and measure of cerebral glucose metabolism as covariates in the analyses. Given that all of these factors and others,

including other cardiovascular risk factors, lifestyle factors, and perhaps even socioeconomic factors could potentially have an effect on brain and/or cognitive function, there are many variables that should be taken to account in future CBF studies in AD.

Limitations of this review include that we only used accessible articles from PubMed that were published in English. Another limitation inherent in including articles from various decades is that several different imaging and processing methods were used to measure CBF in these papers. Papers also used different reference regions to normalize the CBF values. Despite this, the results of CBF in AD compared to CN and of CBF in relation to cognitive test scores were generally consistent. The less consistent results in the MCI group may be due to the small sample size or may be due to differences in the MCI samples that were not accounted for. Additionally, this review only includes papers with AD samples of a certain age, so the number of papers included is relatively small, and some of them have small sample sizes. Due to these limitations and to the observational and correlational nature of the research question, the results and syntheses presented here are meant to summarize and consolidate the existing evidence of altered CBF in MCI/AD and to characterize general patterns in these findings, rather than to make conclusive statements about the degree of these changes.

The results of this review suggest that more research is needed to better understand the spatial and temporal nature of changes in CBF throughout the course of AD, especially in early stages of disease including MCI. In addition, standardization of methods to measure and process CBF would allow results from different studies to be more easily be consolidated or compared. We believe that, in order to best characterize CBF for its potential use as an early noninvasive biomarker for AD, large and diverse

samples of participants must be employed, so that analyses can be completed in multiple brain regions and with multiple factors included as covariates. Longitudinal studies that meet these criteria and include individuals from different disease stages could help to clarify the specific patterns of CBF changes that usually occur during the years leading up to a diagnosis of AD and how altered CBF relates to AD pathologies and cognitive decline.

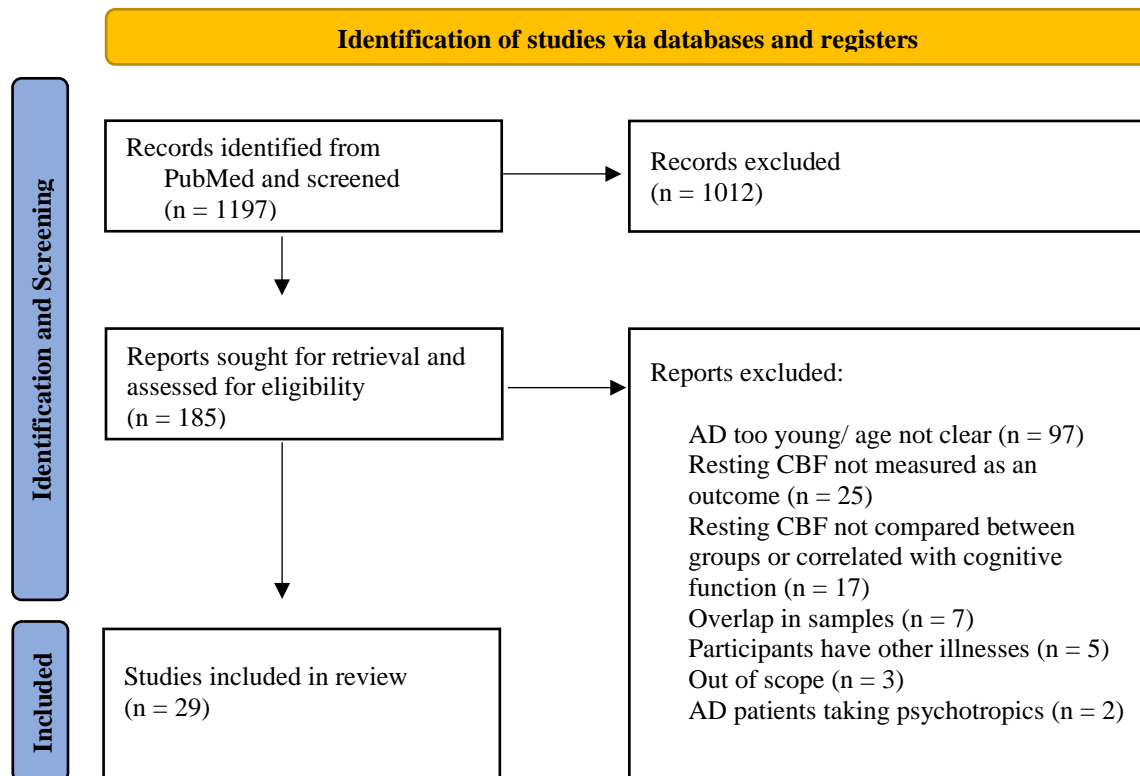


Figure 1. PRISMA flow chart of articles identified, assessed for eligibility, and included in systematic review. Reasons for exclusion are listed. Included papers compare resting CBF between AD/MCI and CN, include an AD sample where over 95% are 60 years old or older, and are written in English.

Table 1. Characteristics of included articles. Columns display authors (A), titles (B), publication date (C), location of study/authors (D), number of participants and diagnostic groups included (E), criteria used to determine diagnoses (F), method used for measurement of CBF (G), and ages of participants in each diagnostic group expressed as mean (SD) (H) for each included paper. The last four columns state whether the paper includes results were included in the synthesis (I) and whether the paper reports CBF for AD (J), MCI (K), and/or in association with cognitive function (L). Abbreviations can be found in the List of Abbreviations (p. xii).

A	B	C	D	E	F	G	H	I	J	K	L
Alegret et al <sup>45</sup>	Brain perfusion correlates of visuoperceptual deficits in mild cognitive impairment and mild Alzheimer's disease	2010	Barcelona, Spain	126 (42 CN, 42 MCI, 42 AD)	NINCDS-ADRDA for AD and Petersen et al criteria for MCI	<sup>99m</sup> Tc-ECD SPECT	CN: 74.7 (4.4) MCI: 76.8 (4.3) AD: 76.4 (4.5)	no	yes	yes	yes
Benoit et al <sup>46</sup>	Brain perfusion in Alzheimer's disease with and without apathy: a SPECT study with statistical parametric mapping analysis	2002	Nice University Memory Center, France	41 (11 CN, 30 AD)	ICD-10 criteria	<sup>99m</sup> Tc-ECD SPECT	CN: 74.1 (9.3) AD: 77.1 (5.6)	no	yes	no	yes
Brown et al <sup>37</sup>	Longitudinal changes in cognitive function and regional cerebral function in Alzheimer's disease: a SPECT blood flow study	1996	Glasgow, Scotland	38 (14 CN, 24 AD)	CAMDEX and DSM-III-R	<sup>99m</sup> Tc-HMPAO SPECT	CN: 72 (2.3) AD: 76 (1.5)  comparison not described	yes	yes	no	yes

Claus et al <sup>47</sup>	Assessment of cerebral perfusion with single-photon emission tomography in normal subjects and in patients with Alzheimer's disease: effects of region of interest selection	1994	Netherlands; Rotterdam Elderly Study	108 (60 CN, 48 AD)	NINCDS-ADRDA	<sup>99m</sup> Tc-HMPAO SPET	CN: 74.1 (0.8) MCI: 72.2 (1.2)	yes	yes	no	no
Dai et al <sup>48</sup>	Mild cognitive impairment and alzheimer disease: patterns of altered cerebral blood flow at MR imaging	2009	Pittsburgh, USA; Cardiovascular Health Study Cognition Study	104 (38 CN, 29 MCI, 37 AD)	described in Lopez et al 2003	CASL MRI	CN: 82.1 (3.6) AD: 83.6 (3.5)	yes	yes	yes	no
Ding et al <sup>49</sup>	Pattern of cerebral hyperperfusion in Alzheimer's disease and amnesic mild cognitive impairment using voxel-based analysis of 3D arterial spin-labeling imaging: initial experience	2014	China	62 (21 CN, 17 MCI, 24 AD)	NINCDS-ADRDA for AD and Petersen et al criteria for MCI	3D pCASL MRI	CN: 69.6 (5.9) MCI: 71.4 (7.6) AD: 74.6 (6.7)	no	yes	yes	no

Encinas et al <sup>50</sup>	Regional cerebral blood flow assessed with <sup>99m</sup> Tc-ECD SPET as a marker of progression of mild cognitive impairment to Alzheimer's disease	2003	Madrid, Spain	42 (21 MCI, 21 AD)  all start with MCI and some progress to AD	International Psychogeriatric Association and the Alzheimer's Disease Cooperative Study, Global Deterioration Scale (GDS) for MCI; NINCDS-ADRDA, DSM-IV, GDS for AD	<sup>99m</sup> Tc-ECD SPET	MCI: 71.6 (8.2) AD: 75.3 (5.5)	no	yes	yes	no
Firbank et al <sup>39</sup>	Cerebral blood flow by arterial spin labeling in poststroke dementia	2011	Newcastle upon Tyne, UK	46 (29 CN, 17 AD)  also a post-stroke group	NINCDS-ADRDA	ASL MRI	CN: 82.9 (3.5) AD: 83.2 (3.7)	yes	yes	no	yes
Hanyu et al <sup>33</sup>	Cerebral blood flow patterns in Binswanger's disease: a SPECT study using three-dimensional stereotactic surface projections	2004	Tokyo, Japan	44 (22 CN, 22 AD)  also a Binswanger's disease group	NINCDS-ADRDA	<sup>123</sup> I-IMP SPECT	CN: 77.1 (5.8) AD: 77.9 (5.5)	yes	yes	no	no

Hanyu et al <sup>51</sup>	The effect of education on rCBF changes in Alzheimer's disease: a longitudinal SPECT study	2008	Tokyo, Japan	81 (28 CN, 53 AD)  AD grouped by level of education, cutoff 12 years	NINCDS-ADRDA	<sup>123</sup> I-IMP SPECT	CN: 75.1 (6.4) AD high education: 76.8 (5.7) AD low education: 75.9 (6.4)	yes	yes	no	no
Harris et al <sup>44</sup>	Cortical circumferential profile of SPECT cerebral perfusion in Alzheimer's disease	1991	Baltimore, Maryland, USA	23 (8 CN, 15 AD)	NINCDS-ADRDA	<sup>123</sup> I-IMP SPECT	CN: 70.1 (4.9) AD: 72.6 (5.9)	yes	yes	no	no
Iizuka & Kameyama <sup>52</sup>	Cholinergic enhancement increases regional cerebral blood flow to the posterior cingulate cortex in mild Alzheimer's disease	2017	Tokyo, Japan	45 (9 CN, 36 AD)  AD grouped by response to treatment; used data from before treatment	NINCDS-ADRDA, DSM-IV-R, and ICD 10 <sup>th</sup> revision	<sup>123</sup> I-IMP SPECT	CN: 77.11 (3.6) AD: 77.6, range 69-89	no	yes	no	no
Jagust et al <sup>53</sup>	The diagnosis of dementia with single photon emission computed tomography	1987	California, USA	14 (5 CN, 9 AD)  also 2 with multi-infarct dementia	NINCDS-ADRDA and DSM-III	<sup>123</sup> I-IMP SPECT	CN: 70 (6) AD: 71 (5)	yes	yes	no	yes

Johnson et al <sup>54</sup>	Single photon emission computed tomography perfusion differences in mild cognitive impairment	2007	Massachusetts, USA	158 (19 CN, 105 MCI, 34 AD)	NINCDS-ADRDA for AD; Clinical Dementia Rating Sum of Boxes for grouping at follow-up	<sup>99m</sup> Tc-HMPAO SPECT	CN: 73.1 (3.6) MCI: 73.7 (5.0) AD: 75.1 (3.9)	no	yes	yes	yes
Kimura et al <sup>55</sup>	Relationship between thyroid hormone levels and regional cerebral blood flow in Alzheimer disease	2011	Oita, Japan	89 (27 CN, 62 AD)	NINCDS-ADRDA	<sup>99m</sup> Tc-ECD SPECT	CN: 75.8 (6.5) AD: 77.3 (6.9)	yes	yes	no	no
Lacalle-Aurioles et al <sup>55</sup>	Is the cerebellum the optimal reference region for intensity normalization of perfusion MR studies in early Alzheimer's disease?	2013	Madrid, Spain	63 (20 CN, 15 MCI, 28 AD)	Winblad criteria for MCI, NINCDS-ADRDA for AD	echo planar MRI for perfusion weighted imaging	CN: 71.7 (7.0) MCI: 70.9 (9.7) AD: 74.7 (7.0)	yes	yes	yes	no
Lee et al <sup>56</sup>	Statistical parametric mapping of brain SPECT perfusion abnormalities in patients with Alzheimer's disease	2003	Taiwan	60 (20 CN, 20 mild AD, 20 moderate AD)	NINCDS-ADRDA for AD, CDR, MMSE and Cognitive Abilities Screening Instruments (CASI) for AD severity	<sup>99m</sup> Tc-HMPAO SPECT	CN: 73.8 (2.8) mild AD: 74.2 (3.0) moderate AD: 74.1 (3.2)	no	yes	no	no

Mubrin et al <sup>57</sup>	Normalization of rCBF pattern in senile dementia of the Alzheimer's type	1989	Yugoslavia	26 (CN and AD)  numbers per group unknown	DSM-III and elimination of alternate diagnoses	<sup>133</sup> Xenon CT	full sample: 76.2 (8.0)	no	yes	no	no
Nagahama et al <sup>58</sup>	Cerebral correlates of the progression rate of the cognitive decline in probable Alzheimer's disease	2003	Shiga, Japan	52 (24 CN, 28 AD)  AD grouped by slowly and rapidly declining at follow-up	NINCDS-ADRDA and DSM-III-R	<sup>99m</sup> Tc-HMPAO SPECT	CN: 69.6 (7.2) slowly declining AD: 71.9 (1.0) rapidly declining AD: 71.6 (1.8)	no	no	no	yes
Obara et al <sup>42</sup>	Cognitive declines correlate with decreased cortical volume and perfusion in dementia of Alzheimer type	1994	Texas, USA	36 (18 CN, 18 AD)	NINCDS-ADRDA and DSM-III-R	<sup>133</sup> Xenon CT	CN: 73.7 (7.0) AD: 75.4 (5.2)	yes	yes	no	yes

Sase et al <sup>59</sup>	Discrimination Between Patients With Alzheimer Disease and Healthy Subjects Using Layer Analysis of Cerebral Blood Flow and Xenon Solubility Coefficient in Xenon-Enhanced Computed Tomography	2017	Osaka, Japan	42 (15 CN, 27 AD)	DSM IV	<sup>133</sup> Xenon CT	CN: 78.6 (4) AD: 81.7 (3.3)	no	yes	no	yes
Schuff et al <sup>60</sup>	Cerebral blood flow in ischemic vascular dementia and Alzheimer's disease, measured by arterial spin-labeling magnetic resonance imaging	2009	California, USA	32 (18 CN, 14 AD)  also a group with subcortical ischemic vascular dementia	NINCDS-ADRDA and DSM IV	ASL MRI	CN: 73 (8) AD: 74 (5)	yes	yes	no	no
Shimizu et al <sup>61</sup>	Differentiation of dementia with Lewy bodies from Alzheimer's disease using brain SPECT	2005	Tokyo, Japan	103 (28 CN, 75 AD)  also a group with dementia with Lewy bodies	NINCDS-ADRDA	<sup>123</sup> I-IMP SPECT	CN: 75.1 (6.4) AD: 75.5 (6.8)	yes	yes	no	no

Sundström et al <sup>62</sup>	Memory-provoked rCBF-SPECT as a diagnostic tool in Alzheimer's disease?	2006	Umeå, Sweden	36 (18 CN, 18 AD)	NINCDS-ADRDA	<sup>99m</sup> Tc-HMPAO SPECT	CN: 69.4 (3.9) AD: 73.2 (4.8)  CN are younger	no	yes	no	no
Takahashi et al <sup>63</sup>	Poor performance in Clock-Drawing Test associated with visual memory deficit and reduced bilateral hippocampal and left temporoparietal regional blood flows in Alzheimer's disease patients	2008	Sagami-hara, Japan	25 (2 CN, 7 MCI, 16 AD)  grouped into 11 with high scores and 14 with low scores on the Clock Drawing Test (CDT), cutoff 9 out of 10	Petersen et al criteria for MCI; NINDS-ADRDA for AD	<sup>99m</sup> Tc-ECD SPECT	high CDT score: 74.4 (6.8) low CDT score: 75.1 (10)	no	no	no	yes
Tateno et al <sup>64</sup>	Usefulness of a blood flow analyzing program 3DSRT to detect occipital hypoperfusion in dementia with Lewy bodies	2008	Sunagawa, Japan	54 (16 CN, 38 AD)  also a group with dementia with Lewy bodies	not clear; the "latest diagnostic criteria"	<sup>99m</sup> Tc-ECD SPECT	CN: 75.8 (5.6) AD: 79.0 (5.3)	yes	yes	no	no

van de Haar et al <sup>65</sup>	Neurovascular unit impairment in early Alzheimer's disease measured with magnetic resonance imaging	2016	the Netherlands	30 (16 CN, 14 MCI/AD)	Dubois criteria for MCI; NINCDS-ADRDA for AD	pCASL MRI	CN: 76.4, range 65-85 MCI/AD: 75.3, range 65-85	yes	yes	no	no
Yew & Nation <sup>66</sup>	Cerebrovascular resistance: effects on cognitive decline, cortical atrophy, and progression to dementia	2017	California, USA; ADNI	232 (112 amyloid-negative CN/MCI, 87 amyloid-positive CN/MCI, 33 AD)	NINCDS-ADRDA for AD; florbetapir PET with cutoff of SUVR 1.11 for amyloid positivity	PASL MRI	CN/MCI amyloid-negative: 69.2 (0.6) CN/MCI amyloid-positive: 73.7 (0.7) AD: 73.2 (1.2)  CN/MCI amyloid-negative group is younger	yes	yes	no	no
Yoshida et al <sup>67</sup>	Protein synthesis in the posterior cingulate cortex in Alzheimer's disease	2011	Suita, Japan	16 (8 CN, 8 AD)	NINCDS-ADRDA	<sup>123</sup> I-IMP SPECT	CN: 72.5 (5.8) AD: 73.0 (5.4)	yes	yes	no	no

Table 2. Risk of bias assessment scores for included articles. Columns display authors (A) as identification for each paper, component scores on the risk of bias assessment for: clearly stated objective (B), clearly defined sample (C), controls that come from the same population as cases (D), consistent inclusion/exclusion criteria for cases and controls (E), cases and controls clearly distinct (F), use of a reliable method to measure CBF (G), blind assessment of CBF when not automated (H), and use of confounding variables in statistical analyses (I). Finally, each paper was given an overall risk of bias assessment score of “poor”, “fair”, or “good”, and the justification for each score is given (J). A modified version of the NIH Quality Assessment of Case-Control Studies was used. Abbreviations can be found in the List of Abbreviations (p. xii).

A	B	C	D	E	F	G	H	I	J
Alegret et al <sup>45</sup>	yes	no	yes	no	yes	yes	not applicable	yes	fair; little information about samples; AD group were all taking AChEIs while the other groups were not, and most CN did not have CT to check for exclusions
Benoit et al <sup>46</sup>	yes	yes	no	not reported	not reported	yes for AD; not reported for CN	not applicable	no	poor; CN are from a different population, scanned separately but “similarly”, not clear whether the inclusion criteria is the same, and cognitive scores for the CN group are not reported
Brown et al <sup>37</sup>	yes	no	yes	yes	yes	yes	yes	no	good
Claus et al <sup>47</sup>	yes	yes	no	yes	yes	yes	yes	yes	good
Dai et al <sup>48</sup>	yes	yes	yes	yes	yes	yes	not applicable	yes	good
Ding et al <sup>49</sup>	yes	yes	not reported	yes	yes	yes	not applicable	no	fair; it is not reported whether the groups are from the same population; only CN are excluded for substance abuse
Encinas et al <sup>50</sup>	yes	yes	yes	yes	yes	yes	yes	no	good
Firbank et al <sup>39</sup>	yes	no	not reported	not reported	yes	yes	yes	no	fair; little information about sample; unclear whether population and/or inclusion criteria are the same between groups



Lee et al <sup>56</sup>	yes	no	not reported	not reported	yes	yes	not applicable	no	fair; little information given about the sample, not clear whether the groups are from the same population or if they have the same inclusion criteria
Mubrin et al <sup>57</sup>	yes	no	not reported	not reported	not reported	yes for imaging; not reported for processing	not reported	no	poor; very little information about samples, especially CN; CN does not have cognitive scores reported
Nagahama et al <sup>58</sup>	yes	yes for cases, no for controls	not reported	yes	not reported	yes	not applicable	no	poor; little information about CN, not sure if they are from the same population as AD; cognitive scores not reported for CN
Obara et al <sup>42</sup>	yes	no	not reported	no	yes	yes	not reported	yes	fair; little information about sample; not sure whether groups are from the same population; inclusion criteria differs slightly between groups
Sase et al <sup>59</sup>	yes	yes	yes	no	yes	yes	not applicable	no	fair; inclusion criteria differs slightly between groups
Schuff et al <sup>60</sup>	yes	yes	yes	yes	yes	yes	not applicable	yes	good
Shimizu et al <sup>61</sup>	yes	yes for cases, no for controls	not reported	no	not reported	yes	not applicable	no	poor; not reported whether the groups are from the same population; only AD are excluded for taking medication that affects the CNS; cognitive exam scores are not reported for CN
Sundström et al <sup>62</sup>	yes	yes	yes	yes	yes	yes	not applicable	no	poor; CN are younger than AD
Takahashi et al <sup>63</sup>	yes	yes	yes	yes	yes	yes	not applicable	no	good

Tateno et al <sup>64</sup>	yes	no	not reported	no	yes	yes	not applicable	no	fair; little information given about the sample, not clear whether the groups are from the same population; only CN have abnormalities on scans as exclusion criteria
van de Haar et al <sup>65</sup>	yes	yes	yes	no	not reported	yes	yes	yes	fair; only AD are excluded for history of stroke; CN are said to complete cognitive exams, but their scores are not reported
Yew & Nation <sup>66</sup>	yes	yes	yes	yes	yes	yes	not applicable	yes	good
Yoshida et al <sup>67</sup>	yes	yes	yes	no	yes	yes	yes	no	fair; inclusion criteria are not the same: all AD have <i>APOE</i> $\epsilon 4$ , but this is not reported for CN

Table 3. CBF in CN and AD individuals in each paper. The sample size for each group is presented for each paper. For each included brain region, it is indicated whether AD has decreased or increased CBF compared to CN, and CBF data from each paper is presented as mean (SD). The notes column defines the specific brain regions and methods used in each paper, where relevant. Abbreviations can be found in the List of Abbreviations (p. xii).

Author	Sample Size	Frontal	Parietal	Temporal	Temporo-parietal	Occipital	Posterior Cingulate	Hippocampus	Thalamus	Notes
Alegret et al <sup>45</sup>	CN: 42 AD: 42			AD < CN  CN: 667 (25) AD: 504 (26)	AD < CN  CN: 1028 (25) AD: 802 (24)		AD < CN  CN: 885 (20) AD: 696 (26)	AD < CN  CN: 716 (23) AD: 535 (22)		Values are eigenvariates from peak voxels where CBF differs between groups; SDs are adjusted for age; data extracted from bar graph. Regions are temporal: left temporal lobe and right temporal pole, temporoparietal: right angular gyrus, and right hippocampus.

Benoit et al <sup>46</sup>	CN: 11 AD: 30	AD < CN  z = 3.79 k = 1322 p = 0.008					AD < CN  z = 3.25 k = 1431 p = 0.005			Results are from comparison of the whole AD group (with and without apathy) and CN; voxels correspond to right medial frontal and right posterior cingulate regions.
Brown et al <sup>37</sup>	CN: 14 AD: 24	AD < CN  CN: 0.854 (0.040) AD: 0.796 (0.086)	AD < CN  CN: 0.890 (0.046) AD: 0.764 (0.104)	AD < CN  CN: 0.917 (0.050) AD: 0.839 (0.077)						Values are regional CBF normalized to calcarine cortex; regions are frontal: low frontal & high frontal; temporal: temporal & posterior temporal; data extracted from bar graph; significance reported with Bonferroni correction
Claus et al <sup>47</sup>	CN: 60 AD: 48	AD < CN  CN: 84.3 (5.6) AD: 80.8 (6.3)		AD < CN  CN: 83.0 (5.2) AD: 76.0 (7.1)	AD < CN  CN: 78.4 (6.8) AD: 70.5 (9.8)	AD < CN  CN: 89.2 (6.1) AD: 86.5 (6.4)				Values are percentages of regional CBF relative to cerebellar CBF; anatomical ROI multi-slice values used.

Dai et al <sup>48</sup>	CN: 38 AD: 37	AD < CN  CN: 52.6 (18.1) AD: 37.0 (11.6)	AD < CN  CN: 53.1 (19.4) AD: 38.4 (13.2)	AD < CN  CN: 51.1 (18.9) AD: 36.0 (8.7)			AD < CN  CN: 61.2 (20.5) AD: 46.4 (15.9)	AD > CN  CN: 42.1 (10.2) AD: 42.7 (13.0)	AD < CN  CN: 45.2 (18.8) AD: 36.9 (19.7)	Regions are frontal: left lateral frontal and left orbitofrontal, parietal: left interior and left superior parietal, and temporal: left superior temporal.
Ding et al <sup>49</sup>	CN: 21 AD: 24	AD > CN  t = -3.95 k = 312 p < 0.01	AD < CN  t = 3.34 k = 391 p < 0.01	AD < CN  t = 3.33 k = 340 p < 0.01		AD < CN  t = 4.77 k = 2569 p < 0.01			AD > CN  t = -3.32 k = 355 p < 0.01	Voxels are: right paracentral, right superior parietal, right middle & inferior temporal, left superior, middle & inferior occipital & cuneus, and left thalamus
Encinas et al <sup>50</sup>	stable MCI: 21 MCI progressing to AD: 21	AD < MCI  MCI: 89.8 (10) AD: 80.8 (7.8)	AD < MCI  MCI: 90.0 (8.6) AD: 82.0 (8.5)	AD < MCI  MCI: 85.0 (9.4) AD: 76.0 (9.0)	AD < MCI  MCI: 87.5 (9.1) AD: 79.5 (7.5)					Values are percentage of regional CBF over cerebellar CBF; comparisons are stable MCI vs. MCI that progress to AD, at baseline; frontal: right and left prefrontal, right and left frontal; parietal: right and left parietal; temporal: right and left temporal, left posterior lateral temporal; temporoparietal: right and left frontoparietotemporal

Firbank et al <sup>39</sup>	CN: 29 AD: 17	AD < CN  CN: 1.82 (0.27) AD: 1.58 (0.28)	AD < CN  CN: 1.70 (0.32) AD: 1.34 (0.31)			AD < CN  CN: 1.55 (0.27) AD: 1.47 (0.29)			AD < CN  CN: 2.68 (1.08) AD: 2.28 (0.71)	Values are GM:WM ratio; one control does not have data for thalamus; statistics are Gabriel post hoc tests; frontal: prefrontal.
Hanyu et al <sup>33</sup>	CN: 22 AD: 22	AD < CN AD: 1.04 (0.47)			AD < CN AD: 1.48 (0.55)	AD < CN AD: 0.95 (0.51)	AD < CN AD: 1.2 (0.5)			Values are z scores normalized to CN values
Hanyu et al <sup>51</sup>	CN: 28 AD: 53	AD < CN  AD: 0.98 (0.55)	AD < CN  AD: 1.20 (0.70)	AD < CN AD: 0.98 (0.61)	AD < CN AD: 1.43 (1.07)	AD < CN AD: 0.77 (0.77)	AD < CN AD: 0.99 (0.52)		AD < CN AD: 0.46 (0.47)	Values are z scores normalized to CN values; combined high and low education AD groups; frontal: superior, middle, inferior, medial, orbital frontal; parietal: superior and inferior parietal; temporal: superior, middle, inferior, and transverse temporal; temporoparietal: supramarginal and angular gyri; occipital: superior, middle, and inferior occipital.

Harris et al <sup>44</sup>	CN: 8 AD: 15	AD < CN  CN: 101.6 (8.8) AD: 91.7 (10.7)			AD < CN  CN: 105.8 (8.2) AD: 89.4 (11.9)	AD < CN  CN: 106.0 (8.9) AD: 97.6 (11.3)				All regions are combined from two slices: at basal ganglia level and superior to it
Iizuka & Kameyama <sup>52</sup>	CN: 9 AD: 36	AD < CN	AD < CN	AD < CN			AD < CN			Results were qualitative in the text and presented in a brain surface figure with a color scale, but it was not feasible to accurately extract values based on color. Comparisons were at baseline and were present in CN vs. responding and/or nonresponding AD before treatment began.
Jagust et al <sup>53</sup>	CN: 5 AD: 9	AD > CN  CN: 1.11 (0.09) AD: 1.16 (0.08)			AD < CN  CN: 1.10 (0.05) AD: 0.93 (0.04)					Values are regional CBF over whole tomographic slice;

Johnson et al <sup>54</sup>	CN: 19 AD: 34	AD < CN z = 3.59 k = 214 corr. p < 0.05	AD < CN z = 5.20 k = 6629 corr. p < 0.05	AD < CN z = 4.01 k = 2117 corr. p < 0.05			AD < CN z = 4.87 k = 862 corr. p < 0.05		AD > CN z = -4.42 k = 1184 corr. p < 0.05	Voxels are located in: left inferior frontal, left inferior parietal, right superior temporal, right posterior cingulate, and left thalamus & striatum; p values are corrected for multiple comparisons.
Kimura et al <sup>35</sup>	CN: 27 AD: 62		AD < CN CN: 35.4 (4.3) AD: 30.5 (5.2)	AD < CN CN: 35.3 (3.6) AD: 30.8 (4.7)	AD < CN CN: 40.4 (4.6) AD: 34.5 (5.9)		AD < CN CN: 41.3 (5.1) AD: 35.9 (5.5)			Regions are: left superior and inferior parietal, left and right middle and inferior temporal, right angular gyrus, and left and right posterior cingulate
Lacalle-Aurioles et al <sup>55</sup>	CN: 20 AD: 28		AD < CN CN: 0.849 (0.032) AD: 0.812 (0.051)	AD > CN CN: 0.778 (0.063) AD: 0.828 (0.069)						Values are regional CBF over whole cortical GM CBF; data was extracted from graphs; regions are: left and right parietal lobe, right medial temporal lobe.
Lee et al <sup>56</sup>	CN: 20 AD: 20	AD < CN z = 4.64 corr. p = 0.007	AD < CN z = 6.87 corr. p < 0.001	AD < CN z = 6.94 corr. p < 0.001						Used moderate AD as the AD group; voxels come from: left middle frontal, right superior parietal, and right superior temporal; cluster sizes not reported; p values corrected for multiple testing.

Mubrin et al <sup>57</sup>	CN: not clear AD: 31		AD < CN		AD < CN					Results are qualitative only; both regions are bilateral.
Obara et al <sup>42</sup>	CN: 18 AD: 17	AD < CN  CN: 42.3 (9.4) AD: 37.5 (4.4)	AD < CN  CN: 43.1 (6.9) AD: 37.7 (4.9)	AD < CN  CN: 43.1 (7.6) AD: 38.2 (6.1)		AD < CN  CN: 39.5 (8.8) AD: 35.9 (4.7)			AD < CN  CN: 51.8 (10.7) AD: 47.0 (9.4)	
Sase et al <sup>59</sup>	CN: 15 AD: 27									This paper measures CBF in 5 mm layers from the surface of the brain. AD < CN in cingulate cortex and in every layer measured; measurements of layers were taken from lateral, superior, anterior, and posterior views. The greatest differences were found in the left lateral view of the third and fourth layers.
Schuff et al <sup>60</sup>	CN: 18 AD: 14	AD < CN  CN: 56.4 (7.9) AD: 41.2 (10.9)	AD < CN  CN: 58.7 (9.8) AD: 43.6 (11.7)	AD < CN  CN: 52.7 (19.1) AD: 45.5 (15.2)						

Shimizu et al <sup>61</sup>	CN: 28 AD: 75	AD < CN AD: 1.08 (0.35)	AD < CN AD: 1.39 (0.55)	AD < CN AD: 1.40 (0.65)		AD < CN AD: 0.90 (0.43)				Values are z scores normalized to CN values
Sundström et al <sup>62</sup>	CN: 18 AD: 18	AD < CN	AD < CN	AD < CN						Voxel-wise comparison are presented graphically but not numerically; frontal region is mainly middle frontal
Tateno et al <sup>64</sup>	CN: 16 AD: 38		AD < CN CN: 42.2 (3.5) AD: 37.2 (3.9)	AD < CN CN: 36.8 (5.3) AD: 33.7 (4.1)	AD < CN CN: 45.2 (4.0) AD: 38.5 (4.9)			AD < CN CN: 30.4 (5.2) AD: 26.3 (3.1)	AD < CN CN: 39.3 (7.2) AD: 34.4 (5.7)	Values were extracted from bar graphs; the temporoparietal data is from the angular gyrus
van de Haar et al <sup>65</sup>	CN: 16 MCI/A D: 14	MCI/A D < CN  CN: 38.9 (7.2) MCI/A D: 33.3 (7.6)	MCI/AD < CN  CN: 39.6 (6.7) MCI/AD : 32.4 (7.4)	MCI/AD < CN  CN: 36.8 (6.2) MCI/AD: 31.1 (7.6)		MCI/AD < CN  CN: 37.9 (8.3) MCI/AD : 30.7 (9.1)				The AD group includes MCI

Yew & Nation <sup>66</sup>	CN: 87 AD: 33	AD < CN CN: 23.2 (3.7) AD: 21.5 (6.2)	AD < CN CN: 30.2 (4.7) AD: 26.3 (7.5)	AD < CN CN: 23.4 (5.2) AD: 21.4 (7.5)				AD < CN CN: 28.0 (5.2) AD: 24.7 (6.9)		The CN are amyloid-positive; data extracted from bar graph; regions are frontal: medial orbital and rostral middle frontal, inferior temporal, and inferior parietal
Yoshida et al <sup>67</sup>	CN: 8 AD: 8	AD > CN CN: 0.80 (0.06) AD: 0.82 (0.09)	AD < CN CN: 0.84 (0.08) AD: 0.79 (0.11)	AD < CN CN: 0.76 (0.03) AD: 0.63 (0.11)			AD < CN CN: 0.84 (0.11) AD: 0.60 (0.11)			Values are regional CBF: occipital cortex CBF ratios; the temporal region is the medial temporal lobe.

Table 4. CBF in CN and MCI individuals in each paper. The sample size for each group is presented for each paper. For each included brain region, it is indicated whether MCI has decreased or increased CBF compared to CN, and CBF data from each paper is presented as mean (SD). The notes column defines the specific brain regions and methods used in each paper, where relevant. Abbreviations can be found in the List of Abbreviations (p. xii).

Author	Sample Size	Frontal	Parietal	Temporal	Temporo-parietal	Occipital	Posterior Cingulate	Hippocampus	Thalamus	Notes
Alegret et al <sup>45</sup>	CN: 42 MCI: 42			MCI < CN CN: 667 (25) MCI: 567 (26)	MCI < CN CN: 1028 (25) MCI: 874 (24)		MCI < CN CN: 885 (20) MCI: 739 (26)	AD < CN CN: 716 (23) MCI: 587 (26)		Values are eigenvariates from peak voxels where CBF differs between CN and AD; SDs are adjusted for age; data extracted from bar graph. Regions are temporal: left temporal lobe and right temporal pole, temporoparietal: right angular gyrus, and right hippocampus.
Dai et al <sup>48</sup>	CN: 38 MCI: 29	MCI < CN CN: 52.6 (18.1) MCI: 50.5 (19.6)	MCI > CN CN: 53.1 (19.4) MCI: 53.4 (18.3)	MCI < CN CN: 51.1 (18.9) MCI: 44.8 (15.6)			MCI < CN CN: 61.2 (20.5) MCI: 47.7 (15.8)	MCI > CN CN: 42.1 (10.2) MCI: 59.6 (17.3)	MCI > CN CN: 45.2 (18.8) MCI: 54.6 (25.4)	Regions are frontal: left lateral frontal and left orbitofrontal, parietal: left interior and left superior parietal, and temporal: left superior temporal.

Ding et al <sup>49</sup>	CN: 21 MCI: 17		MCI < CN  t = 3.83 k = 298 p < 0.01	MCI < CN  t = 3.71 k = 363 p < 0.01		MCI < CN  t = 3.51 k = 350 p < 0.01				Voxels are from: right superior parietal lobule, right middle temporal gyrus, and left cuneus (occipital).
Johnson et al <sup>54</sup>	CN: 19 Decliners: 43					Decliners < CN z = 4.46 p < 0.02				CBF measured at baseline; decliners did not differ cognitively from CN at baseline, but their cognition declined over the following 4 years. Region is right posterior cingulate; cluster size not reported.
Lacalle-Aurioles et al <sup>55</sup>	CN: 20 MCI: 15		MCI > CN  CN: 0.849 (0.032) MCI: 0.855 (0.013)	MCI > CN  CN: 0.778 (0.063) MCI: 0.780 (0.020)						Values are regional CBF over whole cortical GM CBF; data was extracted from graphs; regions are: left and right parietal lobe, right medial temporal lobe.

Table 5. Relationships between CBF and cognition in each paper. For each paper, the sample size column reports the number of individuals and the diagnostic groups included in the CBF and cognition correlation analyses. Abbreviations can be found in the List of Abbreviations (p. xii).

	Sample Size	Correlation between CBF and Cognition	Notes
Alegret et al <sup>45</sup>	126 (CN, MCI, & AD)	CBF in posterior cingulate ( $r = 0.72, p < 0.001$ ) and right temporal pole ( $r = 0.68, p < 0.001$ ) is positively correlated with MMSE score. CBF in posterior cingulate ( $r = 0.55, p < 0.001$ ) and right temporal pole ( $r = 0.48, p < 0.001$ ) is positively correlated with 15-Objects Test score. CBF in posterior cingulate ( $r = 0.46, p < 0.001$ ) and right temporal pole ( $r = 0.40, p < 0.001$ ) is positively correlated with 15 item Boston Naming Test score. CBF in posterior cingulate ( $r = 0.37, p < 0.001$ ) and right temporal pole ( $r = 0.34, p < 0.001$ ) is positively correlated with Poppelreuter test score.	Relationship assessed across all participants; CBF measures are eigenvariates from the named regions.
Benoit et al <sup>46</sup>	30 AD (with and without apathy)	CBF in bilateral lateral parietal cortex is positively correlated with MMSE score. Significant clusters right: ( $z = 3.73, p = 0.015$ ), left: ( $z = 3.64, p = 0.010$ ).	Analysis was voxel-wise. Using the apathy score on the Neuropsychiatric Inventory as a covariate in the correlation did not change the results.
Brown et al <sup>37</sup>	24 AD	Longitudinal change in CAMCOG score is positively correlated with longitudinal change in CBF in right and left low frontal ( $r = 0.69; r = 0.74$ ) and right temporal regions ( $r = 0.62$ ). All $p < 0.05$ ; left low frontal $p < 0.05$ after Bonferroni correction.	Frontal and temporal CBF was positively correlated with language, praxis, and abstraction, but not memory CAMCOG sub-scores in this paper.
Firbank et al <sup>39</sup>	46 (CN and AD)	Global GM/WM CBF does not contribute to the variation in CAMCOG-R score when age, sex, and hippocampal volume are predictors in the model.	
Jagust et al <sup>53</sup>	9 AD	The ratio of CBF in the temporoparietal region: whole tomographic slice is positively correlated with MMSQ score ( $r = 0.81, p < 0.01$ ).	

Johnson et al <sup>54</sup>	124 CN/ MCI	CBF in rostral anterior cingulate and inferior frontal regions was positively correlated with scores on Trailmaking Test Part B ( $p < 0.05$ ), while CBF in caudal anterior cingulate was negatively correlated with scores on the same test ( $p < 0.006$ ). No correlations were seen between anterior cingulate CBF and the California Verbal Learning Test or Self-Ordering Test, or between posterior cingulate CBF and any of the three tests.	
Nagahama et al <sup>58</sup>	28 AD, both rapidly and slowly progressing	CBF in right middle ( $z=4.67$ , $k=458$ , $p<0.001$ ) and superior frontal gyrus ( $z=3.05$ , $k=8$ , $p<0.01$ ) and right inferior parietal cortex ( $z=3.27$ , $k=332$ , $p<0.001$ ) is decreased in patients that decline rapidly compared to those that decline slowly, meaning that their MMSE score declines less than 4 points over 2 to 3 years of follow-up.	Results reported from voxel-wise analysis.
Obara et al <sup>42</sup>	17 AD	Declines in parietal cortical CBF add to the prediction of cognitive decline on the CCSE ( $p = 0.015$ ) when other predictors are decline in cortical volumes and decline in subcortical densities.	CBF, cognition, and tissue volumes and densities were measured every 6 to 12 months for between 2 and 3 years on average.
Sase et al <sup>59</sup>	42 (CN and AD)	CBF: lambda ratio in the third ( $r = 0.66$ , $p < 0.0001$ ) and fourth ( $r = 0.68$ , $p < 0.0001$ ) layer left lateral views is positively correlated with MMSE scores.	Lambda is the Xenon solubility coefficient. CBF and CBF:lambda ratio were decreased in AD compared to CN in this paper.
Takahashi et al <sup>63</sup>	25 (CN, MCI, and AD)	Clock Drawing Test scores are positively correlated with CBF in the left hippocampus ( $\rho = 0.43$ , $p < 0.05$ ), left parietal ( $\rho = 0.37$ ), bilateral pericallosal ( $\rho = 0.35$ ; $0.32$ ), and bilateral angular regions ( $\rho = 0.38$ ; $0.35$ ).	Correlation coefficients are Spearman's rho. Those without p values did not reach significance. Areas that with correlations less than $\rho = 0.32$ were: callosomarginal, precentral, central, right parietal, temporal, posterior, lenticular nucleus, thalamus, right hippocampus, and cerebellum.

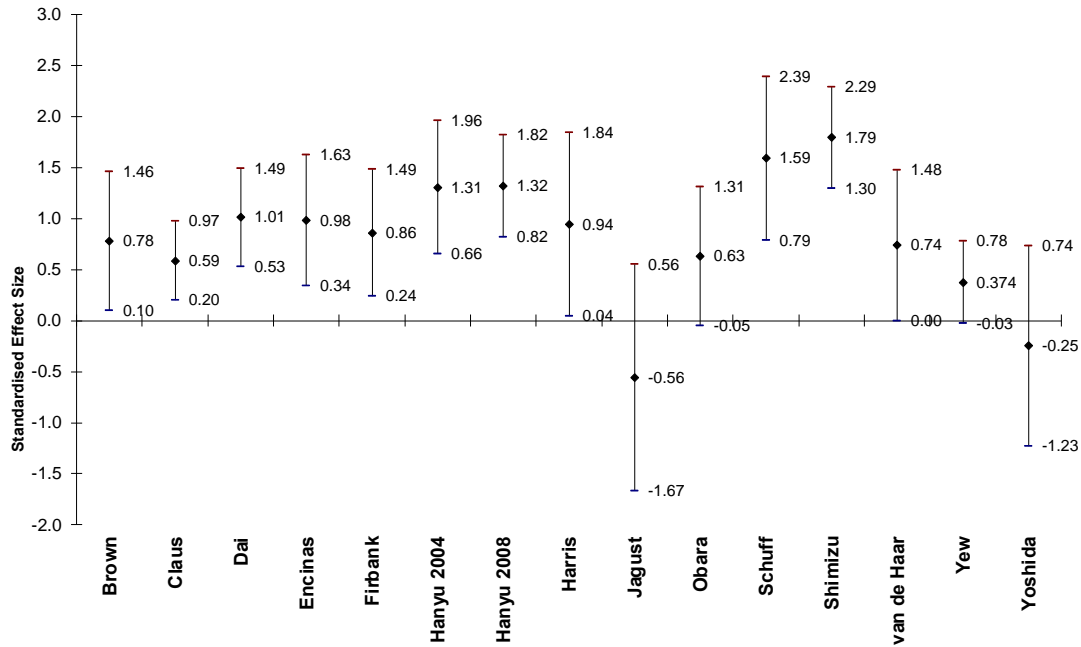


Figure 2. Effect sizes and 95% confidence intervals of frontal lobe CBF in AD relative to CN. Positive effect sizes indicate that CBF is decreased in AD relative to CN. Of 15 papers, 13 reported decreased CBF in AD and two reported increased CBF in AD.

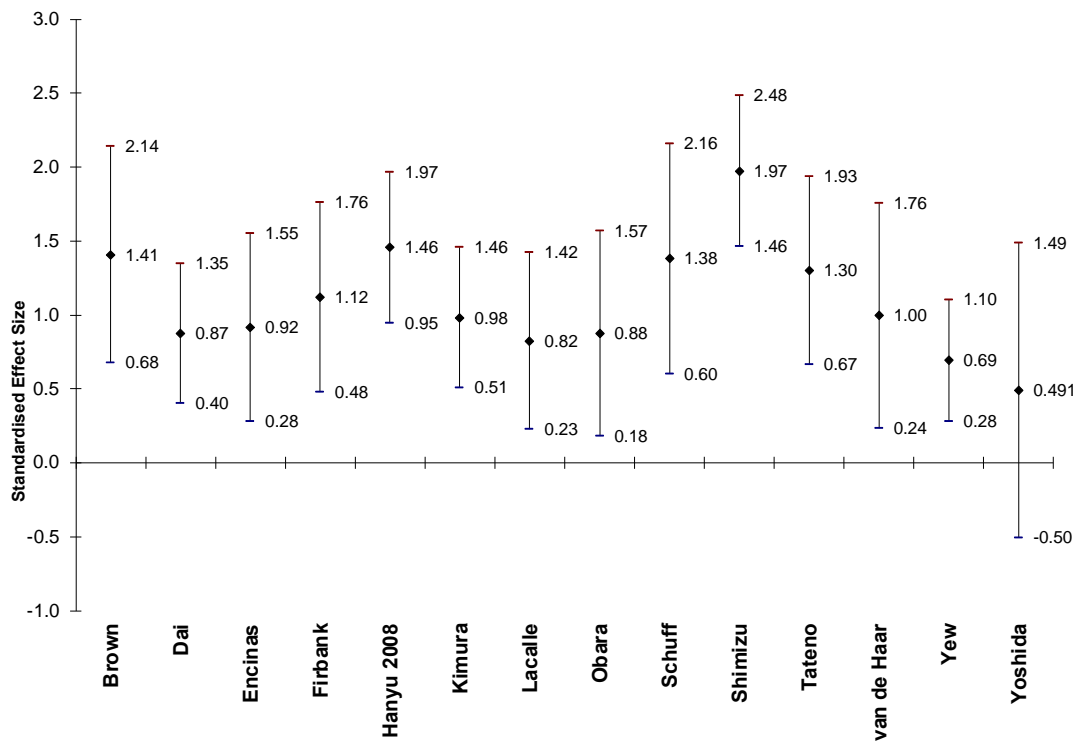


Figure 3. Effect sizes and 95% confidence intervals of parietal lobe CBF in AD relative to CN. Positive effect sizes indicate that CBF is decreased in AD relative to CN. Of 14 papers, all 14 reported decreased CBF in AD.

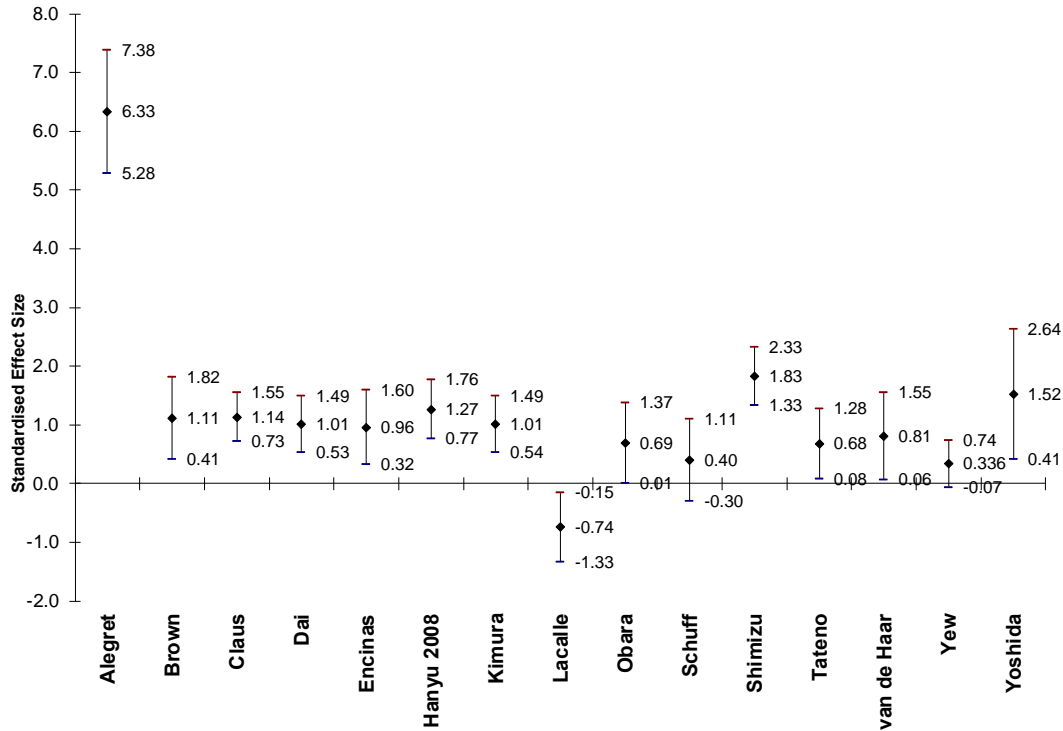


Figure 4. Effect sizes and 95% confidence intervals of temporal lobe CBF in AD relative to CN. Positive effect sizes indicate that CBF is decreased in AD relative to CN. Of 14 papers, 13 reported decreased CBF in AD and one reported increased CBF in AD.

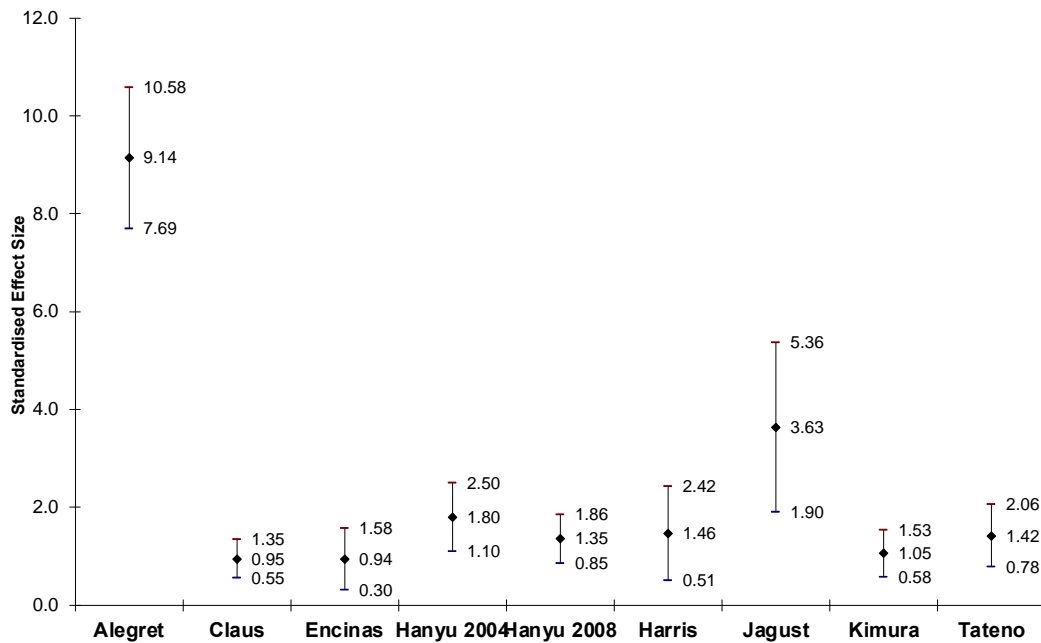


Figure 5. Effect sizes and 95% confidence intervals of temporoparietal CBF in AD relative to CN. Positive effect sizes indicate that CBF is decreased in AD relative to CN. Of nine papers, all nine reported decreased CBF in AD.

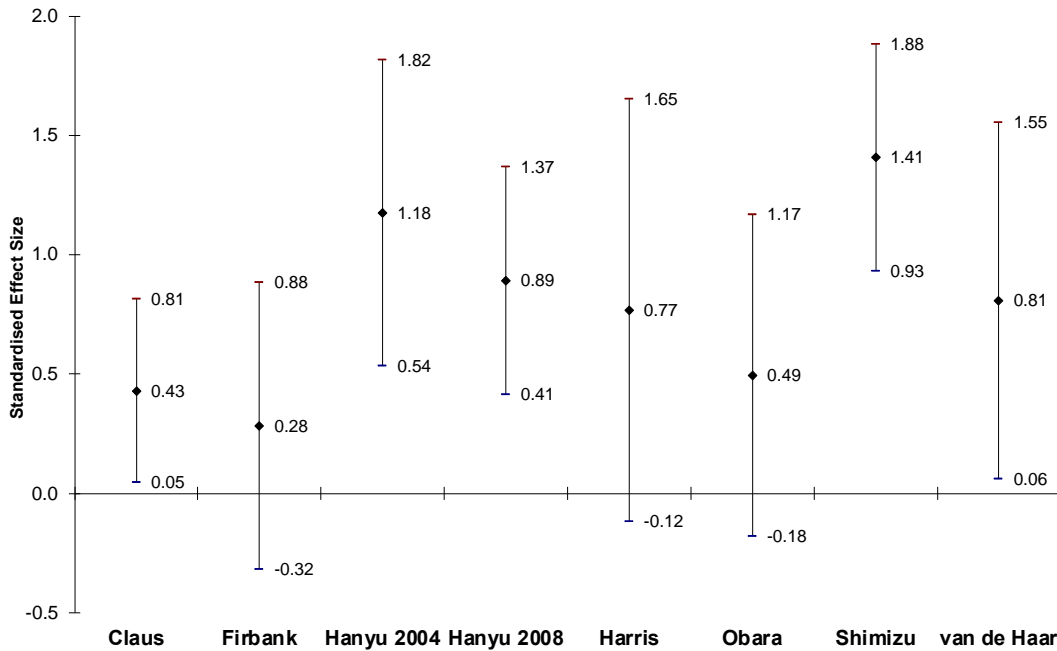


Figure 6. Effect sizes and 95% confidence intervals of occipital lobe CBF in AD relative to CN. Positive effect sizes indicate that CBF is decreased in AD relative to CN. Of eight papers, all eight reported decreased CBF in AD.

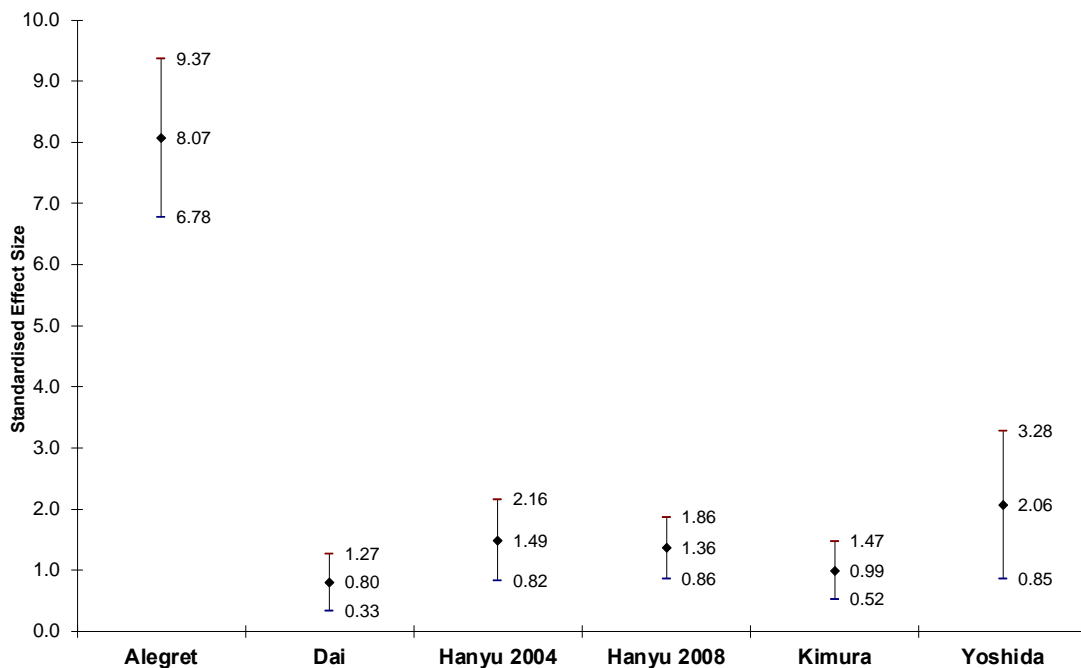


Figure 7. Effect sizes and 95% confidence intervals of posterior cingulate CBF in AD relative to CN. Positive effect sizes indicate that CBF is decreased in AD relative to CN. Of six papers, all six reported decreased CBF in AD.

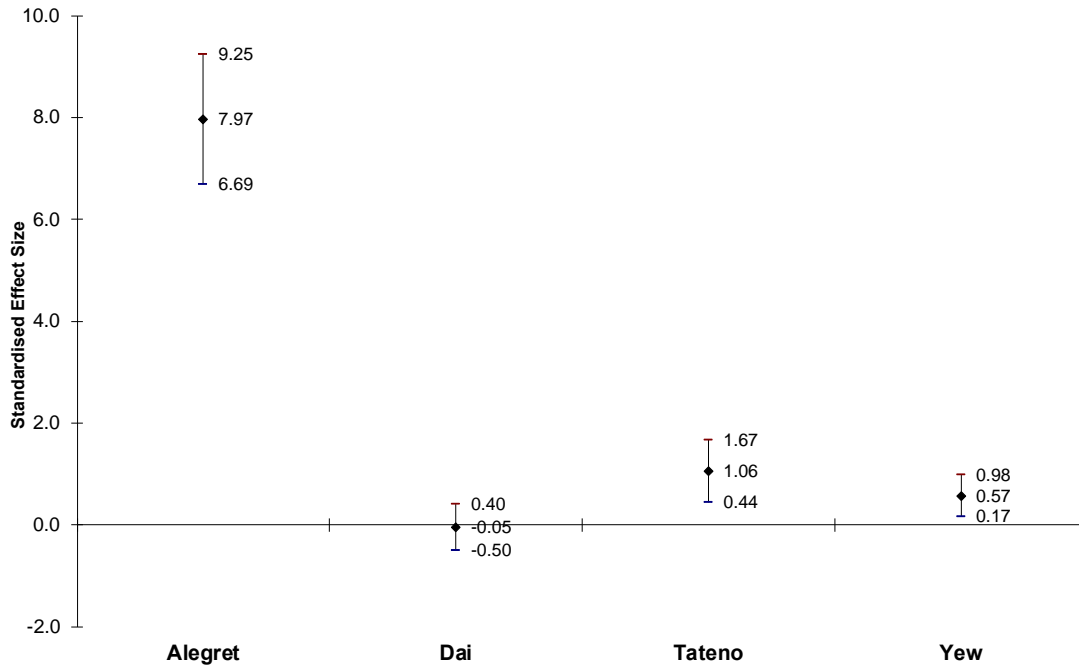


Figure 8. Effect sizes and 95% confidence intervals of hippocampal CBF in AD relative to CN. Positive effect sizes indicate that CBF is decreased in AD relative to CN. Of four papers, three reported decreased CBF in AD and one reported no difference between AD and CN.

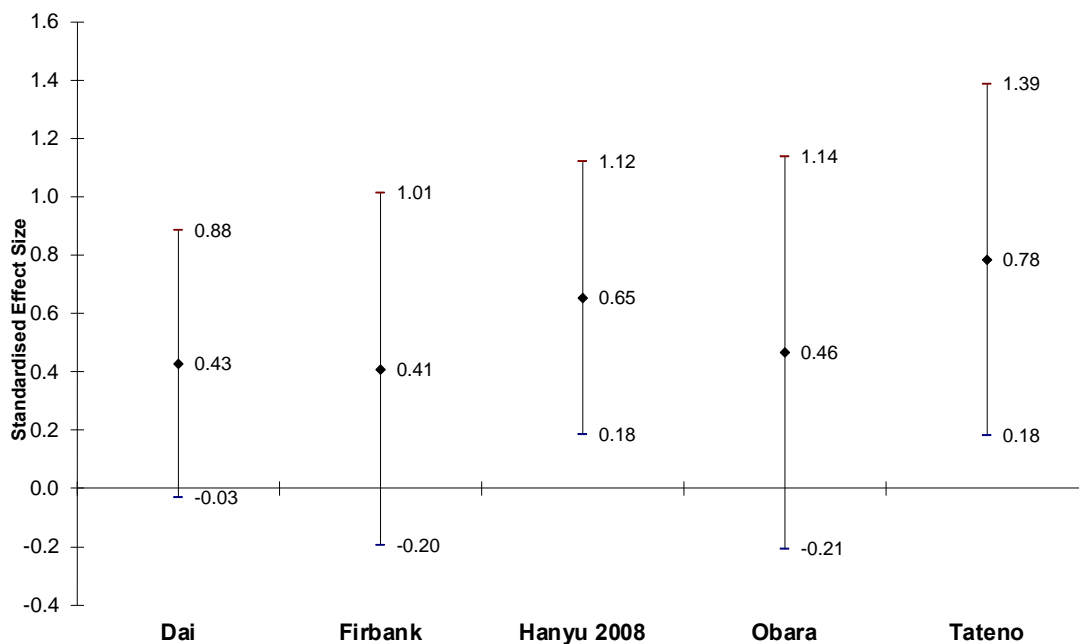


Figure 9. Effect sizes and 95% confidence intervals of thalamic CBF in AD relative to CN. Positive effect sizes indicate that CBF is decreased in AD relative to CN. Of five papers, all five reported decreased CBF in AD.

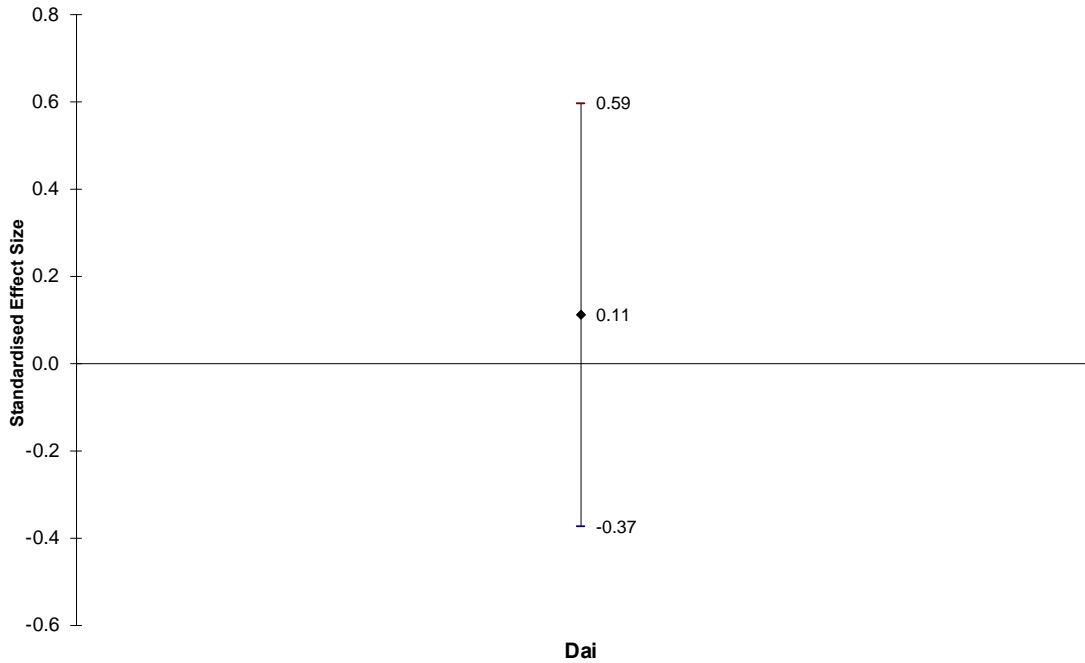


Figure 10. Effect sizes and 95% confidence intervals of frontal lobe CBF in MCI relative to CN. Positive effect sizes indicate that CBF is decreased in MCI relative to CN. One paper reported decreased CBF in MCI.

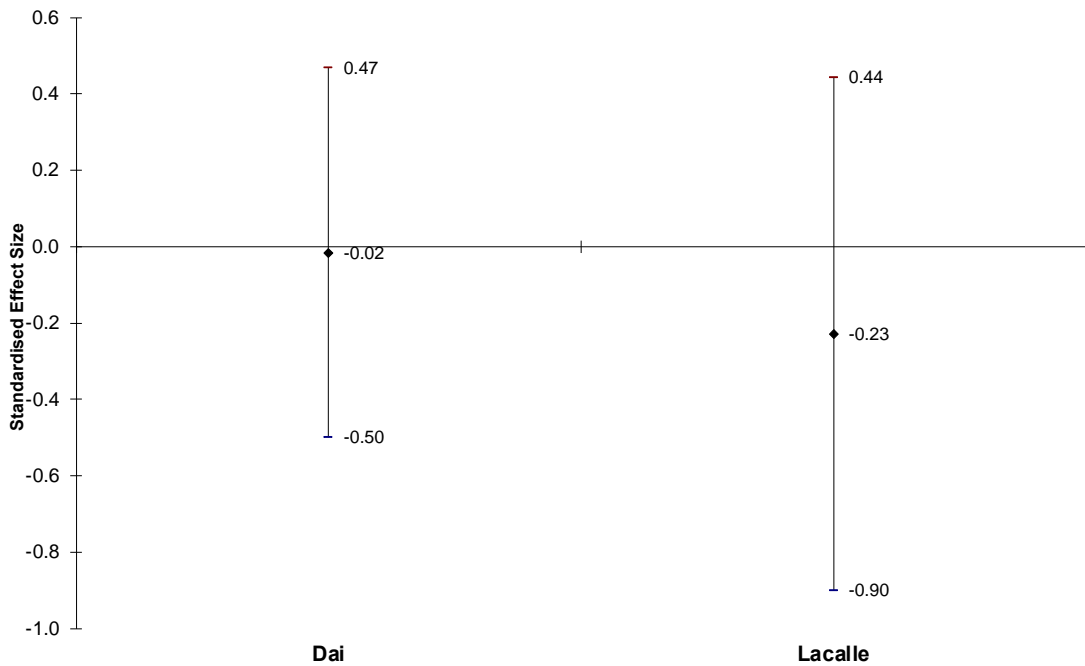


Figure 11. Effect sizes and 95% confidence intervals of parietal lobe CBF in MCI relative to CN. Positive effect sizes indicate that CBF is decreased in MCI relative to CN. Of two papers, one reported decreased CBF in MCI and one reported no difference between MCI and CN.

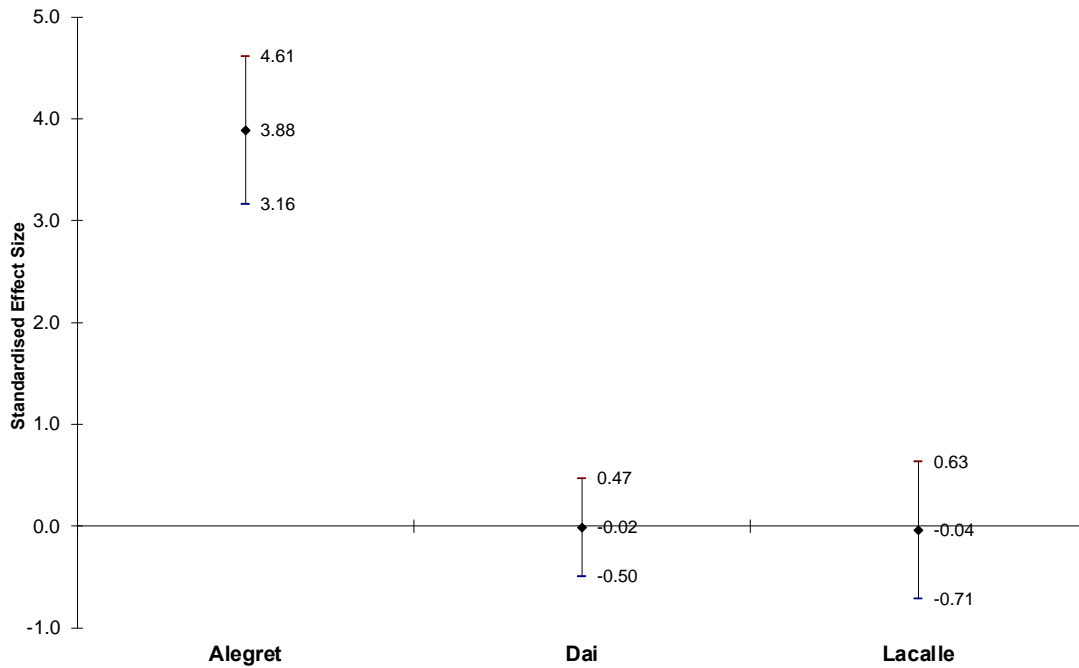


Figure 12. Effect sizes and 95% confidence intervals of temporal lobe CBF in MCI relative to CN. Positive effect sizes indicate that CBF is decreased in MCI relative to CN. Of three papers, one reported decreased CBF in MCI and two reported no difference between MCI and CN.

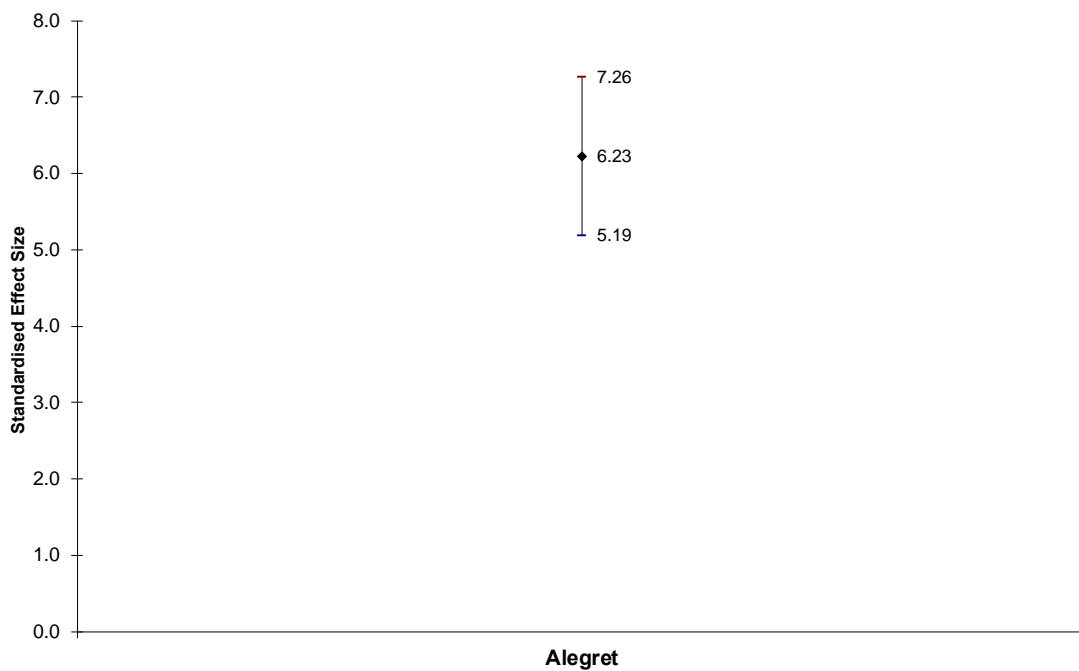


Figure 13. Effect sizes and 95% confidence intervals of temporoparietal CBF in MCI relative to CN. Positive effect sizes indicate that CBF is decreased in MCI relative to CN. One paper reported decreased CBF in MCI.

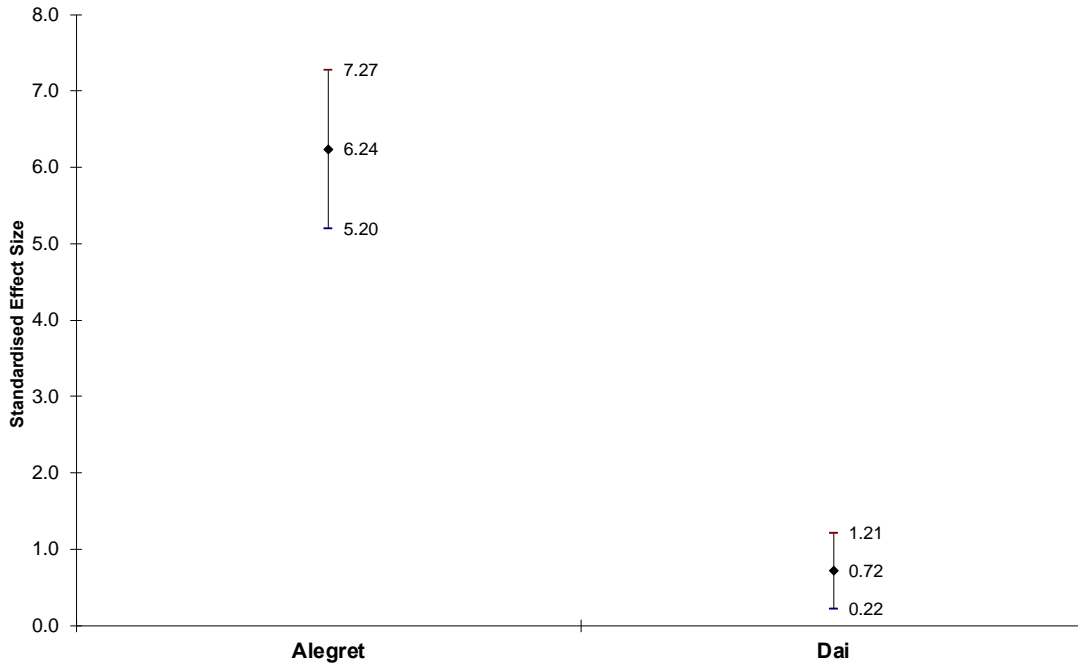


Figure 14. Effect sizes and 95% confidence intervals of posterior cingulate CBF in MCI relative to CN. Positive effect sizes indicate that CBF is decreased in MCI relative to CN. Of two papers, both reported decreased CBF in MCI.

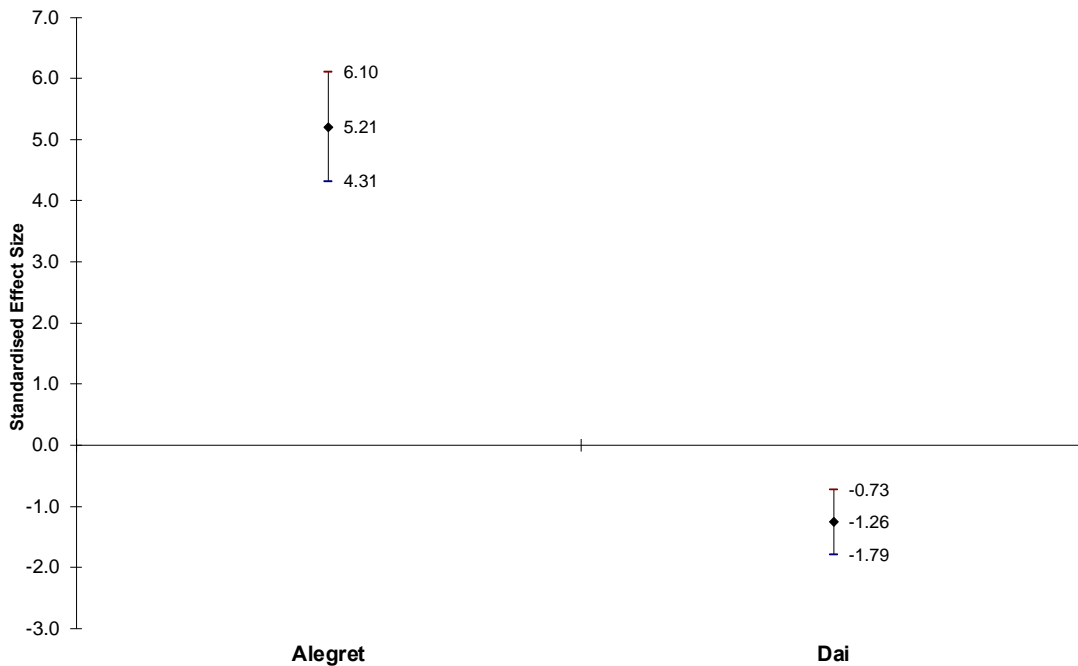


Figure 15. Effect sizes and 95% confidence intervals of hippocampal CBF in MCI relative to CN. Positive effect sizes indicate that CBF is decreased in MCI relative to CN. Of two papers, one reported decreased CBF in MCI and one reported increased CBF in MCI.

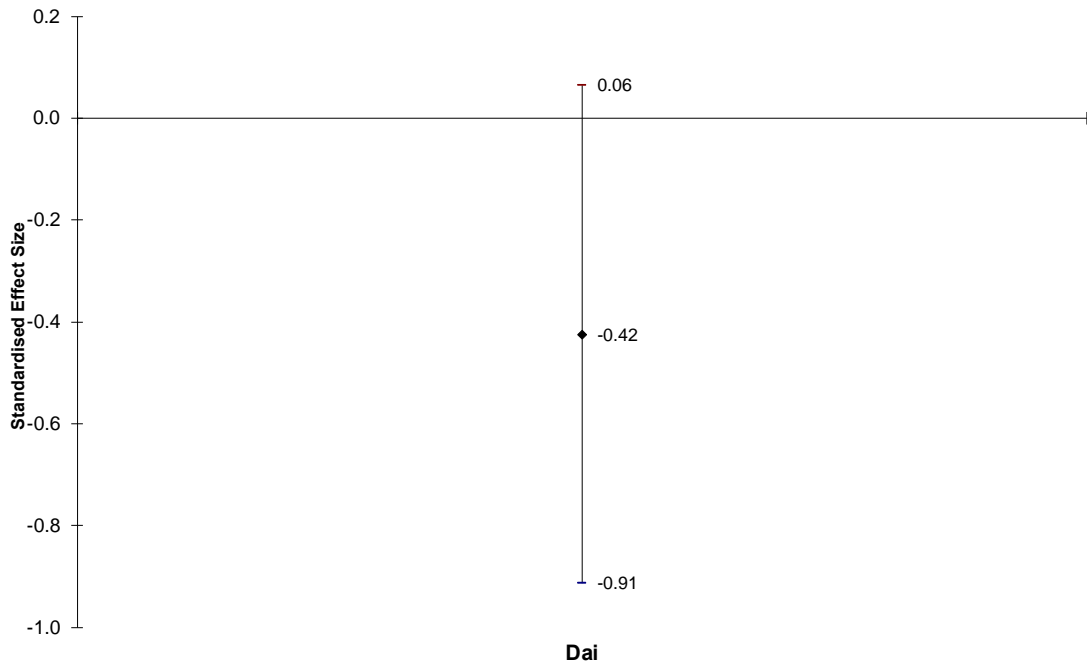


Figure 16. Effect sizes and 95% confidence intervals of thalamic CBF in MCI relative to CN. Positive effect sizes indicate that CBF is decreased in MCI relative to CN. One paper reported increased CBF in MCI.

Table 6. Syntheses of CBF in AD compared to CN by brain region. For each synthesis, the total number of individuals by diagnostic group, number of and authors of studies included, the mean, median and range of Hedge's G effect size across included studies, the overall certainty of the synthesized results, and reasons for the certainty score are presented. The mean and median effect sizes indicated that CBF is decreased in AD compared to CN in all included brain regions. The greatest decreases were found in the temporoparietal region and posterior cingulate. Abbreviations can be found in the List of Abbreviations (p. xii).

Brain Region	Individuals	Studies	Hedge's G; Mean, Median and Range	Certainty	Comments
Frontal	386 cases; 379 controls	14: Brown et al, <sup>37</sup> Claus et al, <sup>47</sup> Dai et al, <sup>48</sup> Firbank et al, <sup>39</sup> Hanyu et al, <sup>33</sup> , Hanyu et al, <sup>51</sup> Harris et al, <sup>44</sup> Jagust et al, <sup>53</sup> Obara et al, <sup>42</sup> Schuff et al, <sup>60</sup> Shimizu et al, <sup>61</sup> van de Haar et al, <sup>65</sup> Yew and Nation, <sup>66</sup> Yoshida et al <sup>67</sup>	0.79; 0.82 (-0.56, 1.79)	low	Certainty lowered because: data extracted from graphs (Brown et al, <sup>37</sup> Jagust et al, <sup>53</sup> Yew and Nation <sup>66</sup> ), several subregions and high and low education groups combined in Hanyu et al, <sup>51</sup> subregions combined in Brown et al, <sup>37</sup> Harris et al <sup>44</sup> ; Notes: two papers with increase in AD (Jagust et al <sup>53</sup> and Yoshida et al <sup>67</sup> ) have very small sample sizes, van de Haar et al <sup>65</sup> has MCI in AD group and Yew and Nation <sup>66</sup> has MCI in CN group. All AD in Yoshida et al <sup>67</sup> are <i>APOE</i> ε4 positive.

Parietal	420 cases; 347 controls	13: Brown et al, <sup>37</sup> Dai et al, <sup>48</sup> Firbank et al, <sup>39</sup> Hanyu et al, <sup>51</sup> Kimura et al, <sup>35</sup> Lacalle-Aurioles et al, <sup>55</sup> Obara et al, <sup>42</sup> Schuff et al, <sup>60</sup> Shimizu et al, <sup>61</sup> Tateno et al, <sup>64</sup> van de Haar et al, <sup>65</sup> Yew and Nation, <sup>66</sup> Yoshida et al <sup>67</sup>	1.11; 1.00 (0.49, 1.97)	moderate	Certainty lowered because: data extracted from graphs (Brown et al, <sup>37</sup> Lacalle-Aurioles et al, <sup>55</sup> Tateno et al, <sup>64</sup> Yew and Nation <sup>66</sup> ), several subregions and high and low education groups combined in Hanyu et al, <sup>51</sup> subregions combined in Brown et al. <sup>37</sup> Notes: van de Haar et al <sup>65</sup> has MCI in AD group and Yew and Nation <sup>66</sup> has MCI in CN group, all AD in Yoshida et al <sup>67</sup> are <i>APOE</i> $\epsilon$ 4 positive.
Temporal	451 cases; 378 controls	13: Brown et al, <sup>37</sup> Claus et al, <sup>47</sup> Dai et al, <sup>48</sup> Hanyu et al, <sup>51</sup> Kimura et al, <sup>35</sup> Lacalle-Aurioles et al, <sup>55</sup> Obara et al, <sup>42</sup> Schuff et al, <sup>60</sup> Shimizu et al, <sup>61</sup> Tateno et al, <sup>64</sup> van de Haar et al, <sup>65</sup> Yew and Nation, <sup>66</sup> Yoshida et al <sup>67</sup>	0.85; 1.01 (-0.74, 1.83)	moderate	Certainty lowered because: data extracted from graphs (Brown et al, <sup>37</sup> Lacalle-Aurioles et al, <sup>55</sup> Tateno et al, <sup>64</sup> Yew and Nation <sup>66</sup> ), several subregions and high and low education groups combined in Hanyu et al, <sup>51</sup> subregions combined in Brown et al <sup>37</sup> ; Notes: one paper with increase in AD (Lacalle-Aurioles et al <sup>55</sup> ) shows same pattern to a lesser extent in MCI; van de Haar et al <sup>65</sup> has MCI in AD group and Yew and Nation <sup>66</sup> has MCI in CN group, all AD in Yoshida et al <sup>67</sup> are <i>APOE</i> $\epsilon$ 4 positive.
Temporo- parietal	247 cases; 166 controls	7: Claus et al, <sup>47</sup> Hanyu et al, <sup>33</sup> Hanyu et al, <sup>51</sup> Harris et al, <sup>44</sup> Jagust et al, <sup>53</sup> Kimura et al, <sup>35</sup> Tateno et al <sup>64</sup>	1.67; 1.42 (0.95, 3.63)	moderate	Certainty lowered because: data extracted from graphs (Jagust et al, <sup>53</sup> Tateno et al <sup>64</sup> ), several subregions and high and low education groups combined in Hanyu et al, <sup>51</sup> subregions combined in Harris et al <sup>44</sup> ; Notes: Jagust et al <sup>53</sup> had the largest effect size despite a small sample size, and this paper also showed a positive correlation between CBF and cognitive scores.

Occipital	261 cases; 209 controls	8: Claus et al, <sup>47</sup> Firbank et al, <sup>39</sup> Hanyu et al, <sup>33</sup> Hanyu et al, <sup>51</sup> Harris et al, <sup>44</sup> Obara et al, <sup>42</sup> Shimizu et al, <sup>61</sup> van de Haar et al <sup>65</sup>	0.78; 0.79 (0.28, 1.41)	low	Certainty lowered due to low cumulative bias rating of constituent papers, several subregions and high and low education groups combined in Hanyu et al, <sup>51</sup> subregions combined in Harris et al <sup>44</sup> ; Notes: van de Haar et al <sup>65</sup> has MCI in AD group.
Posterior Cingulate	182 cases; 123 controls	5: Dai et al, <sup>48</sup> Hanyu et al, <sup>33</sup> Hanyu et al, <sup>51</sup> Kimura et al, <sup>35</sup> Yoshida et al <sup>67</sup>	1.34; 1.36 (0.80, 2.06)	low	Certainty lowered due to low cumulative bias rating of constituent papers, several subregions and high and low education groups combined in Hanyu et al <sup>51</sup> ; Notes: all AD in Yoshida et al <sup>67</sup> are <i>APOE</i> $\epsilon$ 4 positive.
Hippoc- ampus	108 cases; 141 controls	3: Dai et al, <sup>48</sup> Tateno et al, <sup>64</sup> Yew and Nation <sup>66</sup>	0.53; 0.57 (-0.05, 1.06)	low	Certainty lowered because: data extracted from graphs (Tateno et al, <sup>64</sup> Yew and Nation <sup>66</sup> ); Notes: one paper with increase in AD (Dai et al <sup>48</sup> ) shows similar pattern in MCI, but the effect is very small in AD. Yew and Nation <sup>66</sup> has MCI in CN group..
Thalamus	162 cases; 129 controls	5: Dai et al, <sup>48</sup> Firbank et al, <sup>39</sup> Hanyu et al, <sup>51</sup> Obara et al, <sup>42</sup> Tateno et al <sup>64</sup>	0.55; 0.46 (0.41, 0.78)	moderate	Certainty lowered due to low cumulative bias rating of constituent papers, data extracted from graphs (Tateno et al <sup>64</sup> ), several subregions and high and low education groups combined in Hanyu et al <sup>51</sup> ; Notes: Firbank et al <sup>39</sup> is missing this region for one control.

## Chapter 2: Regional Cerebral Blood Flow is Related to Hypertensive Status and Self-Identified Race

### 2.1 Introduction

Alzheimer's disease (AD) affects 6 million adults in the US alone, and this number is projected to more than double to 13 million by 2050.<sup>1</sup> In order to mitigate this increase, the National Plan to Address Alzheimer's Disease included a goal to find a treatment for AD by 2025. A major step in this goal has been to identify and characterize early preclinical biomarkers for AD so that at-risk adults can be treated prior to the onset of significant neurodegeneration, which is likely irreversible. African Americans (AA) are twice as likely as non-Hispanic white Americans (WA) to develop dementia, including AD.<sup>1</sup> Although potential reasons for this increased prevalence of AD in AA have been suggested, it is not yet clear why this is the case. Possible race-related risk factors include prevalence of cardiovascular disease/risk factors (hypertension, obesity, diabetes, tobacco use), length and/or quality of education, quality of or access to healthcare, socioeconomic status, life-long stress, differences in AD-risk genes and their relative effects, and other differences in AD-specific or general neurodegenerative pathology that have not yet been characterized.<sup>68</sup>

Cerebrovascular risk factors are known risk factors for AD; cerebrovascular damage is a common pathology in individuals in preclinical and clinical stages of AD. This is consistent with the two-hit hypothesis of AD, which posits that early AD-specific pathology (soluble amyloid beta) acts alongside general cerebrovascular risk factors to initiate and exacerbate cerebrovascular damage, which ultimately reinforces amyloid beta

deposition, tau aggregation, neurodegeneration, and cognitive decline.<sup>13</sup> Along with other cardiovascular risk factors, hypertension is more prevalent in AA than WA.<sup>69</sup>

Hypertension may also cause more complications in AA.<sup>70</sup> Chronic hypertension causes arterial stiffening, atherosclerosis, and a shift of the autoregulatory curve which, among other changes, results in a tendency for the microvasculature to be constricted rather than dilated.<sup>11</sup> In this hyper-constricted brain environment, chronic cerebral hypoperfusion results. A lack of adequate oxygen and nutrients causes neurons to elicit inflammatory responses and to release reactive oxygen species (ROS). This causes further damage to the vasculature, and it creates an environment that increases amyloid beta, which in turn promotes further vessel constriction.<sup>11</sup> Hypertension-induced hypoperfusion and AD pathology thus reinforce and exacerbate one another. Cerebrovascular dysfunction and decreased CBF are present in older adults at risk for AD prior to other pathologies, implying that it is a causal factor in the development of AD.<sup>71</sup>

Because AA have a higher prevalence of hypertension than WA, it has been suggested that this is the reason for increased prevalence of AD in AA; perhaps the higher prevalence of hypertension in this population results in a greater burden of cerebrovascular pathology.<sup>68</sup> However, it is also possible that AA have more cerebrovascular dysfunction than WA independent of hypertension and other cardiovascular disease. In support of this theory, there is some evidence that AA have decreased CBF compared to WA, regardless of vascular risk. Clark et al<sup>68,72</sup> found decreased perfusion in AA compared to WA, independent of several vascular risk factors and suggested that lower flow was correlated with risk factors in the AA group only. Hurr et al<sup>73</sup> found that even in college-aged individuals with no vascular risk factors, AA have

a decreased vasodilatory response to hypercapnia compared to WA. Thayer and Koenig<sup>74</sup> and Allen et al<sup>75</sup> suggest different relationships between global resting CBF and high frequency heart rate variability in AA and WA, where the correlation is positive in WA and negative in AA. These previous studies suggest that cerebrovascular dysfunction is related to race independent of vascular risk factors, yet there is still a paucity of information about CBF in AA vs. WA.

Here, we assess the relationships between CBF, hypertension (HT), and cognition in AA and WA from two independent samples of older adults who are cognitively normal (CN), have subjective cognitive decline (SCD), or mild cognitive impairment (MCI). The goal is to determine whether CBF is decreased in AA, and, if so, whether this is due to hypertension or to an independent effect of race on CBF. We hypothesize that hypertensive individuals of both races will have decreased CBF in *a priori* regions of interest (ROIs) and in widespread regions in voxel-wise analyses. We also hypothesize that AA will have decreased CBF compared to WA, perhaps in distinct regions from those effected by hypertension. If CBF differs by race independently from effects of hypertension, it supports the idea that ethnicity/race should be considered among other risk factors when characterizing and standardizing early biomarkers of AD. If there are differences in how AD-related pathology and, more generally, neurodegenerative processes and cognitive decline occur in AA compared to WA, it is critical that we clarify and understand the causes of those differences. This could lead to individualized biomarkers for diagnosis, risk-assessment, clinical trial enrollment, and targeted treatment, without which we could inadvertently design treatments that are not generalizable to the diverse population of older adults in the US and around the world.

## 2.2 Methods

### Participants

This study included 135 participants (46 CN, 45 SCD, 44 MCI) from the Indiana Memory and Aging Study (IMAS), a cohort followed by the Indiana Alzheimer's Disease Research Center (IADRC), who were at least sixty years of age. All participants had 3D pCASL MRI, T1-weighted structural MRI, a clinical assessment, apolipoprotein E (*APOE*) genotyping, and Montreal Cognitive Assessment (MoCA) scores. Diagnoses were determined by clinician consensus. SCD was defined as a score of 20 or more on the first 12 items of the 20-item Cognitive Change Index (CCI-20)<sup>76</sup> reflecting increased subjective memory concerns and the absence of a measurable cognitive deficit, with or without increased levels of informant-based concerns.<sup>7</sup> Using standard criteria, an individual was diagnosed with MCI if the participant and/or an informant had a significant complaint about their cognition and they scored 1.5 standard deviations or more below normal on objective tests of cognitive functioning, either in memory or another cognitive domain. Additionally, individuals diagnosed with MCI by definition do not show a significant decline in daily functioning. All procedures were approved by the Indiana University School of Medicine Institutional Review Board. Informed consent was obtained according to the Declaration of Helsinki and the Belmont Report. In addition, this study included a replication sample using a subset of age-, sex-, and diagnosis-matched African Americans (AA) and white Americans (WA; 14 CN, 14 significant memory concern [SMC], 14 MCI) from the Alzheimer's Disease Neuroimaging Initiative (ADNI). As described in the ADNI-2 Clinical Protocols

(adni.loni.usc.edu/methods/documents/), SMC individuals had a self-report significant memory concern measured with the CCI, cognitive test scores within the normal range, a Clinical Dementia Rating (CDR) score of 0, and no concern of progressive memory impairment by the informant. Data for this replication sample were obtained from the ADNI database (adni.loni.usc.edu). The ADNI was launched in 2003 by Principal Investigator Michael W. Weiner, MD. The primary goal of ADNI has been to measure the progression of MCI and early AD utilizing a combination of MRI, positron emission tomography (PET), other biological markers, and clinical and neuropsychological assessments. Up-to-date information can be found at [www.adni-loni.org](http://www.adni-loni.org). The subset from ADNI used here included individuals that were at least sixty years of age and had 2D PASL MRI, T1-weighted structural MRI, and medical history, and MoCA sub-scores. 39 of these 42 of individuals had MoCA total scores.

### Structural MRI

Both IMAS and ADNI samples underwent high-resolution T1-weighted magnetization-prepared rapid acquisition gradient echo (MPRAGE) scans, which were used as structural images to normalize the ASL images during processing. The individual structural MRI images were segmented, and the gray matter images were smoothed with a FWHM kernel of 6x6x6 mm. These methods have been previously described.<sup>77</sup> Region of interest (ROI) - based CBF was calculated for the IMAS sample using SPM12 and FreeSurfer 6 for the following bilateral regions: frontal (inferior frontal [pars orbitalis, pars opercularis, pars triangularis], superior frontal), hippocampus, putamen, temporal (superior temporal, middle temporal, inferior temporal), thalamus, anterior cingulate

(caudal anterior cingulate, rostral anterior cingulate), posterior cingulate, and lateral occipital. ROIs made up of multiple sub-regions were calculated by weighted average.

## ASL MRI

For the IMAS sample, pseudo-continuous ASL (pCASL) MRI scans were obtained on a Siemens 3T Prisma scanner by Fair QII with multi-slice interleaved saturation sequence. The acquisition parameters were: TR= 3790 ms, TE= 40.7 ms, T1= 700 ms, FOV= 240 mm x 240 mm, slice number= 54, thickness= 2.50 mm, image matrix= 64 x 64, and voxel size 2.5 x 2.5 x 2.5 mm<sup>3</sup>.

For the ADNI sample, structural and ASL images were downloaded from the ADNI database. Pulsed ASL (PASL<sup>78</sup>) MRI scans were obtained on 3T scanners by QUIPS II with thin-slice T11 periodic saturation sequence.<sup>79</sup> The acquisition parameters were: TR= 3400 ms, TE= 12 ms, T11= 700 ms, T12= 1900 ms, FOV= 256 mm x 256 mm, slice number= 24 (axial), thickness= 4 mm, and image matrix= 64 x 64.

Scans from both samples were further processed in the same manner, which has been previously described.<sup>77</sup> Individuals' ASL images were aligned to their first ASL image and coregistered to their structural MRI image. The structural MRIs and the coregistered ASL images were then coregistered to a T1 template. Pairs of ASL images were subtracted and then averaged for a mean perfusion image. A previously described method was used to calculate mean cerebral blood flow (CBF) maps from the mean perfusion images (<http://cfn.upenn.edu/perfusion/software.htm>). The gray matter images from the structural MRI were resliced to be coregistered to the mean perfusion images, thresholded for voxels > 0.75, smoothed with a FWHM kernel at 6x6x6 mm, and

thresholded for voxels  $> 0.20$  to create individualized gray matter masks. These gray matter masks were applied to the mean CBF maps, which were then normalized to Montreal Neurological Institute (MNI), resampled to  $2 \text{ mm}^3$  voxels, smoothed with a FWHM kernel of  $6 \times 6 \times 6 \text{ mm}$ , and masked to exclude the cerebellum. All processing steps were completed in Statistical Parametric Mapping 12 (SPM12; Wellcome Department of Cognitive Neuroscience, London, UK).

### Statistical Analyses

The demographic and clinical variables, including global CBF and total gray matter volume, were compared between diagnostic groups using one-way ANOVA for continuous variables and chi-square test for categorical variables. Regional mean CBF was used as the dependent variable in a multiple regression model with age, sex, total gray matter volume, hypertension status, and/or race as independent variables to assess correlations between race, hypertension, and regional CBF. Partial Pearson correlation was used to assess the relationship between regional CBF and MoCA score, with age, sex, years of education completed, and total gray matter volume as covariates. These analyses and all scatterplots were completed in IBM SPSS 25. Selected analyses were repeated on a voxel-wise basis using multiple regression with CBF maps as the dependent variable and hypertension status and/or race, age, sex, and total gray matter volume as independent variables and covariates as appropriate. Voxel-wise results are reported at  $p=0.001$  uncorrected,  $k=150$  for the IMAS sample and at  $p=0.01$  uncorrected,  $k=150$  for the smaller ADNI sample. All voxel-wise analyses were completed using SPM12. Beta map displays were made using MRICroGL.

### 2.3 Results

Demographics for the local IMAS sample are given in Table 7. In this sample, there was a greater proportion of hypertension in AA than in WA. AA also had a greater proportion of women in this sample. Finally, AA had lower MoCA scores and lower gray matter volumes than WA. There were no differences in age, diagnostic makeup, *APOE*  $\epsilon$ 4 positivity, global CBF, or years of education completed between WA and AA in this sample. Demographics for the ADNI sample are given in Table 8. In this sample, AA had lower gray matter volumes than WA. There were no other differences between the WA and AA groups in this sample.

The relationship between regional CBF and hypertensive status was assessed in the IMAS sample with age, sex, and total gray matter volume as covariates. Hypertensive individuals had lower CBF than normotensive individuals in all regions (Table 9). Corresponding voxel-wise analysis resulted in decreased CBF in hypertensive individuals mainly in widespread frontal and temporal regions (Table 10, Figure 17). In the ADNI sample, voxel-wise analysis demonstrated decreased CBF in hypertensive individuals in the left thalamus (not shown). There were no regions of increased CBF in hypertensive individuals in either sample.

The relationship between regional CBF and race (WA or AA) was assessed in the IMAS sample with age, sex, and total gray matter volume as covariates. There was no statistically significant relationship between CBF and race in any of the hypertension-related regions, but there was a nonsignificant trend for lower CBF in AA in all regions (Table 11). Voxel-wise results, with hypertensive status included as a covariate, suggest

that CBF is lower in occipitoparietal regions in AA (Table 12, Figure 18A). In the ADNI sample, voxel-wise analysis with hypertension as a covariate showed decreased CBF in AA in primary motor, visual motor, and visual association regions (Table 13, Figure 18B). Additionally, in the IMAS sample, there was decreased CBF in WA in the right insula (Table 14, Figure 19A). In the ADNI sample, there was decreased CBF in WA in regions of frontal and temporal cortex, the hippocampus, and the thalamus (Table 15, Figure 19B). Voxel-wise beta values from these analyses showed similar overall patterns in both samples. AA had lower CBF relative to WA in more posterior and lateral regions, while WA had decreased CBF in relatively anterior and medial regions relative to AA (Figure 20).

ROI-based analyses were used to assess the relationship between CBF in race-dependent regions and scores on the Montreal Cognitive Assessment (MoCA) in both samples. Age, sex, years of education, and total gray matter volume were used as covariates. CBF in the voxel-wise cluster located in the fusiform (in which CBF is decreased in AA in the IMAS sample) was positively correlated with MoCA delayed memory sub-score in the IMAS sample. Although it did not reach statistical significance, the same pattern of positive correlation was present in the AA group in the ADNI sample. Finally, combining the two samples still resulted in a positive correlation between this region of CBF and the MoCA delayed memory score (Table 16, Figure 21).

## 2.4 Discussion

Here, we found differences in CBF between African Americans and non-Hispanic white Americans that were not fully explained by the higher prevalence of hypertension

in African Americans. Despite limited sample sizes and the use of two ASL MRI methods, we found the same overall spatial pattern of group-wise CBF differences in two independent samples using voxel-wise analyses. Finally, we found a positive correlation between CBF and delayed memory score in a region where CBF was decreased in AA. While not conclusive, our findings suggest differences in cerebrovascular function between AA and WA that are not fully attributed to hypertension and that may be related to cognitive decline.

Across AA and WA, hypertensive individuals had decreased CBF in widespread frontal and temporal brain regions, a smaller region in the occipital lobe, and in all of the *a priori* hypertension-related ROIs. These findings agree with previous literature, which report widespread decrease in CBF in hypertensive individuals, and in particular with Beason-Held et al,<sup>80</sup> which reports decreases in prefrontal, anterior cingulate, and occipital regions. The frontal lobe has been reported as a region showing lower CBF in hypertensive individuals in a number of previous studies.<sup>81-85</sup> It may be that the frontal lobe is especially vulnerable to the structural and functional changes that hypertension causes in the cerebrovasculature.<sup>86</sup> The area of the brain supplied by the middle cerebral artery, and especially the anterior/middle cerebral artery watershed regions located in the frontal lobes, are particularly vulnerable to hypoperfusion.<sup>81,87</sup> In addition, damage to the frontal-subcortical white matter tracts could further exacerbate issues in the frontal lobes; frontal white matter may be particularly vulnerable to hypertension.<sup>86</sup> In support of the major effects of hypertension centering on the frontal lobe, vascular dementia involves executive dysfunction as one of the earliest cognitive symptoms, as opposed to problems with memory that occur in classic AD.<sup>88</sup> However, as mentioned above there are global

changes in CBF related to hypertension, and many studies have found decreased CBF in a variety of brain regions in hypertension, including the parietal lobe, hippocampus, putamen, and globus pallidus.<sup>89,90</sup> Our findings are consistent with decreased CBF in hypertensive individuals and with the concept that anterior brain regions might be particularly susceptible.

In both independent samples, there was a pattern of decreased posterior CBF and increased anterior CBF in AA relative to WA. None of the *a priori* hypertension-based ROIs were significantly different between these two groups in the IMAS sample. With hypertension included in the model, CBF was decreased in AA in regions including the secondary visual area and fusiform (IMAS), primary and visual motor and visual association areas (ADNI). Relative to WA, CBF was increased in AA in regions including the insula (IMAS), dorsal entorhinal, temporal pole, inferior frontal, dorsolateral prefrontal, caudate, thalamus, and hippocampus (ADNI). The greater number of regions of increased CBF in AA in ADNI may be due to greater power of race in the comparison between AA and WA in this sample since the groups are the same size, whereas the IMAS sample contains considerably more WA than AA. When these voxel-wise analyses were repeated without hypertensive status in the model, AA also had decreased CBF in the temporal pole and along the frontoparietal border in the IMAS sample. The other results were not grossly different from the original analyses (*data not shown*). This suggests that the groupwise differences in CBF presented here are relatively independent of hypertensive status.

There have been few studies comparing CBF between AA and WA, but from previous literature we would expect CBF to be decreased in AA compared to WA.<sup>68,72,73</sup>

To our knowledge, no studies have reported specific brain regions in which CBF is higher in AA. In addition, CBF differences by race would be hypothesized to be observed in the same brain regions that are affected by hypertension if the effect is mediated by hypertension rather than race. In fact, some studies have suggested that race could be a proxy for severe hypertension.<sup>91</sup> However, our results do not support the conclusion that differences in CBF between AA and WA are due to the differing prevalence of hypertension in these groups. We also found some regions of increased CBF in AA, which could be compensatory in nature and/or could reflect distinct patterns of brain function in older age in AA and WA. Alternatively, it is possible that due to the nature of ASL MRI, the posterior/anterior dichotomy may be due to a difference in arterial transit times, in which transit is faster in AA. This would result in more blood in anterior regions than in posterior regions at the time of imaging, as blood flows from posterior to anterior regions of the brain. Future imaging studies are needed to determine whether arterial transit times differ between AA and WA older adults so that this factor can be taken into account when characterizing CBF and other neuroimaging biomarkers of AD (i.e., amyloid and tau PET scans).

Although there are few studies comparing CBF between AA and WA, there are several studies that have reported differences in hemodynamics and vascular damage between the two groups that were not explained by vascular risk factors. Caughey et al<sup>92</sup> reported a positive correlation between common carotid artery intima-media thickness and posterior silent brain infarctions and lacunes in AA, but not in WA. Since posterior brain regions are not directly supplied by the common carotid artery, Caughey et al<sup>92</sup> suggested that the observed hypoperfusion in AA may be reflective of dysfunctional

subcortical small vessels. AA have also been reported to have decreased mean blood flow velocity in the vertebral artery<sup>93</sup>, attenuated vascular responses<sup>94</sup>, and greater levels of cognitive decline with respect to the level of white matter damage, a sign of cerebrovascular dysfunction.<sup>95</sup>

When CBF in regions of relative decrease in AA was compared to the delayed memory sub-score of the MoCA, we found a positive correlation in the IMAS sample and in the AA group of the ADNI sample, although this did not reach significance, potentially due to smaller sample size. Combining data of both samples resulted in positive correlations for both groups. This suggests that CBF in this region is important for cognitive functions that decline in AD. The brain region involved in this correlation included the left fusiform. The fusiform is involved in visual processing, particularly distinguishing the identity of an object and whether two objects belong to the same category. It is also involved in recognizing faces and “sight words,” or knowing what a word is by recognizing it rather than sounding it out.<sup>96</sup> Although the fusiform has mostly been associated with the memory of faces,<sup>97,98</sup> one may speculate that in order to remember a word list, the participant must mentally picture either an image of the word or the item it describes. Convit et al<sup>99</sup> found that fusiform gyrus volume used alongside hippocampal volume added power to distinguish between individuals with MCI and those with AD, suggesting that it is related to AD-associated cognitive decline. Future studies are warranted to better understand the groupwise differences in CBF and cognitive correlates of the fusiform. It is possible that AA are particularly vulnerable to decreased CBF and other neurodegenerative and AD-related processes in posterior brain regions including the fusiform. If so, this may result in cognitive decline consistent with a clinical

diagnosis of AD more quickly than would typically occur in WA with the same general level of brain pathology.

The possibility of AA reaching the threshold for a clinical diagnosis of AD earlier is conceptually in agreement with the Weathering Hypothesis, which posits that AA biologically age more quickly than their WA counterparts due to social stressors, lower socioeconomic status, poorer access to healthcare, and related factors that can lead to an early accumulation of health problems.<sup>100</sup> While this construct was described with respect to earlier physical deterioration, chronic stress would also ultimately contribute to mental deterioration either directly or indirectly through physiological (i.e. cardiovascular) pathways. It has been reported that AA have older brain ages, measured by atrophy and white matter lesions, relative to their biological ages than WA.<sup>101</sup> The concept of the Weathering Hypothesis and older brain age in AA could mean that AA manifest clinical symptoms of AD at a lower threshold of brain pathology than WA. This is important with respect to higher prevalence of AD in AA; the Alzheimer's Association Trajectory Report has stated that delaying the onset of dementia by five years would decrease the projected 2050 national prevalence by 5.7 million people.

Limitations of this study include the small percentage of African American individuals in the IMAS sample and the moderate size of the matched subset from the ADNI. This sample size may have been underpowered, but we did still find an overall pattern of groupwise CBF differences that was consistent between the two samples. Future studies with a larger number of AA participants are warranted. This study should be considered preliminary and contributes to the evidence that there may be race-related differences in cerebrovascular function related to cognitive decline. Another limitation is

that the hypertensive status is from a single time point at age 60 or older. Midlife hypertension, as well as chronic hypertension, is most predictive of cognitive decline in later life.<sup>11</sup> The cross-sectional design of this study gives us an idea of CBF differences based on HT and race, but future longitudinal studies are needed to compare temporal changes in CBF in these groups. Finally, race was defined by self-identification, but future studies with larger sample sizes may benefit from using GWAS to genetically define the degree of European and African ancestry for each individual. While this would help to specifically investigate cerebrovascular differences based on genetic differences, self-identification may better encompass other potential explanations for race-related differences, including social factors.

In conclusion, we found that there are differences in regional CBF between African Americans and white Americans, independent of hypertension. CBF in at least one of these regions is positively correlated with delayed memory cognitive test scores. These results support the premise that potential early biomarkers of AD should be assessed with respect to ethnicity/race along with other known and potential AD risk factors. Doing so will ensure that biomarkers are accurate for diverse populations that are at an increased risk for AD.

Table 7. Demographic and Clinical Variables in the IMAS sample. Abbreviations can be found in the List of Abbreviations (p. xii).

IMAS	All (n=135)	White (n=107)	AA (n=28)	Comparison
Age	71.51 ± 7.27	71.83 ± 7.30	70.29 ± 7.13	p=0.318
Sex (%F)	65.9	60.7	85.7	p=0.013*
Diagnosis (%SCD, %MCI)	33.3, 32.6	31.8, 36.4	39.3, 17.9	p=0.171
Hypertension (%)	54.1	47.7	78.6	p=0.003*
APOE ε4 (%)	49.6	49.5	50.0	p=0.965
Education (years)	16.45 ± 2.57	16.65 ± 2.55	15.68 ± 2.55	p=0.074
MoCA Score	24.26 ± 3.62	24.66 ± 3.61	22.71 ± 3.30	p=0.011*
Gray Matter Volume (L)	0.5981 ± 0.0708	0.6046 ± 0.0716	0.5732 ± 0.0628	p=0.036*
Global CBF (mL/100g/min)	24.50 ± 6.08	24.78 ± 6.41	23.45 ± 4.54	p=0.306

Table 8. Demographic and Clinical Variables in the ADNI sample. Abbreviations can be found in the List of Abbreviations (p. xii).

ADNI	All (n=42)	White (n=21)	AA (n=21)	Comparison
Age	73.02 ± 5.51	73.05 ± 5.53	73.00 ± 5.62	p=0.978
Sex (%F)	66.7	66.7	66.7	p=1.000
Diagnosis (%SCD, %MCI)	33.3, 33.4	33.3, 33.4	33.3, 33.4	p=1.000
Hypertension (%)	61.9	57.1	66.7	p=0.525
APOE ε4 (%) [7 AA missing]	31.0 [37.0]	42.9	19.0 [28.6]	p=0.392
Education (years)	16.24 ± 2.56	16.52 ± 2.66	15.95 ± 2.48	p=0.475
MoCA Score	23.64 ± 3.56	24.20 ± 3.00	23.05 ± 4.06	p=0.321
Gray Matter Volume (L)	0.5680 ± 0.0734	0.5931 ± 0.0839	0.5429 ± 0.0517	p=0.025*
Global CBF (mL/100g/min)	23.85 ± 4.78	23.73 ± 5.39	23.96 ± 4.20	p=0.875

Table 9. Correlations between ROI-based CBF and hypertension status in IMAS. Hypertension was associated with decreased CBF in all a priori brain regions, with age, sex and total gray matter volume as covariates. Abbreviations can be found in the List of Abbreviations (p. xii).

ROI CBF	Standardized Coefficient ( $\beta$ )	t	p
Frontal	-0.312	-4.025	<0.001*
Hippocampus	-0.259	-3.364	0.001*
Putamen	-0.323	-4.007	<0.001*
Temporal	-0.313	-4.016	<0.001*
Thalamus	-0.206	-2.627	0.010*
Anterior Cingulate	-0.306	-3.941	<0.001*
Posterior Cingulate	-0.301	-3.835	<0.001*
Lateral Occipital	-0.313	-4.015	<0.001*

Table 10. Correlations between voxel-wise CBF and hypertension status in IMAS. Regions of decreased CBF associated with hypertension with age, sex and total gray matter volume as covariates.  $p=0.001$ ,  $k=150$ .

k	ROI	X	Y	Z	Brodmann area	t	p
517800	left primary motor	-64	-12	26	4	6.52	<0.001
	right orbital frontal	4	34	-8	11	6.47	<0.001
	left frontal eye fields	-22	30	54	8	6.43	<0.001
	left dorsolateral prefrontal	-44	22	36	9	6.39	<0.001
	left medial temporal	-68	-36	8	21	6.39	<0.001
	right temporal pole	54	12	-28	38	6.24	<0.001
	right orbital frontal	2	40	-16	11	6.17	<0.001
	right insula	40	0	2	13	6.11	<0.001
	left primary auditory	-62	-20	6	41	6.07	<0.001
	left premotor and supplementary motor	-40	0	52	6	6.04	<0.001
	right superior temporal	64	-12	0	22	6.03	<0.001
	left superior temporal	-64	-28	8	22	6.03	<0.001
	left superior temporal	-62	-12	2	22	5.99	<0.001
	left temporal pole	-56	6	-20	38	5.94	<0.001
	left medial temporal	-64	-14	-8	21	5.88	<0.001
372	right primary visual	2	-74	10	17	4.07	<0.001
	left secondary visual	-6	-70	6	18	4.04	<0.001
	left primary visual	-14	-78	10	17	3.77	<0.001
179	right secondary visual	12	-86	-12	18	3.68	<0.001
	right visual association	26	-76	-14	19	3.57	<0.001

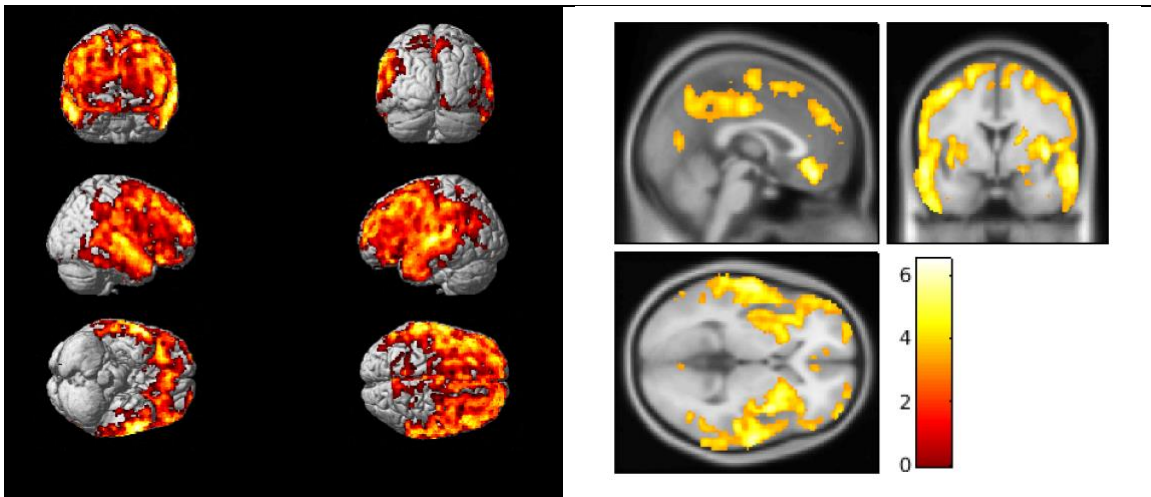


Figure 17. Visualization of correlations between voxel-wise CBF and hypertension status in IMAS. Hypertensive individuals have decreased CBF in widespread frontal and temporal regions. Covariates: age, sex, and total gray matter volume.  $p=0.001$ ,  $k=150$ .

Table 11. Correlations between ROI-based CBF and self-identified race in IMAS. There are trends in all a priori brain regions for African Americans to have lower CBF than white Americans, with age, sex and total gray matter volume as covariates.

ROI CBF	Standardized Coefficient ( $\beta$ )	t	p
Frontal	-0.078	-0.929	0.355
Hippocampus	-0.061	-0.743	0.459
Putamen	-0.117	-1.347	0.180
Temporal	-0.093	-1.112	0.268
Thalamus	-0.062	-0.756	0.451
Anterior Cingulate	-0.102	-1.219	0.225
Posterior Cingulate	-0.088	-1.042	0.299
Lateral Occipital	-0.089	-1.053	0.294

Table 12. Decreased voxel-wise CBF in self-identified African Americans in IMAS. Regions of decreased CBF in African Americans with age, sex, total gray matter volume, and hypertension status as covariates.  $p=0.001$ ,  $k=150$ .

k	ROI	X	Y	Z	Brodmann area	t	p
233	right secondary visual	0	-90	30	18	4.86	<0.001
1055	left fusiform	-68	-50	-8	37	4.32	<0.001
	left fusiform	-66	-52	-2	37	4.24	<0.001

Table 13. Decreased voxel-wise CBF in self-identified African Americans in ADNI. Regions of decreased CBF in African Americans with age, sex, total gray matter volume, and hypertension status as covariates.  $p=0.01$ ,  $k=150$ .

k	ROI	X	Y	Z	Brodmann area	t	p
202	left primary motor	-36	-32	60	4	4.09	<0.001
162	left primary motor	-2	-24	60	4	3.94	<0.001
161	left visual motor	-20	-60	64	7	3.83	<0.001
	left visual motor	-4	-66	60	7	3.11	0.002
174	right visual association	48	-66	8	19	3.79	<0.001
	right visual association	42	-76	16	19	3.48	0.001

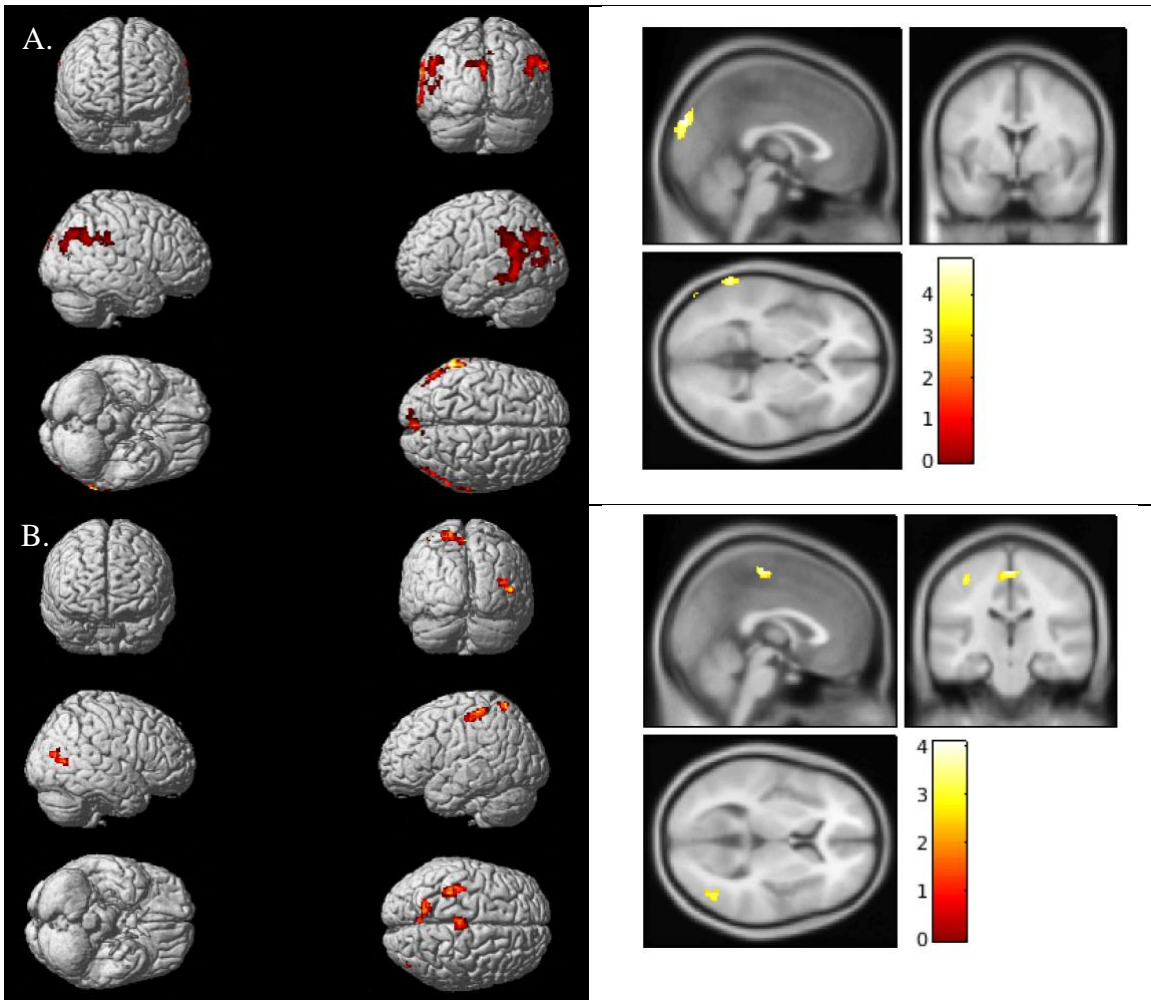


Figure 18. Visualizations of decreased voxel-wise CBF in self-identified African Americans in IMAS (A) and ADNI (B). African Americans have decreased CBF in occipitoparietal regions in IMAS and in primary motor, visual motor, and visual association regions in ADNI, compared to white Americans.  $p < 0.001$  (IMAS) or  $p < 0.01$  (ADNI),  $k = 150$ .

Table 14. Increased voxel-wise CBF in self-identified African Americans in IMAS. Regions of increased CBF in African Americans with age, sex, total gray matter volume, and hypertension status as covariates.  $p = 0.001$ ,  $k = 150$ .

k	ROI	X	Y	Z	Brodmann area	t	p
258	right insula	30	-26	18	13	5.03	<0.001

Table 15. Increased voxel-wise CBF in self-identified African Americans in ADNI. Regions of increased CBF in African Americans with age, sex, total gray matter volume, and hypertension status as covariates.  $p=0.01$ ,  $k=150$ .

k	ROI	X	Y	Z	Brodmann area	t	p
272	left dorsal entorhinal	-32	6	-16	34	3.77	<0.001
	left temporal pole	-42	8	-32	38	3.80	<0.001
277	left pars opercularis	-40	10	8	44	4.51	<0.001
	left dorsolateral prefrontal	-44	30	14	46	3.85	0.002
	left pars opercularis	-52	20	30	44	3.81	0.005
232	left caudate	-6	8	2	N/A	4.38	<0.001
	left caudate	-12	0	16	N/A	4.29	<0.001
647	left thalamus	-2	-16	12	N/A	3.93	<0.001
	left thalamus	-10	-32	6	N/A	3.93	<0.001
	left thalamus	-16	-32	4	N/A	3.81	<0.001
	left hippocampus	-20	-38	2	N/A	3.78	<0.001
	left hippocampus	-28	-34	-4	N/A	3.06	0.002

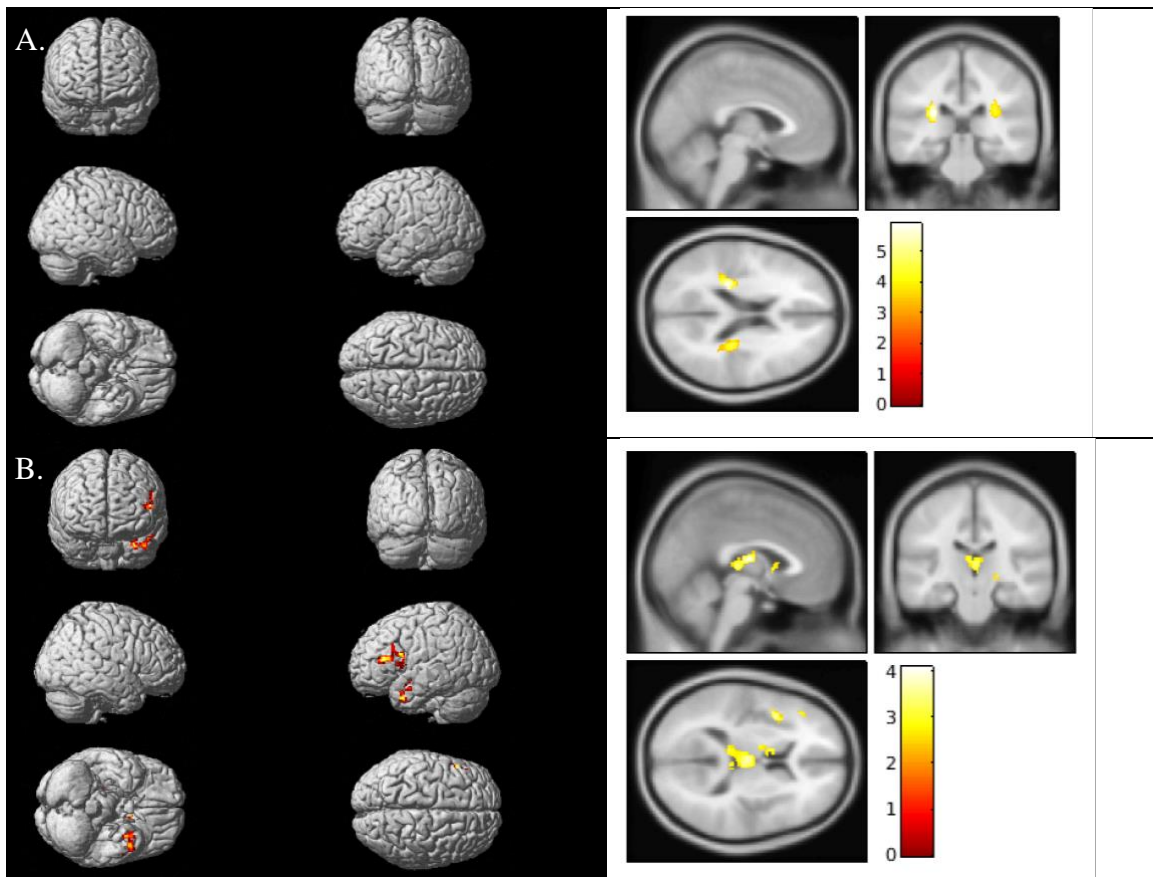


Figure 19. Visualizations of increased voxel-wise CBF in self-identified African Americans in IMAS (A) and ADNI (B). African Americans have increased CBF in the insula in IMAS and in frontal, temporal, hippocampal, and thalamic regions in ADNI, compared to white Americans.  $p<0.001$  (IMAS) or  $p<0.01$  (ADNI),  $k=150$ .

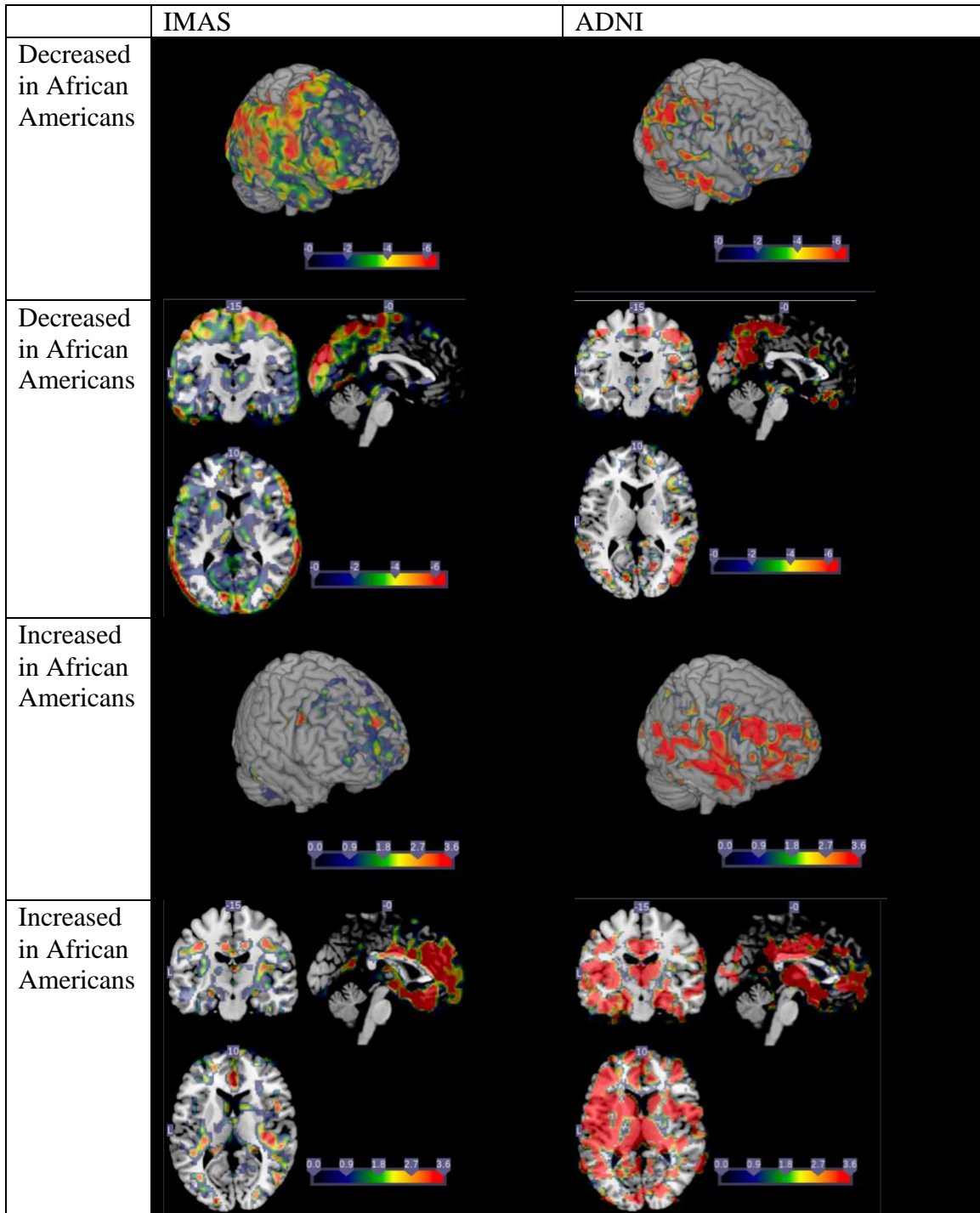
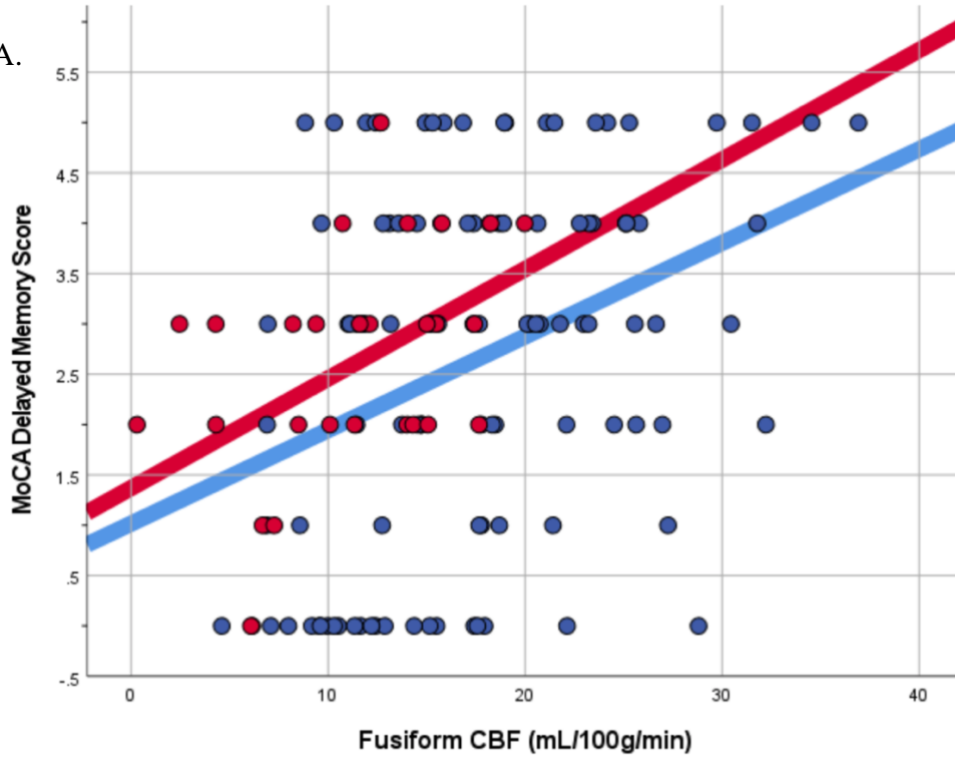


Figure 20. Visualization of voxel-wise beta values in correlations of CBF and self-identified race in IMAS and ADNI. Both samples show a general pattern of decreased CBF in posterior and lateral brain regions with increased CBF in anterior and medial brain regions in AA compared to WA with age, sex, total gray matter volume, and hypertension status as covariates.

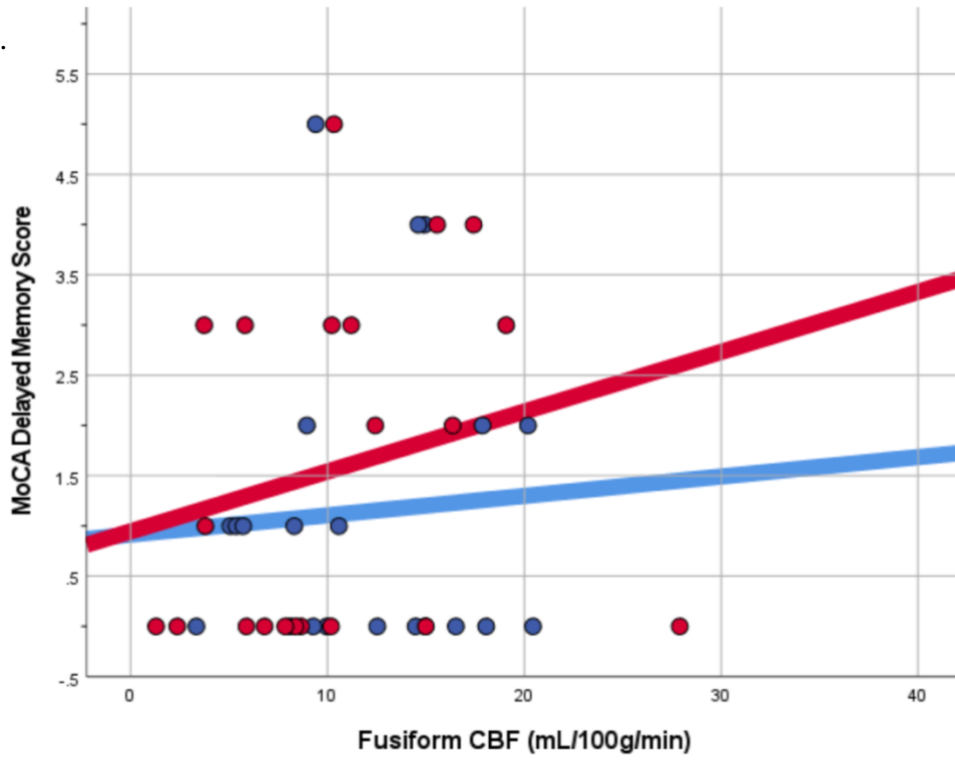
Table 16. Correlations between cluster CBF and MoCA delayed memory sub-score in IMAS and ADNI. CBF in the fusiform was positively correlated with the MoCA delayed memory sub-score in African Americans and white Americans from IMAS, the full IMAS sample, white Americans from combined IMAS and ADNI samples, and the full combined IMAS and ADNI samples. Covariates were age, sex, years of education, and total gray matter volume.

	Sample Size (n)	r	p
IMAS: Full	135	0.220	0.011*
IMAS: AA	28	0.469	0.021*
IMAS: WA	107	0.220	0.026*
ADNI: Full	42	0.119	0.478
ADNI: AA	21	0.180	0.490
ADNI: WA	21	0.098	0.709
Combined: Full	177	0.261	0.001*
Combined: AA	49	0.179	0.239
Combined: WA	128	0.283	0.001*

A.



B.



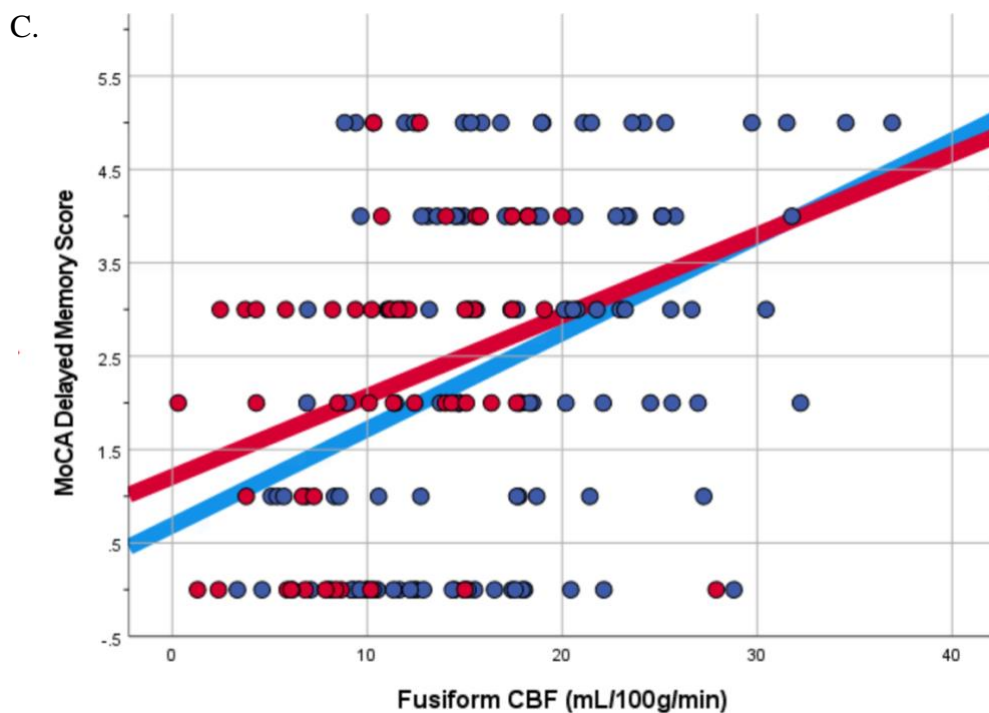


Figure 21. Scatterplots of correlations between fusiform CBF and MoCA delayed memory sub-score in IMAS (A), ADNI (B), and combined samples (C). As presented in Table 16, positive correlations were found in the IMAS and combined samples. Although not statistically significant, the associations in the ADNI sample were positive as well. Red = AA. Blue = WA.

## Chapter 3: Amyloid and Tau Pathology are Associated with Cerebral Blood Flow in Nondemented Older Adults with and without Genetic and Vascular Risk Factors

### 3.1 Introduction

Alzheimer's disease (AD) is the leading cause of dementia; over 6 million older adults in the U.S. have AD, and this number is projected to double over the next thirty years.<sup>1</sup> Thus, the U.S. Department of Health and Human Services has issued a plan to treat and prevent AD by 2025. It has been suggested by the results of multiple studies and clinical trials that an effective treatment for AD will likely need to be preventative.<sup>7,102</sup> Although there are some promising exceptions, treatments targeting amyloid and tau pathology that are administered after the emergence of clinical symptoms have generally been unable to restore cognitive function.<sup>103,104</sup> Therefore, it is imperative to find reliable and accurate biomarkers for the earliest, preclinical stages of AD, so that older adults who would benefit from preventative treatment may be identified. One such potential early biomarker is quantitative cerebral blood flow (CBF).

CBF is known to be decreased in individuals with AD compared to healthy individuals of the same age.<sup>105</sup> This decrease has also been shown to be more than would be expected given the amount of atrophy in these individuals, suggesting that altered CBF is itself a pathologic phenomenon in AD.<sup>106</sup> These results have led to the development of the two-hit hypothesis of AD, which posits that vascular risk factors and amyloid accumulation exacerbate one another and eventually lead to tau aggregation, neurodegeneration, and cognitive decline.<sup>13,107</sup> This differs from the long-standing amyloid cascade hypothesis, which states that amyloid deposition triggers the onset and

propagation of the complex pathologies and symptoms that comprise AD.<sup>12</sup> Evidence for the two-hit model of AD includes the fact that vascular risk factors like hypertension, diabetes mellitus, and obesity are also risk factors for AD.<sup>108</sup> Chronic hypertension, in particular, has been shown to cause cerebral microvascular damage, which both worsens and is worsened by amyloid beta aggregation. It has been suggested that altered CBF may occur very early in the course of AD, before cognitive symptoms and even potentially amyloid and tau aggregation.<sup>109</sup> Given that this early alteration of CBF may play a role in initiating the cascade of pathological changes culminating in AD, it is an intriguing potential early biomarker.

While altered CBF has been described as one of the earliest changes in AD, its typical spatial and temporal pattern throughout the disease course is not yet fully defined. It has been shown in several studies that CBF increases in some brain regions in individuals on the AD spectrum, especially in preclinical and prodromal AD.<sup>110,111</sup> Altered CBF is largely characterized by hypoperfusion by the time individuals have some level of cognitive decline.<sup>112</sup> Increased CBF in early, preclinical stages may be compensatory in response to other AD-related pathologies, like amyloid or tau aggregation. Indeed, global CBF is positively correlated with cognitive test scores.<sup>113</sup> Vascular risk factors such as hypertension and genetic risk factors including the apolipoprotein E (*APOE*)  $\epsilon 4$  allele may play a role in whether individuals have a compensatory increase in CBF and for how long that compensation is able to be maintained despite pathology and vascular dysfunction. It will also be important for us to elucidate the spatial and temporal relationships between altered CBF and other AD-related pathologies, including amyloid and tau aggregation.

According to the literature, CBF tends to be negatively correlated with both amyloid and tau pathology,<sup>114-119</sup> but there are also studies, mostly in individuals with preclinical AD, in which positive correlations between CBF and these pathologies have been reported.<sup>120-124</sup> It has been established that both hypertension and *APOE*  $\epsilon$ 4 positivity are related to increased amyloid beta aggregation and are associated with cerebrovascular dysfunction and decreased CBF.<sup>125-128</sup> It is the goal of this research to assess the relationships between CBF and amyloid and tau pathologies in older nondemented adults and to determine whether the presence of the *APOE*  $\epsilon$ 4 allele and hypertension affect those relationships.

Extensive characterization of altered CBF in the context of preclinical AD will solidify whether it is an effective early biomarker. Here, we assess the relationships between CBF and global cortical amyloid and medial temporal lobe (MTL) tau pathology, using arterial spin labeling (ASL) MRI and PET imaging in older nondemented adults. We also assess the interaction effects of *APOE*  $\epsilon$ 4 positivity and hypertension on the relationship of CBF with amyloid and tau in this sample. We hypothesize that amyloid and tau pathologies will be negatively correlated with CBF overall, although there may be certain regions of positive correlation as well, given the early stage of disease in this sample. We also hypothesize that individuals with hypertension or at least one *APOE*  $\epsilon$ 4 allele will be less likely to have a compensatory positive correlation between CBF and AD-related pathologies.

## 3.2 Methods

### Participants

This study included 78 participants (30 CN, 25 SCD, 23 MCI) from the Indiana Alzheimer's Disease Research Center (IADRC) who were at least sixty years of age. All participants had a 3D pCASL MRI, T1-weighted structural MRI, amyloid PET scan with either [<sup>18</sup>F]florbetapir or [<sup>18</sup>F]florbetaben and tau PET scan with [<sup>18</sup>F]florataucipir. All participants also had a clinical assessment and *APOE* genotyping. Three (3) additional participants who otherwise met these requirements were excluded because their pCASL MRI scans were poor quality. Diagnoses were determined by clinician consensus. SCD was defined as a score of 20 or more on the first 12 items of the 20-item Cognitive Change Index (CCI-20)<sup>76</sup> reflecting increased subjective memory concerns and the absence of a measurable cognitive deficit, with or without increased levels of informant-based concerns.<sup>7</sup> Using standard criteria, an individual was diagnosed with MCI if the participant and/or an informant had a significant complaint about their cognition and they scored 1.5 standard deviations or more below normal on objective tests of cognitive functioning, either in memory or another cognitive domain. Additionally, individuals diagnosed with MCI by definition do not show a significant decline in daily functioning. All procedures were approved by the Indiana University School of Medicine Institutional Review Board. Informed consent was obtained according to the Declaration of Helsinki and the Belmont Report.

## pCASL MRI

Pseudo-continuous ASL (pCASL) MRI scans were obtained on a Siemens 3T Prisma scanner by Fair QII with multi-slice interleaved saturation sequence. The acquisition parameters were: TR= 3790 ms, TE= 40.7 ms, T1= 700 ms, FOV= 240 mm x 240 mm, slice number= 54, thickness= 2.50 mm, image matrix= 64 x 64, and voxel size 2.5 x 2.5 x 2.5 mm<sup>3</sup>.

Processing steps have been previously described.<sup>77</sup> All images were aligned to the first pCASL image and coregistered to the individual's structural MRI image. The structural MRI's and the coregistered pCASL images were then coregistered to a T1 template. The individual T1-weighted structural MRI images were segmented, and the grey matter images were smoothed with a FWHM kernel of 6x6x6 mm. Pairs of pCASL images were subtracted and then averaged for a mean perfusion image. A previously described method was used to calculate mean cerebral blood flow (CBF) maps from the mean perfusion images (<http://cfn.upenn.edu/perfusion/software.htm>). The grey matter images from the structural MRI were resliced to be coregistered to the mean perfusion images, thresholded for voxels > 0.75, smoothed with a FWHM kernel at 6x6x6 mm, and thresholded for voxels > 0.20 to create individualized grey matter masks. These grey matter masks were applied to the mean CBF maps, which were then normalized to Montreal Neurological Institute (MNI), resampled to 2 mm<sup>3</sup> voxels, smoothed with a FWHM kernel of 6x6x6 mm, and masked to exclude the cerebellum. All processing steps were completed in Statistical Parametric Mapping 12 (SPM12; Wellcome Department of Cognitive Neuroscience, London, UK). Lobar CBF was calculated using SPM12 and the

following ROIs from Automated Anatomical Labeling (AAL): frontal, limbic, parietal, temporal, and occipital.

### Amyloid PET

Each participant in the PET sample underwent either [ $^{18}\text{F}$ ]florbetapir (AmyVid; Eli Lilly and Co.) or [ $^{18}\text{F}$ ]florbetaben (NeuraCeq; Life Molecular Imaging, formerly Piramal Imaging) scans. For the [ $^{18}\text{F}$ ]florbetapir scans, 10 mCi of [ $^{18}\text{F}$ ]florbetapir was injected intravenously, followed by a 50-minute uptake period. Individuals were then imaged on a Siemens mCT for 20 minutes with continuous list mode data acquisition. For [ $^{18}\text{F}$ ]florbetaben scans, 8 mCi of [ $^{18}\text{F}$ ]florbetaben was injected intravenously, followed by a 90-minute uptake period. These participants were then also imaged on a Siemens mCT for 20 minutes with continuous list mode data acquisition. For both types of scans, a computed tomography scan was acquired for scatter and attenuation correction. The list mode data were then rebinned into four 5-minute frames and reconstructed using parameters defined in the Alzheimer's Disease Neuroimaging Initiative (ADNI) protocol (<http://adni.loni.usc.edu>). These parameters include corrections for scatter and random coincidence events, attenuation, and radionuclide decay. These 5-minute frames were then spatially aligned to the participants' T1-weighted structural MRI, motion corrected, and normalized to MNI space using SPM12. The PET image frames were averaged to create a static image over the acquisition time period for each individual (50-70 minutes for [ $^{18}\text{F}$ ]florbetapir and 90-110 minutes for [ $^{18}\text{F}$ ]florbetaben), and standardized uptake value ratio images (SUVR) were generated using a whole cerebellar region of interest from the Centiloid project. For this study, the global cortical amyloid measure used was

calculated as Centiloid units. Both types of scans were processed with the Centiloid algorithm at a voxel-wise level as defined by the Centiloid project (<http://www.gain.org/Centiloid-project/>).<sup>129</sup> Global cortical Centiloid data was then extracted from both scan types using MarsBaR. Amyloid positivity was recorded at the time of amyloid PET scanning and was defined as global cortical amyloid >21 Centiloid units.

### Tau PET

All participants in the PET sample underwent a [<sup>18</sup>F]flortaucipir PET scan. 10 mCi of [<sup>18</sup>F]flortaucipir was injected intravenously, followed by a 75-minute uptake period. Individuals were then imaged on a Siemens mCT for 30 minutes by continuous list mode data acquisition. These data were rebinned into six 5-minute frames, and scans were reconstructed using a standard scanner software program (Siemens, Knoxville, TN) according to the ADNI protocol (<http://adni.loni.usc.edu>). The middle four 5-minute frames (80-100 minutes) were motion corrected, normalized to MNI space using each subject's T1-weighted structural MRI, averaged to create a static image, intensity normalized to the cerebellar crus to create SUVR images, and smoothed with an 8 mm full-width half-maximum Gaussian kernel, all using SPM12. For this study, the medial temporal lobe (MTL) SUVR was used. The constituent ROIs were generated from FreeSurfer, and the bilateral mean MTL (average of fusiform gyri, parahippocampal gyri, and entorhinal cortex) SUVR values were extracted for each participant using MarsBaR. For interaction analyses, tau positivity was defined as MTL tau SUVR greater than the third quartile value in this sample (1.151).

## Statistical Analyses

The demographic and clinical variables, as well as global CBF, total grey matter volume, and amyloid and tau PET measures were compared between diagnostic groups using one-way ANOVA for continuous variables and chi-square test for categorical variables. Stepwise multiple regression model (entry  $p=0.10$ , removal  $p=0.20$ ) with dependent variable lobar CBF and independent variables diagnostic group, age, sex, hypertension status, *APOE*  $\epsilon 4$  status, and total grey matter volume were used to determine which demographic/clinical variables are correlated with CBF in this sample. Amyloid and tau PET measures were used as the dependent variable in a multiple regression model with age, sex, hypertension status, *APOE*  $\epsilon 4$  status, and total grey matter volume as independent variables to assess correlations between these measures and demographic/clinical variables. Partial Pearson correlation was used to assess the relationship between lobar CBF and amyloid or tau PET measure, with age, sex, total grey matter volume, hypertension status, and *APOE*  $\epsilon 4$  status as covariates. Analyses including CBF were repeated on a voxel-wise basis using multiple regression with CBF maps as the dependent variable and amyloid or tau PET measure, age, sex, total grey matter volume, and hypertension status as independent variables and covariates as appropriate. A voxel-wise two-way ANCOVA model was used to assess interactions of amyloid/tau positivity and hypertension/*APOE*  $\epsilon 4$  status with age, sex, and total grey matter volume as covariates. CBF was extracted from significant clusters and modeled as the dependent variable in linear regression to visualize interactions. Voxel-wise results are listed at  $p=0.01$ ,  $k=250$  and shown at  $p=0.05$ ,  $k=250$  for display purposes, and scatterplots are presented using CBF extracted from clusters significant at  $p=0.01$ . All

voxel-wise analyses were completed using SPM12. Other statistical analyses and all graphs were created in IBM SPSS 25.

### 3.3 Results

#### Demographics

Demographics for this sample are given in Table 17. The MCI group had a greater global cortical Centiloid value than the CN and SCD groups. Diagnostic groups also differed by prevalence of hypertension; the SCD group had the highest prevalence of hypertension, followed by MCI, and then by CN. Finally, the groups differed by proportion of women. CN had the greatest proportion of women, followed by SCD, and then by MCI.

#### CBF vs. Demographics

Mean CBF from each lobe was entered into a stepwise multiple regression with diagnosis, age, sex, hypertension status, *APOE*  $\epsilon$ 4 status, and total grey matter volume as independent variables. Age and hypertension were negatively correlated with CBF in all lobes (Table 18). No correlations were found between CBF and diagnosis, *APOE*  $\epsilon$ 4 status, or total grey matter volume. The interaction variable for age by hypertension status was not statistically significant in any of the lobes. Voxel-wise regressions were used to model the spatial relationships between CBF and age and hypertension with age, sex, and gray matter volume as covariates where appropriate (Figure 22;  $p=0.05$ ,  $k=250$ ).

### PET vs. Demographics

The global cortical Centiloid and the MTL tau SUVR data were used as dependent variables in a stepwise regression model with age, sex, hypertension status, *APOE*  $\epsilon$ 4 status, and total grey matter volume as independent variables. The global cortical Centiloid value was associated with *APOE*  $\epsilon$ 4 status ( $\beta=0.414$ ,  $t=3.964$ ,  $p<0.001$ ). MTL tau SUVR was associated with hypertension status ( $\beta=-0.223$ ,  $t=-1.997$ ,  $p=0.049$ ).

### PET vs. Lobar CBF

Partial correlations were completed for lobar CBF with global cortical Centiloid and MTL tau SUVR, with age, sex, and total grey matter volume as covariates. There were no significant correlations in any of the lobes between CBF and global cortical Centiloid or MTL tau SUVR. The addition of hypertension status and *APOE*  $\epsilon$ 4 status as covariates did not change the results.

### PET vs. Voxel-wise CBF

Using voxel-wise regression models with global cortical Centiloid and MTL tau SUVR, with age, sex, and total grey matter volume as covariates, MTL tau SUVR was negatively correlated with CBF in the left hippocampus and left parahippocampal gyrus ( $p=0.01$ ,  $k=250$ ; Table 19, Figure 23). General patterns of the correlations between MTL tau SUVR and CBF are shown in Figure 24 ( $p=0.05$ ,  $k=250$ ). There were no statistically significant correlations with global cortical Centiloid at the  $p=0.01$ ,  $k=250$  level. However, results at  $p=0.05$ ,  $k=250$  include negative correlations between global cortical Centiloid and CBF in the left parahippocampal region and amygdala (Figure 25).

## PET vs. Voxel-wise CBF: Interaction Analyses

In order to determine whether *APOE*  $\epsilon 4$  status or hypertension status affected the relationship between amyloid or tau PET measures and CBF, a voxel-wise two-way ANCOVA was used, with CBF as the dependent variable, amyloid or tau positivity and *APOE*  $\epsilon 4$  or hypertension status as independent variables, and age, sex, and total gray matter volume as covariates. Only the amyloid by hypertension interaction reached significance at  $p=0.01$ ,  $k=250$  (Table 20). CBF in the left visual motor, supramarginal, fusiform, visual association, and secondary visual areas is positively associated with global cortical Centiloid in hypertensive individuals and negatively associated with global cortical Centiloid in normotensive individuals (Figures 26, 27, and 28). CBF values from the three clusters were extracted for all individuals and put into a regression model with global cortical Centiloid, hypertension status, age, sex, total gray matter volume, and hypertension status by global cortical Centiloid interaction as independent variables. The interaction variable was positive in all three clusters ( $\beta=0.598$ ,  $t=-4.023$ ,  $p<0.001$ ;  $\beta=0.517$ ,  $t=3.347$ ,  $p=0.001$ ;  $\beta=0.463$ ,  $t=3.248$ ,  $p=0.002$ ). Spatial patterns of this interaction are presented in Figure 29. Parietal, temporoparietal, temporal, and occipital regions are involved. The main effect of amyloid status was significant mostly in inferior temporal regions (Figure 30;  $p=0.05$ ,  $k=250$ ), while the main effect of hypertension status was significant in widespread frontal, temporal, and temporoparietal regions (Table 21,  $p=0.01$ ,  $k=250$ ; Figure 31,  $p=0.05$ ,  $k=250$ ). Results of the other three interactions are shown at  $p=0.05$ ,  $k=250$ . The interaction effect of amyloid status by *APOE*  $\epsilon 4$  status on CBF was significant in orbital frontal, pre- and supplementary motor, and dorsolateral prefrontal cortex (Figure 32). The interaction effect of tau status by hypertension status

on CBF was interestingly similar to that of amyloid by *APOE*  $\epsilon 4$  and was significant in frontal eye fields, dorsolateral prefrontal cortex, primary motor, primary auditory, and temporoparietal regions (Figure 33). The interaction effect of tau status by *APOE*  $\epsilon 4$  status on CBF was significant in the parahippocampal region, primary motor, primary visual, fusiform, pars orbitalis, and dorsolateral prefrontal cortex (Figure 34).

### 3.4 Discussion

Here we found that CBF is negatively correlated with both MTL tau aggregation and, to a lesser degree, global cortical amyloid aggregation in older adults at risk for Alzheimer's disease. There was also an interaction effect of global cortical amyloid and hypertension status on CBF in this sample; global cortical amyloid and CBF were positively correlated in hypertensive individuals and negatively correlated in normotensive individuals. Negative correlations between CBF and MTL tau aggregation were present in the parahippocampal gyrus and hippocampus. Negative correlations between CBF and amyloid beta aggregation were also present in the parahippocampal gyrus and amygdala. Negative correlations between amyloid pathology and CBF have been extensively documented in previous studies. There have been fewer studies addressing the relationship between tau pathology and CBF, but most of them have likewise reported negative correlations.

Negative correlations between amyloid pathology and CBF have been heavily documented. Several animal models of chronic hypoperfusion have been shown to develop amyloid pathology.<sup>130-134</sup> Animal models of amyloid pathology likewise develop decreased CBF,<sup>135,136</sup> and amyloid beta directly causes constriction of capillaries when

applied to animals *in vivo*<sup>137,138</sup> and to fixed human samples *in vitro*.<sup>139</sup> Likewise, some studies involving participants with a mix of preclinical and clinical AD or clinical AD alone have shown negative correlations between amyloid pathology and CBF in entorhinal regions, the precuneus, and throughout the cortex.<sup>117,118</sup> Chen et al,<sup>140</sup> on the other hand, reported a positive correlation between amyloid beta and CBF in the anterior cingulate gyrus in a mixed sample including AD patients. Additionally, Takahashi et al<sup>141</sup> reported that out of eight MCI/AD patients who were amyloid positive, only four of them had an AD pattern of hypoperfusion on SPECT scans.

Studies involving only nondemented participants have also resulted in complex findings. Michels et al<sup>142</sup> and Tosun et al<sup>119</sup> both reported negative correlations between amyloid PET and CBF in regions including frontal, temporal, parietal, and occipital lobes, cingulate cortex, and cerebellum. Tosun et al<sup>123</sup> presented a CBF signature of amyloid positivity in individuals with early MCI that included both regions of hypoperfusion and regions of hyperperfusion. In a sample of amyloid-positive CN individuals, amyloid was positively correlated with CBF in frontal and temporal lobes, insula, dorsal striatum, hippocampus, and amygdala.<sup>122</sup> Finally, in a longitudinal <sup>15</sup>O PET study, it was reported that decreases in CBF in the parietal lobe, cingulate gyrus, thalamus, and midbrain, as well as increases in CBF in the frontal and parietal lobes over several years predicted amyloid positivity via [<sup>11</sup>C]PiB PET.<sup>124</sup>

Previous studies concerning the relationship between tau and CBF have reported negative correlations. Unlike amyloid pathology, tau tracks both spatially and temporally with disease severity and brain dysfunction. Therefore, as tau pathology progresses in its characteristic pattern over the disease course, lower CBF progresses similarly.<sup>143,144</sup>

Similarly to the amyloid literature, animal models of hypoperfusion develop increased tau pathology,<sup>145,146</sup> and animal models of tau pathology develop hypoperfusion.<sup>147-150</sup> In human studies including either a mix of diagnoses including clinical AD or only clinical AD, there have been findings of negative correlations between tau pathology and CBF in temporal, parietal, and occipital lobes, and entorhinal cortex.<sup>114-116</sup> Okamura et al<sup>151</sup> reported that the ratio of (increased) tau in cerebrospinal fluid (CSF) to (decreased) posterior cingulate CBF was an adequate predictor for progression from MCI to AD. Studies in CN individuals report a mix of results, similar to amyloid pathology studies in preclinical AD. Hays et al<sup>152</sup> reported a negative correlation between CSF tau and CBF in the anterior cingulate cortex. Stomrud et al<sup>121</sup> reported a negative correlation between CSF tau and CBF in the medial frontal lobe, as well as a positive correlation between tau and CBF in the frontotemporal border zone. Another study reported that asymptomatic individuals with the same amount of tau pathology as individuals with MCI had increased CBF in the medial temporal lobe and thalamus over time.<sup>120</sup> Although there are fewer studies focused on the relationship between tau pathology and CBF compared to amyloid pathology, it appears that a similar pattern of findings is emerging.

Interacting relationships among multiple risk factors and pathologies in AD have been previously studied; specifically, the effect of *APOE*  $\epsilon 4$  on relationships between CBF and other AD pathologies or symptoms has been reported. Two papers<sup>153,154</sup> reported a positive correlation between CBF and cognition in *APOE*  $\epsilon 4$ -negative CN individuals and a negative correlation between CBF and cognition in *APOE*  $\epsilon 4$ -positive CN individuals. Hays et al<sup>152</sup> found a negative relationship between tau in the cerebrospinal fluid and CBF in the anterior cingulate in *APOE*  $\epsilon 4$ -positive but not *APOE*

$\epsilon 4$ -negative individuals. *APOE*  $\epsilon 4$  may act either alongside or synergistically with amyloid beta to exacerbate neurodegeneration.<sup>155</sup> These interactions make sense given the established relationships between *APOE*  $\epsilon 4$  and AD pathologies amyloid and tau. *APOE*  $\epsilon 4$  is clearly associated with increased amyloid beta aggregation, most likely by reducing the clearance of amyloid beta from the brain and increasing its production.<sup>156-159</sup> It has also been reported that *APOE*  $\epsilon 4$  carriers have increased levels of tau in the medial temporal lobe.<sup>160,161</sup>

Our finding of positive correlations between amyloid beta aggregation and CBF in hypertensive individuals was the opposite of the interaction effect we expected hypertension to have, but previous findings of positive associations between amyloid beta pathology and CBF in nondemented older individuals suggest that this finding could be meaningful. As shown by the diverse findings reported in the literature, the relationship between amyloid pathology and CBF in older adults on the AD spectrum is very complex.

Here, we found negative correlations between global cortical amyloid pathology, MTL tau pathology, and MTL CBF. These findings are in agreement with previous reports of negative correlations between CBF and AD pathology in preclinical AD. They also are in agreement with evidence of the temporal and spatial correlation between tau pathology and brain dysfunction in AD. While we did not see positive correlations between CBF and amyloid or tau pathology in the whole sample, as have also been reported in preclinical populations, this may be due to our small sample size. There also may be distinct time courses for compensation in response to amyloid beta and tau pathology that are dependent on other pathologies and risk factors. We also report that

hypertension was associated with decreased CBF in this sample. This has been reported previously.<sup>162</sup> It has been described that chronic hypertension shifts microvascular regulation in favor of constriction, which leads to decreased CBF in hypertensive individuals.<sup>163</sup> As the two-hit hypothesis of AD posits, vascular risk factors such as hypertension lead to cerebrovascular dysfunction that both aggravates and is aggravated by amyloid and tau pathology.

Finally, we found an interaction of amyloid beta aggregation and hypertension on CBF in older adults without dementia. While amyloid and CBF were negatively correlated as expected in normotensive individuals, they were positively correlated in hypertensive individuals. To our knowledge, this is the first report of this interaction. Not only does this suggest that hypertension status may alter the interpretation of altered CBF as a biomarker, it also suggests that cerebral vascular function is differentially affected by AD pathology in older adults with and without cardiovascular risk factors during preclinical stages of disease. The direction of the interaction was not expected; individuals with the risk factor hypertension seemed to have more of a compensatory response (increased CBF) to amyloid beta pathology. This may suggest that the combined presence of risk factors and pathologies do not always favor loss of function in early disease stages. There is not yet a standard time course of when compensation turns to failure of compensation, and it likely differs for each individual based on their comorbidities, cardiovascular health, lifestyle choices like diet and exercise, and demographic, genetic, and environmental variables. Another possibility is that our findings were different than expected because we defined hypertension as presence or absence of the condition at the time of imaging, but midlife hypertension confers the

greatest risk for AD in old age.<sup>164</sup> It has also been reported that hypotension in old age, especially following midlife hypertension, is a risk factor for AD as well.<sup>165</sup>

Surprisingly, we did not find interactions between hypertension status and tau or *APOE*  $\epsilon 4$  and either amyloid or tau at our chosen level of statistical significance in this sample. It could be that hypertension and amyloid beta have relatively more independent effects on the cerebral vasculature than the other risk factor and pathology pairs. In support of this, we did find correlations between global cortical amyloid and *APOE*  $\epsilon 4$  and between MTL tau and hypertension status in this sample. This is also in agreement with the two-hit hypothesis of AD, in which cardiovascular risk and amyloid beta aggregation culminate to initiate and propagate the pathological processes in AD. At a more liberal statistical significance level, we did find brain regions with *APOE*  $\epsilon 4$  by amyloid beta and tau interaction effects on CBF. With larger sample sizes, these interactions may prove to be meaningful. It is also possible that these interactions would be detectable and meaningful during later disease stages but not in preclinical stages.

This study was limited by its modest sample size. Some of the voxel-wise correlations between CBF and PET biomarkers reached significance only when an extent threshold of  $p < 0.05$  was used, and a larger sample size could have led to more statistically significant results suggesting a clearer picture of correlative patterns. In order to detect the correlation between global cortical amyloid and CBF at  $p = 0.01$ ,  $k = 250$ , the sample size would need to be 200. Future studies should use larger sample sizes of individuals with preclinical AD, so that statistical power is adequate to elucidate the complex relationships between CBF, amyloid, tau, and other AD-related pathologies. We also used global cortical Centiloid and MTL tau SUVR as our measures from PET

imaging. It would be ideal to retain the spatial information in both the PET and ASL images in order to determine areas of spatial overlap between AD pathologies and altered CBF.

Our findings suggest that global cortical amyloid and MTL tau pathology are both associated with decreased MTL CBF in older adults at risk for AD. Amyloid pathology's correlation with CBF was affected by hypertension status. This suggests a complex relationship between amyloid pathology and CBF that depends partially on cardiovascular health. Altered CBF is likely both an instigator and an outcome of increased amyloid and tau pathology, and these and other factors interact both spatially and temporally in the environment of an at-risk brain. CBF as a biomarker can be used in the future to identify those at risk so that they can enter clinical trials and/or receive treatment, track disease progression in both treated and untreated individuals, and perhaps to help elucidate the complex mechanisms that initiate AD and drive its progression.

Table 17. Demographic and clinical variables by diagnostic group. Abbreviations can be found in the List of Abbreviations (p. xii).

PET	All (n=78)	CN (n=30)	SCD (n=25)	MCI (n=23)	Group Comparison
Age	71.71 ± 6.78	71.13 ± 6.53	71.00 ± 7.12	73.22 ± 6.78	p=0.448
GM Volume (mg)	569,769 ± 59,277	576,393 ± 57,148	566,463 ± 63,286	564,723 ± 59,372	p=0.739
Hypertension	52.6%	26.7%	80.0%	56.5%	p<0.001*
Sex (F)	65.4%	80.0%	64.0%	47.8%	p=0.050*
APOE ε4 positive	43.6%	46.7%	32.0%	52.2%	p=0.338
Average Global CBF (mL/100g/min)	24.14 ± 6.24	25.01 ± 7.98	23.58 ± 4.82	23.62 ± 5.04	p=0.630
Amyloid PET (Centiloid)	19.41 ± 32.12	10.91 ± 26.13	11.10 ± 24.49	39.54 ± 38.16	p=0.001* MCI > CN&SCD
Tau PET (SUVR)	1.11 ± 0.11	1.09 ± 0.07	1.09 ± 0.08	1.15 ± 0.16	p=0.110

Table 18. Correlation of age and hypertension status with lobar CBF. Increasing age and hypertension were both associated with decreased CBF in all lobes.

Lobar CBF	Independent Variable retained in Model	Standardized Coefficient ( $\beta$ )	t	p
Frontal	Age	-0.335	-3.312	0.001
	Hypertension Status	-0.326	-3.221	0.002
Limbic	Age	-0.320	-3.033	0.003
	Hypertension Status	-0.239	-2.265	0.026
Parietal	Age	-0.284	-2.691	0.009
	Hypertension Status	-0.281	-2.671	0.009
Temporal	Age	-0.331	-3.199	0.002
	Hypertension Status	-0.277	-2.677	0.009
Occipital	Age	-0.313	-2.982	0.004
	Hypertension Status	-0.258	-2.453	0.016

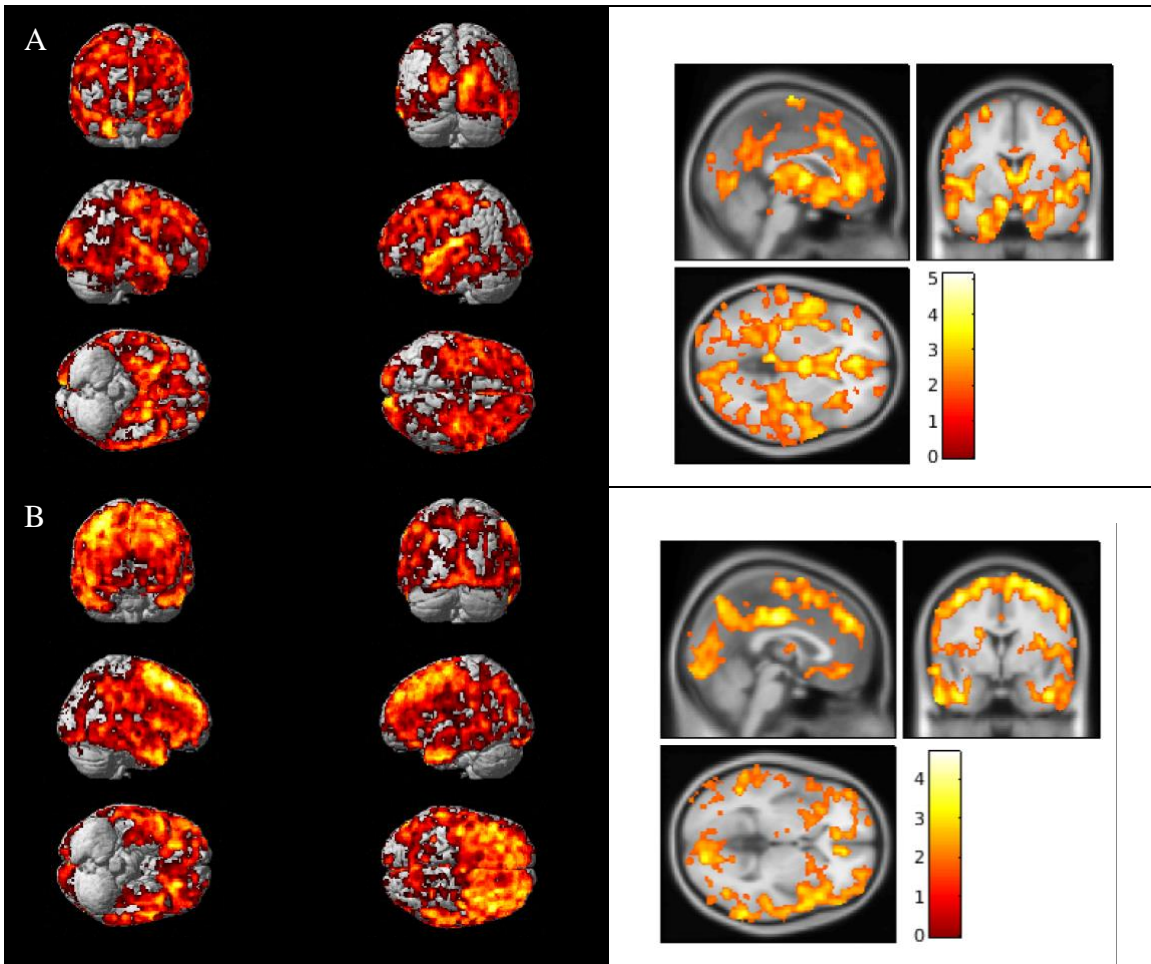


Figure 22. Negative correlations between voxel-wise CBF and age (A) and hypertension status (B). Covariates are age (in the hypertension analysis), sex, and total gray matter volume.  $p=0.05$ ,  $k=250$ .

Table 19. Negative correlations between voxel-wise CBF and MTL tau SUVR.  $p=0.01$ ;  $k= 250$ .

	k	ROI	X	Y	Z	Brodmann area	t	p
MTL tau SUVR	444	left parahippocampal gyrus	-22	-22	-20	36	4.63	<0.001
		left hippocampus	-14	-12	-18	N/A	3.60	<0.001

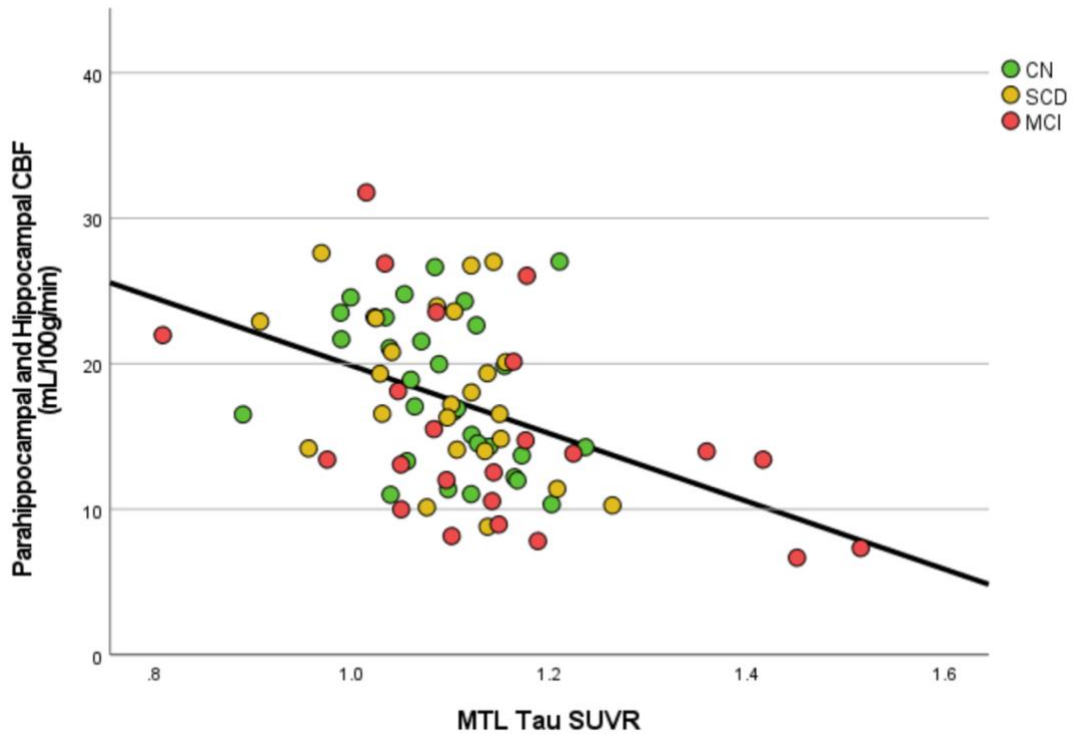


Figure 23. Scatterplot of negative correlations between voxel-wise CBF and MTL tau SUVR. Parahippocampal and hippocampal CBF are from the significant cluster in the voxel-wise analysis. Green = CN, yellow = SCD, red = MCI.

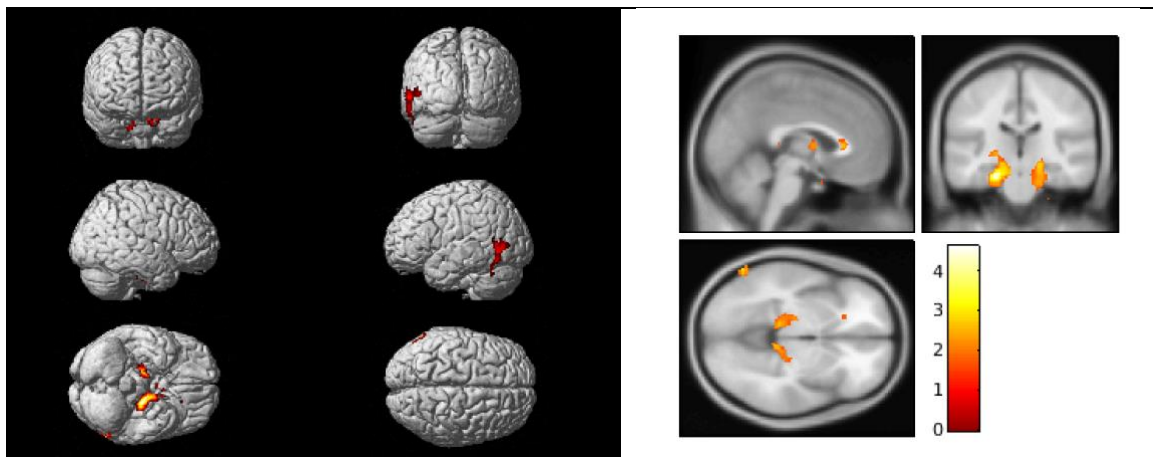


Figure 24. Visualization of negative correlations between voxel-wise CBF and MTL tau SUVR. Parahippocampal and hippocampal CBF are decreased in those with increased MTL tau, with age, sex and total gray matter volume as covariates.  $p=0.05$ ,  $k= 250$ .

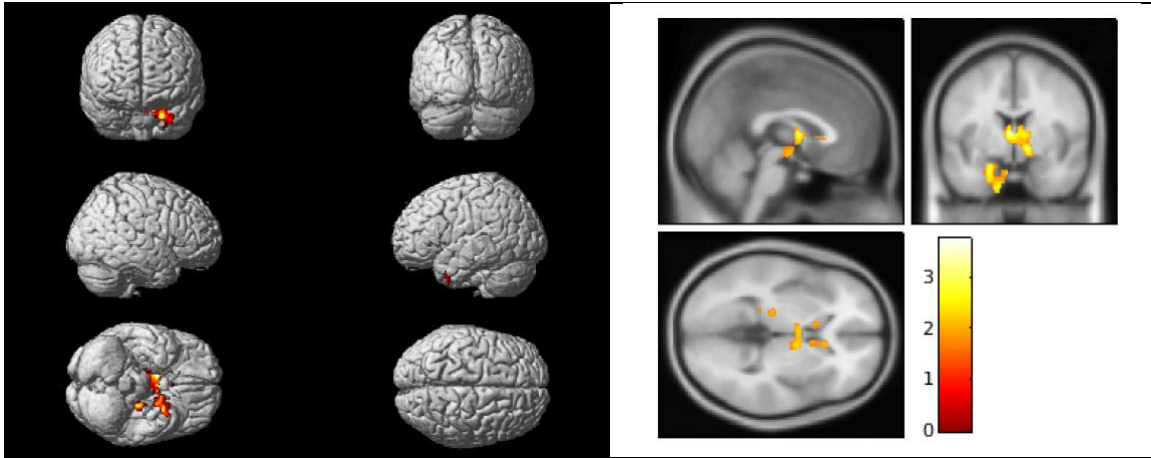


Figure 25. Visualization of negative correlations between voxel-wise CBF and global cortical Centiloid. CBF is decreased in the amygdala and parahippocampal region in those with increased global cortical Centiloid, with age, sex and total gray matter volume as covariates.  $p=0.05$ ,  $k= 250$ .

Table 20. Amyloid positivity by hypertension status interaction effect on voxel-wise CBF.  $p=0.01$ ;  $k= 250$ .

	k	ROI	X	Y	Z	Brodmann area	F	p
amyloid x hypertension interaction	558	left visual motor	-26	-54	38	7	18.57	<0.001
		left supramarginal	-50	-40	32	40	16.29	<0.001
	343	left fusiform	-50	-38	-22	37	11.61	0.001
		left fusiform	-44	-54	-2	37	10.96	0.001
	561	left visual association	-24	-48	-6	19	14.41	<0.001
		left secondary visual	-18	-76	-4	18	12.53	0.001

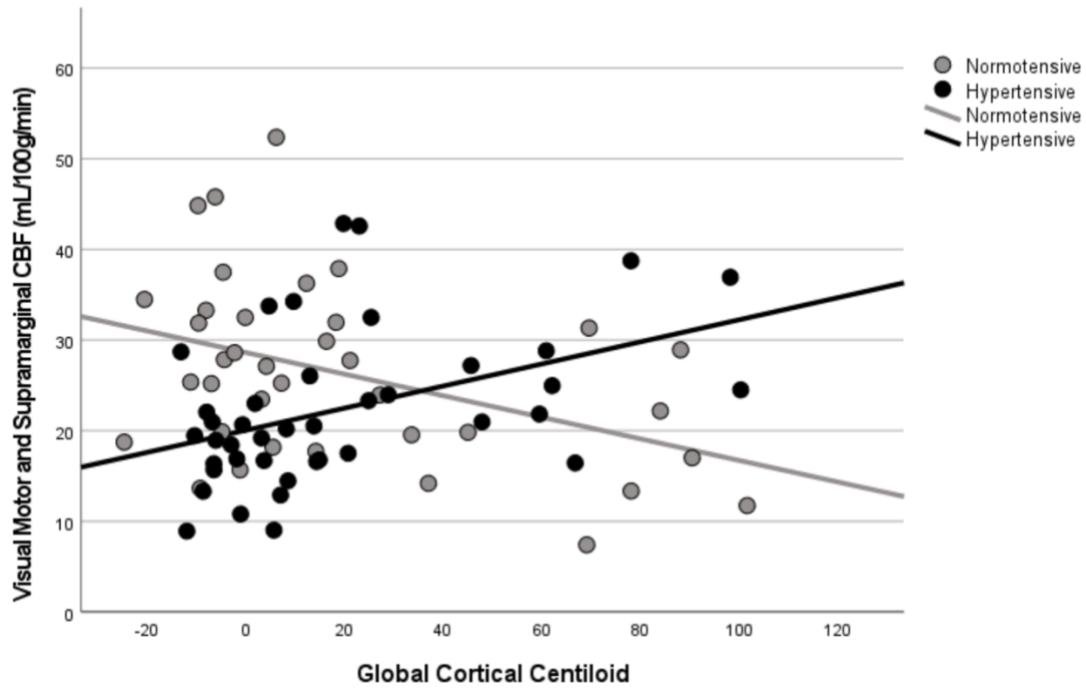


Figure 26. Global cortical Centiloid by hypertension status interaction effect on visual motor and supramarginal CBF. CBF is from a significant cluster in the voxel-wise interaction analysis. In visual motor and supramarginal regions, CBF is positively associated with global cortical Centiloid in hypertensive individuals and negatively associated with global cortical Centiloid in normotensive individuals. Black = individuals with hypertension, gray = individuals without hypertension.

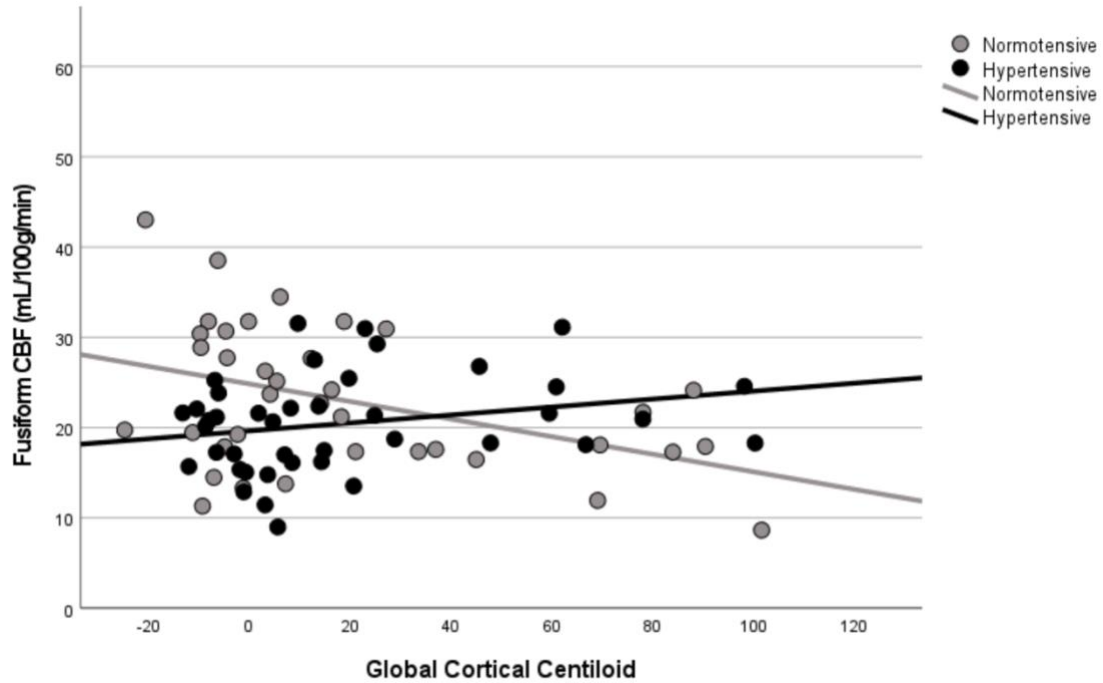


Figure 27. Global cortical Centiloid by hypertension status interaction effect on fusiform CBF. CBF is from a significant cluster in the voxel-wise interaction analysis. In the fusiform, CBF is positively associated with global cortical Centiloid in hypertensive individuals and negatively associated with global cortical Centiloid in normotensive individuals. Black = individuals with hypertension, gray = individuals without hypertension.

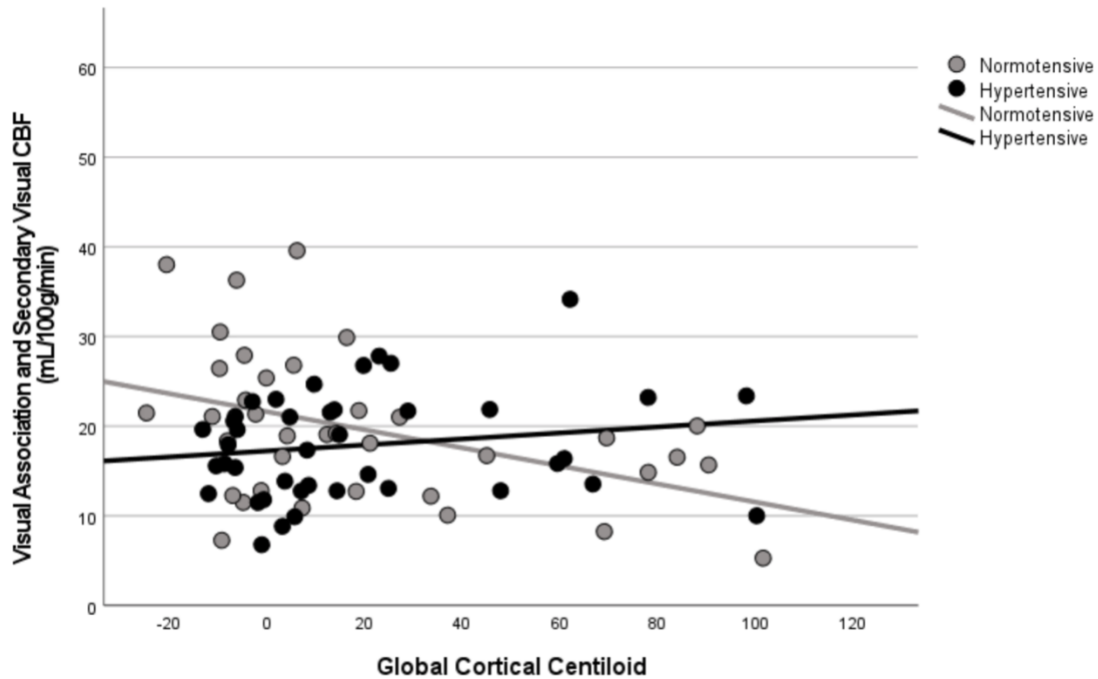


Figure 28. Global cortical Centiloid by hypertension status interaction effect on visual association and secondary visual CBF. CBF is from a significant cluster in the voxel-wise interaction analysis. In visual association and secondary visual regions, CBF is positively associated with global cortical Centiloid in hypertensive individuals and negatively associated with global cortical Centiloid in normotensive individuals. Black = individuals with hypertension, gray = individuals without hypertension.

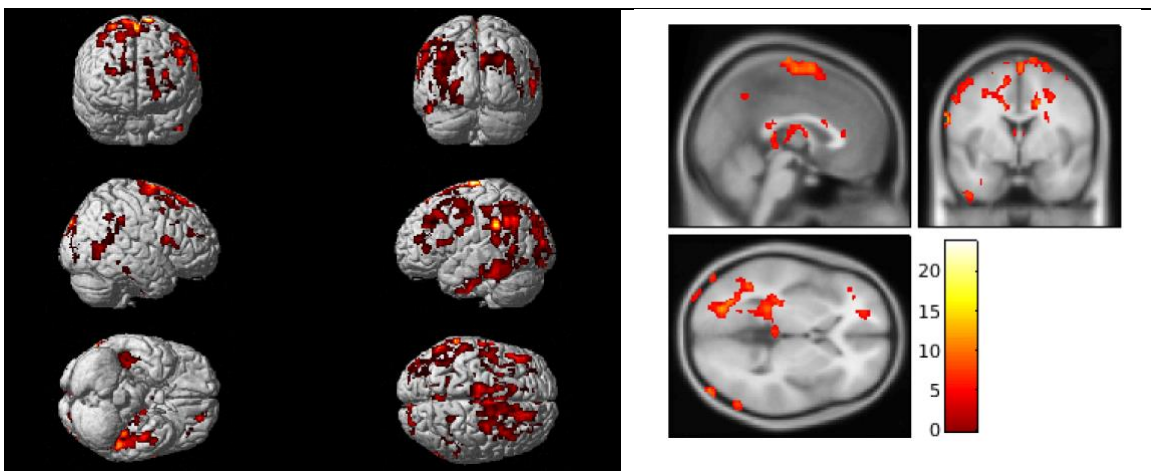


Figure 29. Visualization of amyloid positivity by hypertension status effect on voxel-wise CBF. The interaction of amyloid positivity and hypertension affects CBF in parietal, temporoparietal, temporal, and occipital regions, with age, sex and total gray matter volume as covariates.  $p=0.05$ ,  $k=250$

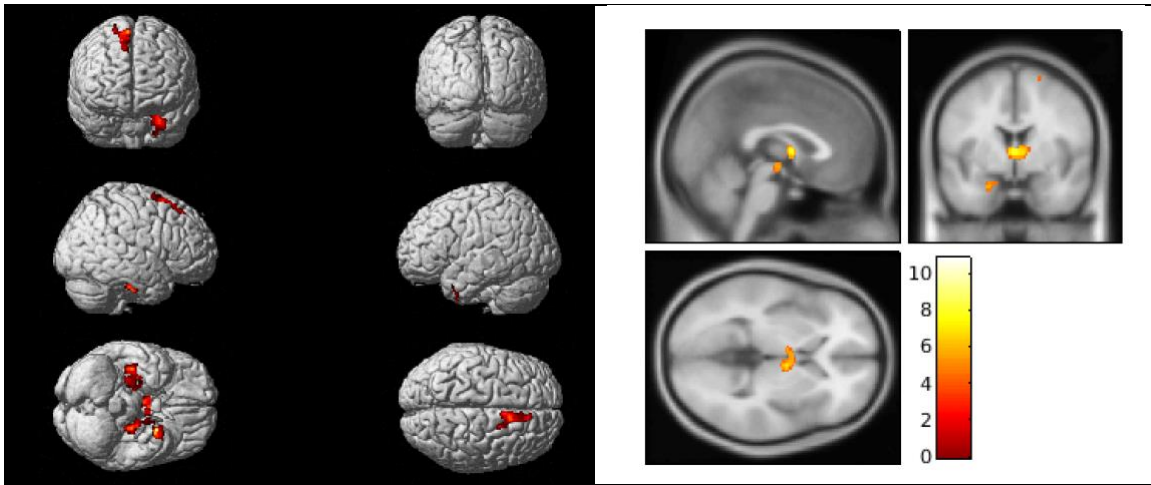


Figure 30. Visualization of amyloid positivity main effect on voxel-wise CBF. In the amyloid positivity by hypertension interaction model, global cortical Centiloid has a main effect on CBF in mainly inferior temporal regions.  $p=0.05$ ,  $k= 250$ .

Table 21. Hypertension main effect on voxel-wise CBF. Regions of CBF where there is a main effect of hypertension status in the amyloid positivity by hypertension interaction model.  $p=0.01$ ;  $k= 250$ .

	k	ROI	X	Y	Z	Brodmann area	F	p
Hypertension main effect on CBF	11729	right frontal eye fields	42	22	48	8	29.08	<0.001
		left dorsolateral PFC	-46	24	36	9	27.97	<0.001
		left pre and supplementary motor	-30	-6	62	6	24.94	<0.001
	812	right temporal pole	48	14	-30	38	21.66	<0.001
		right inferior temporal gyrus	44	0	-34	20	18.04	<0.001
		right temporal pole	44	14	-38	38	16.30	<0.001
	339	left temporal pole	-40	4	-36	38	20.96	<0.001
		left temporal pole	-36	14	-32	38	11.07	0.001
	425	left pars orbitalis	-24	28	-12	47	19.37	<0.001
		left orbital frontal	-22	38	-12	11	16.49	<0.001
	282	right anterior PFC	10	42	12	10	17.48	<0.001

		right anterior PFC	4	46	-10	10	14.71	<0.001
		right dorsal ACC	6	36	-4	32	13.42	<0.001
	340	right supramarginal	62	-34	44	40	10.38	0.002
	452	left supramarginal	-60	-36	42	40	16.87	<0.001
		left supramarginal	-64	-40	24	40	12.78	0.001
	498	right pars orbitalis	26	24	-14	47	14.14	<0.001
		right pars orbitalis	26	36	-10	47	13.06	0.001
		right orbital frontal	16	18	-20	11	12.27	0.001
	396	left angular gyrus	-46	-58	50	39	9.82	0.003

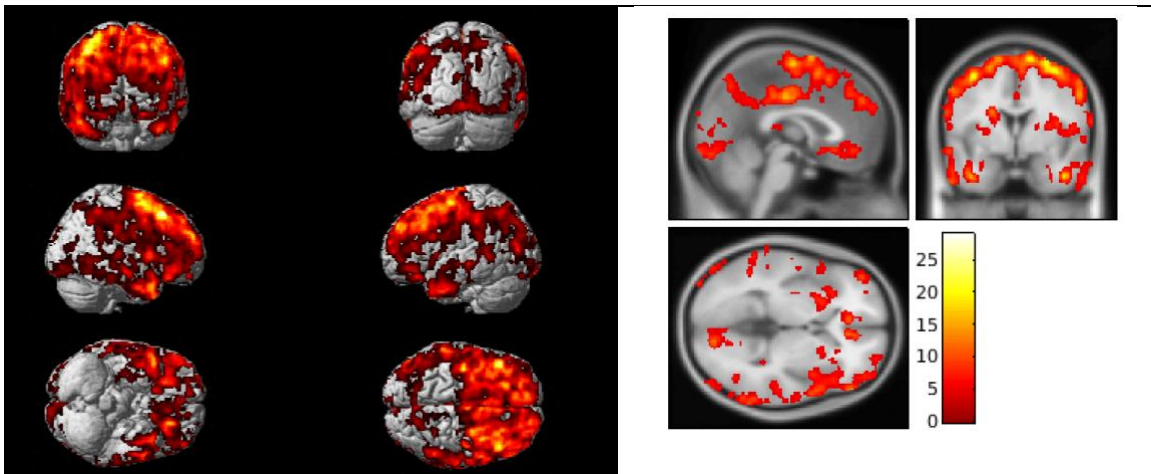


Figure 31. Visualization of hypertension main effect on voxel-wise CBF. In the amyloid positivity by hypertension interaction model, hypertension status has a main effect on CBF in widespread frontal, temporal, and temporoparietal regions.  $p=0.05$ ,  $k= 250$ .

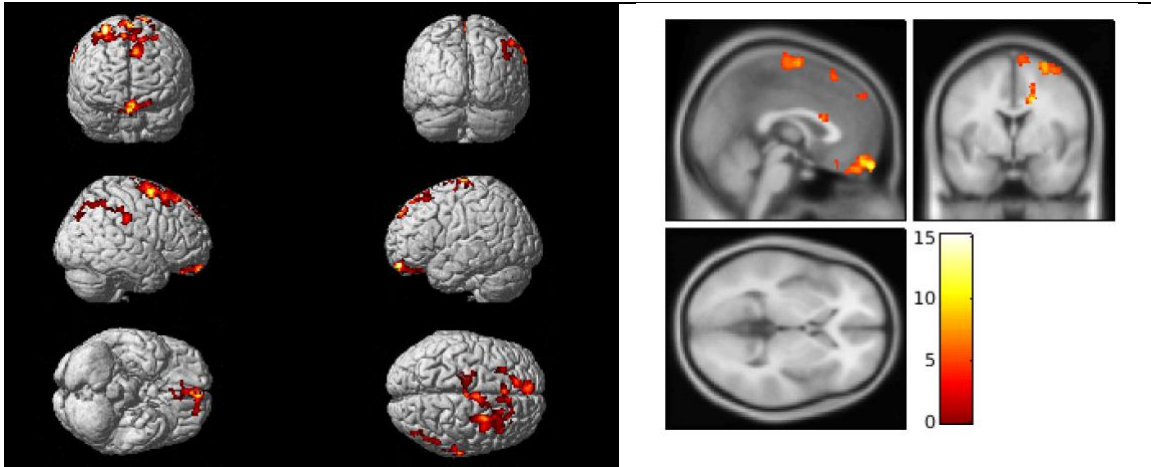


Figure 32. Visualization of amyloid positivity by *APOE*  $\epsilon 4$  positivity effect on voxel-wise CBF. The interaction of amyloid positivity and *APOE*  $\epsilon 4$  affects CBF in prefrontal and supplementary motor regions, with age, sex and total gray matter volume as covariates  $p=0.05$ ,  $k= 250$ .

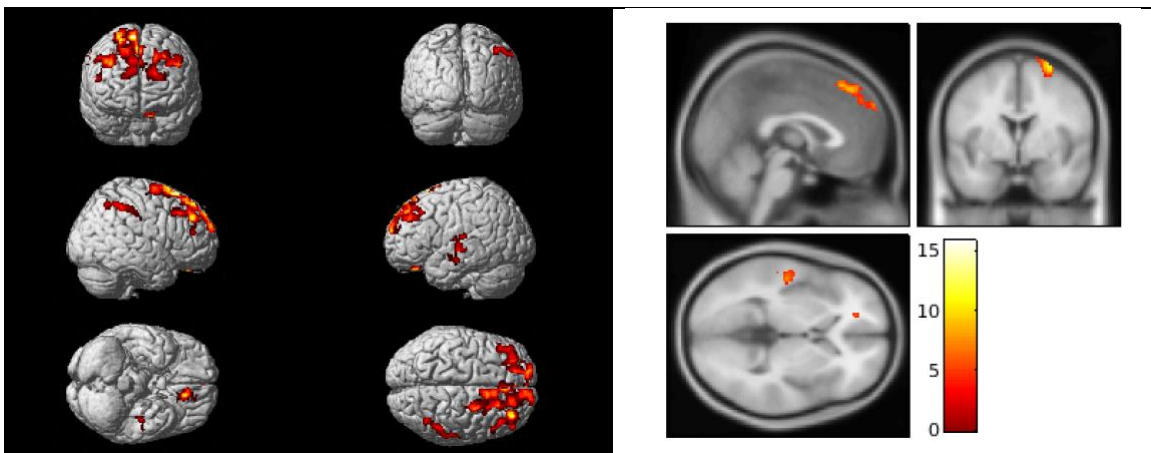


Figure 33. Visualization of MTL tau positivity by hypertension status effect on voxel-wise CBF. The interaction of MTL tau positivity and hypertension affects CBF in prefrontal, primary motor and auditory, and temporoparietal regions, with age, sex and total gray matter volume as covariates.  $p=0.05$ ,  $k= 250$ .

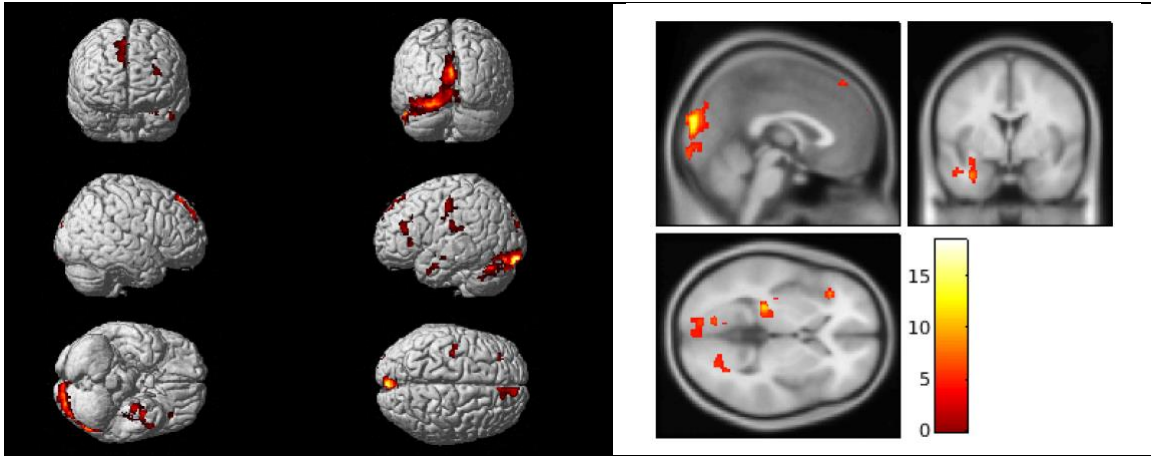


Figure 34. Visualization of MTL tau positivity by *APOE*  $\epsilon 4$  positivity effect on voxel-wise CBF.  $p=0.05$ ,  $k= 250$ . The interaction of MTL tau positivity and *APOE*  $\epsilon 4$  affects CBF in parahippocampal, primary motor and visual, occipital, and prefrontal regions, with age, sex and total gray matter volume as covariates.  $p=0.05$ ,  $k= 250$ .

## Chapter 4: Memory Concerns in the Early Alzheimer's Disease Prodrome: Regional Association with Tau Deposition

### 4.1 Introduction

Alzheimer's disease (AD), the leading cause of neurodegenerative dementia associated with aging, affects over 5 million adults in the United States and is predicted to increase to 16 million affected by 2050.<sup>166</sup> There are presently no approved pharmacological treatments that can stop the progression of AD. Treatment is likely to be most effective during the preclinical or early prodromal stages of AD, before substantial permanent neurodegenerative and cognitive damage has occurred. Therefore, there has been considerable recent interest in measures to identify older adults at highest risk for progression to AD who may benefit most from early intervention.<sup>7,167</sup>

Adults with subjective cognitive decline (SCD) in the presence of normal neuropsychological test scores are at an increased risk of progression to AD. These adults have been shown to progress to mild cognitive impairment (MCI) and eventually AD or a related dementia at a higher rate than cognitively normal (CN) adults who do not have SCD.<sup>7,168-172</sup> Adults with SCD also show subtle, subclinical differences in objective cognitive performance compared to adults without SCD and experience more functional decline over time.<sup>173</sup> Therefore, it has been suggested that SCD is potentially a preclinical stage of AD.<sup>173</sup> However, SCD has also been linked to depression, other affective disorders, and personality traits.<sup>171,174-177</sup> Therefore, it is necessary to determine the factors that influence the clinical and prognostic significance of SCD.

In addition to capturing self-based estimates of SCD, investigators often also assess the extent of concerns about cognitive decline from an informant (spouse, child, other caregiver, or clinician). Informant-based cognitive concerns are particularly important in the later stages of cognitive decline, when individuals' insight into their own cognitive problems diminishes and informant perceptions of cognition are more accurate.<sup>176,178,179</sup> In CN adults, however, self- and informant perceptions of cognitive decline are both predictive of future progression to MCI or AD, and the use of both measures together is a better predictor than either measure alone.<sup>169</sup> This finding suggests that, in very early stages of disease, both at-risk adults and their informants can provide important information about subclinical cognitive decline. Thus, using both sources of concern together may provide complementary information regarding subtle pathological changes in adults in very early preclinical stages of AD. Many adults with SCD exhibit structural and pathological changes that are typically associated with MCI or AD. For example, adults with SCD show patterns of neurodegeneration, such as decreased gray matter and hippocampal volumes, that are similar to those seen in adults with MCI.<sup>76,180,181</sup> Similarly, some adults with SCD and early mild cognitive impairment (EMCI) show AD-related pathology, such as amyloid plaques, tau tangles, and cerebrospinal fluid (CSF) profiles that are similar to those observed in AD (decreased levels of amyloid and increased levels of total and phosphorylated tau).<sup>182-184</sup> Adults with SCD or EMCI who also show AD-like pathology are more likely to progress to later stages of MCI or AD.<sup>184,185</sup> Tau aggregation is an important biomarker of disease severity along the spectrum of preclinical and clinical stages of AD. It has been previously established from measurements of tau in CSF and postmortem studies of brain tissue that

tau aggregation correlates with both neurodegeneration and the resultant cognitive decline temporally and spatially during progression of AD.<sup>186,187</sup> The recent development of tau-specific radiotracers has allowed in vivo positron emission tomography (PET) measurement and visualization of the spatial distribution of tau aggregation for the first time.<sup>188</sup> Tau radiotracers have permitted in vivo correlation of tau aggregation and other markers of disease progression, including increased cognitive decline, amyloid deposition, and CSF measures of amyloid and tau.<sup>189</sup> Spatial information about the tau anatomical distribution has also been shown to provide important clinical information; brain regions with high levels of tau aggregation often correspond to declines in cognitive functions related to those regions.<sup>161</sup>

Because tau aggregation correlates spatially with brain areas implicated in cognitive decline, it is possible that self-based memory concerns correlate more strongly with tau aggregation in brain regions involved in introspection or internal thought processes, for example, the medial prefrontal cortex. More generally, the frontal cortex has been implicated in several aspects of conscious internal processing, such as planning, decision-making, and inhibition of actions by thinking through consequences. It is possible that preclinical pathological changes in frontal brain regions would be noticeable to the patient before causing outward changes in behavior due to impacts on the processes of internal thought. On the other hand, informant memory concerns may correlate more strongly with tau aggregation in brain regions typically seen in patients with MCI and AD, as these may be involved in common initial symptoms of AD (i.e., memory decline) that are more likely to be noticed by an observer.

To determine how self- and informant perceptions of cognitive decline are each related to tau deposition in the early stages of AD, we assessed the relationship between self- and informant scores on the memory subscale of the Test of Everyday Cognition (ECog<sup>190</sup>), as well as the association of each with regional and global tau aggregation as measured by the tau PET radiotracer [<sup>18</sup>F]flortaucipir (T-807; AV-1451). Our goal was to evaluate the relationship between self- and informant memory concerns and tau deposition to investigate the biological basis for the predictive power of cognitive concerns and whether the self- and informant concerns could be utilized as part of a screening protocol to assess preclinical AD in individual adults. We included older adults enrolled in the Alzheimer's Disease Neuroimaging Initiative (ADNI) who were defined as CN controls, had significant memory concerns (SMCs), or had EMCI. These adults comprise a continuum of risk for developing clinical AD. A subset of the CN older adults are amyloid negative and apolipoprotein E gene (*APOE*)  $\epsilon$ 4 noncarriers and thus are at risk for AD due to age alone and are on the “low-risk” end of the continuum. On the “high-risk” end are adults with EMCI who have subtle cognitive decline, presence of self- and informant cognitive concerns, and are amyloid positive and/or *APOE*  $\epsilon$ 4 carriers. We examined the association of self- and informant ECog memory scores with one another and with tau aggregation in all participants. Following these analyses, we completed a subanalysis using only participants who are amyloid positive because these participants are at a relatively higher risk of developing AD. We hypothesized that self- and informant ECog memory scores would be mildly correlated with one another, and that higher ECog memory scores (indicating greater perceived memory decline) would be associated with increased levels of tau. Finally, we also hypothesized that self- and

informant scores would potentially correlate with the distribution of tau aggregation in spatially different patterns of association throughout the brain.

## 4.2 Methods

### Participants

Data used in the preparation of this article were obtained from the ADNI database (<http://adni.loni.usc.edu>; Supplementary Material). For up-to-date information, see <http://www.adni-info.org>. The 82 participants included in this study were diagnosed as CN older adults, SMC participants, or EMCI participants by the ADNI-2 procedures manual criteria (<http://www.adni-info.org>). According to these criteria, 40 CN participants had no subjective or informant complaint of cognitive decline and performed normally on the Wechsler Logical Memory Delayed Recall (LM-delayed) and the Mini-Mental State Examination (MMSE). 11 SMC participants expressed subjective memory concerns on the CCI<sup>191,192</sup> (total score from first 12 items  $\geq 16$ ) but had no significant informant complaint of cognitive decline and performed normally on the LM-delayed and MMSE. Finally, 31 EMCI participants had subjective, informant, and/or clinician complaint of cognitive decline, memory function approximately one standard deviation (SD) below normal on the LM-delayed, a MMSE total score greater than 24, and functioning at a level that precluded a diagnosis of AD. For the amyloid-positive group, we included only CN, SMC, and EMCI participants who were amyloid positive ( $n = 36$ ; 15 CN, 4 SMC, and 17 EMCI) on the [<sup>18</sup>F]florbetapir PET scan closest to the [<sup>18</sup>F]flortaucipir PET scan, using data generated by the University of California, Berkeley, and downloaded from the ADNI site (global standardized uptake value ratio

[SUVR] > 1.11).<sup>193</sup> The percentage of subjects that were amyloid positive did not differ by the diagnostic group.

### Clinical and Cognitive Assessments

Clinical and cognitive performance data were obtained from the ADNI database (<http://adni.loni.usc.edu>). Participants were given clinical and cognitive tests as described in the ADNI-2 manual ([www.adni-info.org](http://www.adni-info.org)). For the primary analyses, we used self- and informant ECog memory scores, which are the averages of ratings on the eight questions in the memory section of the ECog. The ECog score from the test given closest in time to the [<sup>18</sup>F]flortaucipir scan was used [full sample: mean (SD) = 145.5 (186.8) days; amyloid-positive sample: mean (SD) = 128.4 (158.2) days], which did not differ by the diagnostic group.

### [<sup>18</sup>F]flortaucipir PET scans

Preprocessed [<sup>18</sup>F]flortaucipir PET scans were downloaded from the ADNI Laboratory of Neuro Imaging (LONI; <http://adni.loni.usc.edu>) site. These scans were preprocessed using standard techniques in Statistical Parametric Mapping 8 (SPM8), including normalization to Montreal Neurologic Institute (MNI) space. Then, SUVR images were created by intensity normalization using a cerebellar crus reference region. Regional mean SUVR was extracted from subject-specific regions of interest (ROIs), including the bilateral mean parahippocampal gyri, frontal lobe, parietal lobe, and global cortex. ROIs were generated from the closest in time structural MRI scan using FreeSurfer, version 5.1.

## Statistical analysis

Partial Pearson correlations were used to assess the association between self- and informant ECog memory scores and with tau aggregation in the target ROIs using SPSS Statistics, version 24 (IBM Corporation, Somers, NY). Covariates for these analyses included age, sex, and years of education. Furthermore, *APOE*  $\epsilon$ 4 carrier status (where positive is having at least one *APOE*  $\epsilon$ 4 allele and negative is not having an *APOE*  $\epsilon$ 4 allele regardless of whether the other alleles are *APOE*  $\epsilon$ 2 or *APOE*  $\epsilon$ 3) and Geriatric Depression Scale (GDS) total score were tested as potential covariates in secondary analyses. The associations were assessed in the whole group of participants, as well as in amyloid-positive participants only and in amyloid-negative participants only.

$\chi^2$  tests were used to evaluate the association of sex, *APOE*  $\epsilon$ 4 positivity, or amyloid positivity with the diagnostic group. A one-way analysis of variance (ANOVA) was used to assess differences in age, years of education, a composite memory score, GDS score, self-ECog memory score, and informant ECog memory score by the diagnostic group. Again, these associations were examined using all participants and in amyloid-positive participants only. Post hoc differences were evaluated after Bonferroni adjustment for multiple comparisons, with  $P < .05$  after correction considered significant.

## Voxelwise analysis

In addition, the associations of self- and informant ECog memory scores and [ $^{18}$ F]flortaucipir SUVR were evaluated on a whole-brain voxelwise basis in SPM8 using a multiple linear regression model, masked for the gray plus white matter, and including age, sex, and years of education as covariates. Significance was set at a voxelwise

threshold of  $P < .005$  (uncorrected for multiple comparisons) and a minimum cluster size (k) of 675 voxels, which corresponds to a clusterwise threshold of  $P < .05$  (familywise error [FWE] correction for multiple comparisons). Talairach Daemon was used to identify brain regions of significant clusters. As in the regional analyses, the voxelwise analyses included an initial analysis using the whole sample and a follow-up analysis included amyloid-positive participants only.

### 4.3 Results

#### Demographics

Effects of diagnosis on demographics, neuropsychological test scores, and self- and informant ECog memory scores are shown in Table 22 for all participants and in Table 23 for amyloid-positive participants. For all participants, as expected, participants with EMCI had lower memory performance with lower composite scores than CN participants ( $P = .007$ ). Participants with EMCI had higher informant ECog memory scores than CN participants ( $P < .001$ ). Sex was significantly different across diagnostic groups such that men made up a greater percentage of the EMCI group, whereas women made up a greater percentage of the CN group ( $P = .049$ ). There were no significant differences in age, years of education, GDS scores, *APOE*  $\epsilon 4$  positivity, amyloid positivity, or self-ECog memory scores between diagnostic groups. For amyloid-positive participants, participants with EMCI had lower memory composite scores than CN participants ( $P = .045$ ). Participants with EMCI also had higher informant ECog memory scores than CN participants ( $P = .019$ ). No significant differences in age, years of

education, sex, GDS scores, *APOE*  $\epsilon$ 4 genotype, or self-ECog memory scores were observed between diagnostic groups.

#### Association of self- and informant ECog memory scores

Self-ECog memory scores were only mildly correlated with informant ECog memory scores, after covariate adjustment, when all participants were included ( $r = 0.362$ ,  $r_p = 0.001$ ). When only amyloid-positive participants were included, the correlation between self- and informant ECog memory scores did not reach statistical significance ( $r = 0.243$ ,  $r_p = 0.173$ ).

#### Regional analysis in all participants

Self-ECog memory scores were significantly correlated with tau aggregation, after covariate adjustment, in all four ROIs (parahippocampal:  $r_p = 0.293$ ,  $P = .009$ ; frontal:  $r_p = 0.329$ ,  $P = .003$ ; parietal:  $r_p = 0.291$ ,  $P = .009$ ; and global:  $r_p = 0.306$ ,  $P = .006$ ; Fig. 35A). Informant ECog memory scores were similarly significantly associated with tau aggregation in all four regions, but the correlation with tau aggregation in the parietal region was the strongest (parahippocampal:  $r_p = 0.283$ ,  $P = .011$ ; frontal:  $r_p = 0.259$ ,  $P = .021$ ; parietal:  $r_p = 0.411$ ,  $P < .001$ ; and global:  $r_p = 0.296$ ,  $P = .008$ ; Fig. 35B).

#### Regional analysis in amyloid-positive participants

When only amyloid-positive participants were included, self-ECog memory scores were again significantly correlated with tau aggregation in all four regions, and the

strongest association was in the frontal lobe (parahippocampal:  $r_p = 0.411$ ,  $P = .018$ ; frontal:  $r_p = 0.517$ ,  $P = .002$ ; parietal:  $r_p = 0.352$ ,  $P = .044$ ; and global:  $r_p = 0.459$ ,  $P = .007$ ; Fig. 36A). Alternatively, informant ECog memory scores were significantly correlated with tau aggregation in all regions except for the frontal region (parahippocampal:  $r_p = 0.347$ ,  $P = .048$ ; frontal:  $r_p = 0.341$ ,  $P = .052$ ; parietal:  $r_p = 0.514$ ,  $P = .002$ ; and global:  $r_p = 0.416$ ,  $P = .016$ ), and the strongest correlation with tau aggregation was in the parietal region (Fig. 36B). When only amyloid-negative participants were included, neither self- nor informant ECog memory scores were correlated with tau aggregation in any of the ROIs (*data not shown*).

#### Interaction analysis

To determine whether there is a significant interaction of source of cognitive concern (self vs. informant) and location of tau deposition (frontal vs. parietal), we calculated the difference scores by subtracting informant ECog memory scores from self-ECog memory scores and mean frontal parietal from mean frontal [ $^{18}\text{F}$ ]flortaucipir SUVR. We then evaluated the association between these two difference scores. A statistically significant concern source-by-region interaction was observed in which self-scores are preferentially associated with tau aggregation in frontal regions and informant scores are preferentially associated with tau aggregation in parietal regions, both in all participants and in amyloid-positive participants (Fig. 37). Including either *APOE*  $\epsilon 4$  allele positivity or GDS scores as additional covariates did not change the observed pattern of results in either the full sample or the amyloid-positive only sample (*data not shown*).

## Voxelwise analyses

To assess the spatial differences between the associations with tau and self- and informant ECog memory scores without the bias of using our predetermined ROIs, we performed voxelwise analyses in SPM8. In all participants, the self–ECog memory scores were associated with tau in the following regions: bilateral frontal lobe (middle, medial, superior, and inferior frontal gyri), left frontal subgyral region, right temporal lobe (middle, superior, inferior, and fusiform gyri and subgyral region), bilateral precentral gyrus, left postcentral gyrus, bilateral cingulate gyrus, bilateral anterior cingulate, bilateral posterior cingulate, right parahippocampal gyrus, right precuneus, right insula, right uncus, and anterior lobe of right cerebellum (clusterwise threshold of  $P < .05$  FWE; Table 24; Fig. 38A). Informant ECog memory scores were associated with tau aggregation in the following regions: bilateral frontal lobe (middle, medial, and superior frontal gyri), right frontal subgyral region, bilateral temporal lobe (middle, inferior, and fusiform gyri), left superior temporal gyrus, right supramarginal gyrus, bilateral precentral gyrus, right inferior parietal lobule, right occipital lobe (middle and superior occipital gyri), left inferior occipital gyrus, bilateral precuneus, left cuneus, bilateral posterior cingulate, bilateral cingulate gyrus, right insula, bilateral posterior lobe of cerebellum, and anterior lobe of left cerebellum (clusterwise threshold of  $P < .05$  FWE; Table 25; Fig. 38B).

In amyloid-positive participants, self–ECog memory scores were associated with tau aggregation in the following regions: bilateral frontal lobe (middle, inferior, and subcallosal gyri), left medial frontal gyrus, right temporal lobe (middle and inferior temporal gyri), right precentral gyrus, bilateral anterior cingulate, right putamen, right

uncus, right insula, and anterior lobe of right cerebellum (clusterwise threshold of  $P < .05$  FWE; Table 26; Fig. 38C). Informant ECog memory scores were associated with tau aggregation in the following regions: bilateral frontal lobe (middle, medial, superior, and inferior gyri and subgyral region), bilateral middle temporal gyrus, right supramarginal gyrus, left superior temporal gyrus, bilateral precentral gyrus, right postcentral gyrus, bilateral precuneus, bilateral cingulate gyrus, bilateral posterior cingulate, left cuneus, right insula, and posterior lobe of right cerebellum (clusterwise threshold of  $P < .05$  FWE; Table 26; Fig. 38D).

#### 4.4 Discussion

In this study, we found that self- and informant memory concerns are both correlated with tau aggregation in at-risk adults, but that the overall spatial patterns of associations differ between the two measures of subjective memory concern. We found that self- and informant ECog memory scores are only mildly correlated with one another in at-risk adults and are not correlated with one another in the subset of amyloid-positive adults, suggesting that the two measures of subjective memory complaints may be somewhat independent and provide complementary information. The results from our ROI-based analyses suggest that self-based memory complaints are most strongly associated with tau aggregation in the frontal lobes, whereas informant memory complaints are most strongly associated with tau aggregation in the parietal lobes. These differences in patterns of correlation were enhanced when only amyloid-positive participants were included, and significant source-by-region interactions were found in both the full analysis and the sub-analysis of amyloid-positive individuals. There were no

correlations found when only amyloid-negative participants were included, suggesting that the patterns of association found are specifically present in adults at higher risk for developing AD, which supports the idea that these subjective memory tools may be useful for optimizing screening techniques in the population of at-risk adults. In addition to our regional analyses, we evaluated the associations with voxel-wise analyses to lessen the bias imposed by our predetermined ROIs. Although these analyses revealed regions of overlap between the correlations of tau aggregation with self- and informant memory concerns, they resulted in the same general patterns found with the ROI-based analyses. Specifically, both self- and informant memory concerns were associated with tau aggregation in the frontal and temporal lobes when all participants were included, while the informant memory concerns were also associated with tau aggregation in posterior brain regions, including the parietal and occipital lobes. When only amyloid-positive participants were included, the self-based memory concerns were significantly associated with tau aggregation in bilateral frontal lobes and the right temporal lobe, while the informant memory concerns were also correlated with tau burden in the left parietal lobe and bilateral occipital lobes.

Our data suggest that self-based memory concerns correlate more strongly with tau aggregation in regions typical of conscious internal thought processes (i.e., frontal lobe, specifically the medial prefrontal region), while informant memory concerns correlate more strongly with tau aggregation in posterior regions typical of more progressed MCI and AD patients. These posterior regions may be involved with the more outward signs of cognitive decline that can be noticed by an observer who knows the individual well. In support of this implication of our results, the voxel-wise analysis

revealed that only self-based memory concerns were correlated with tau aggregation in the bilateral anterior cingulate, while only informant memory concerns were correlated with tau aggregation in the supramarginal gyri. The anterior cingulate has been shown to be involved in decision-making,<sup>194</sup> while the supramarginal gyrus is involved in language perception and processing.<sup>195</sup> While correlations within these specific brain regions are interesting, future research focused on the relationship between subjective memory concerns and regional pathology will be necessary to confirm the relationships that we observe here.

Because both self-based cognitive complaints and pathological changes in the frontal lobe have been shown to be correlated with depression,<sup>171,174,175,196</sup> we used GDS scores as a covariate along with age, sex, and years of education to ensure that depressive symptomology was not a confound in the observed correlations. The inclusion of this score as a covariate did not significantly change the patterns of association; the self-based memory concerns were still significantly correlated to tau in the frontal region (*data not shown*). Individuals' depressive symptoms have been shown to increase informant-based cognitive complaints in other studies as well,<sup>179,197</sup> but the pattern of association between informant based memory concerns and tau was not changed when GDS scores were used as a covariate (*data not shown*). It is still possible that some of the participants experienced subtle depressive symptoms that were not reflected in the GDS scores but still influenced their perceptions of their own cognitive functioning. Future studies exploring the interactions between depression, cognitive concerns, and AD pathophysiology are warranted.

Overall, our findings suggest that subjective memory concerns have the potential to be optimized and used as part of a screening protocol for AD-related pathology and disease progression in adults with preclinical or prodromal stages of AD. Along with the differing regions of tau association between the two measures of subjective memory concern, this finding suggests that using both self- and informant measures together may provide important complementary information, such that high scores on both measures may suggest a greater overall tau burden in the brain. Finally, these results provide a potential biological explanation for the previous finding that using self- and informant memory concerns together is a better predictor of future progression to MCI or AD than either measure alone.<sup>169</sup>

This study does have some potential limitations. First, our sample size, especially in the amyloid-positive sub-analysis, was relatively small, which could lead to bias. Although we included all available CN, SMC, and EMCI participants in ADNI-2 who had tau scans at the time of our analyses, we recognize that the CN group had more *APOE*  $\epsilon$ 4 carriers than expected in the general population and that the amyloid positivity surprisingly did not differ between the diagnostic groups. Second, we also acknowledge that there may have been unforeseen selection bias in the ADNI-2 study. Future studies in larger samples will help to support the present findings. In addition, the SMC group from ADNI-2 was defined on the basis of subjective- or self-based memory complaints but not informant-based concerns. Therefore, there was not a group in this study for participants who had solely informant-based complaints in the context of normal or above average cognitive functioning. Third, this study only evaluated cross-sectional data; future studies with longitudinal data are needed to address changes in self- and informant concerns

across the disease spectrum and their association with changes in AD pathophysiology. Evaluating whether CN individuals who later progress to AD show different patterns of self- and/or informant cognitive concerns and differing patterns of association of these concerns with AD pathology could further validate quantitative assessment of memory concerns as a useful screening tool. Finally, we used Talairach Daemon to define the brain regions from our voxel-wise analysis. Although this atlas is not specific to our study or to an aging population, we felt that it was the most appropriate tool to use in this case. A standardized atlas specific for older adults has not been defined in the literature, and our small sample size kept us from producing our own study-specific atlas. We do not expect that extensive atrophy should confound the results of the Talairach Daemon atlas in our preclinical AD population, and we visually inspected labeled regions for accuracy. However, we acknowledge that use of this nonspecific atlas may have caused minor labeling issues in our aging participants.

In summary, we demonstrated that both self- and informant memory concerns are associated with tau aggregation in adults at risk for AD. Furthermore, we found that self- and informant memory concerns correlate with tau aggregation in spatially different patterns of association throughout the brain. Overall, these findings suggest that both self- and informant memory concerns have the potential to be used as part of a screening process for preclinical AD and that they may also provide complementary information about both future conversion and AD-related pathological patterns. Although future studies are needed, it may be the case that the discrepancy between self- and informant memory concerns could help determine the location of tau aggregation for individuals, thus adding information for better detection, diagnosis, and prognosis of future decline.

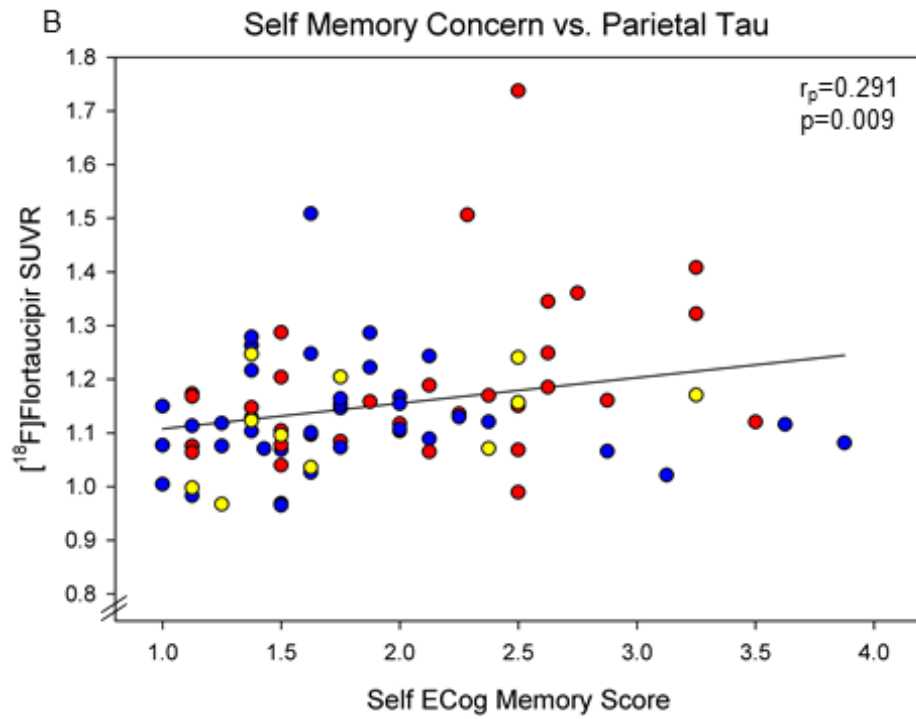
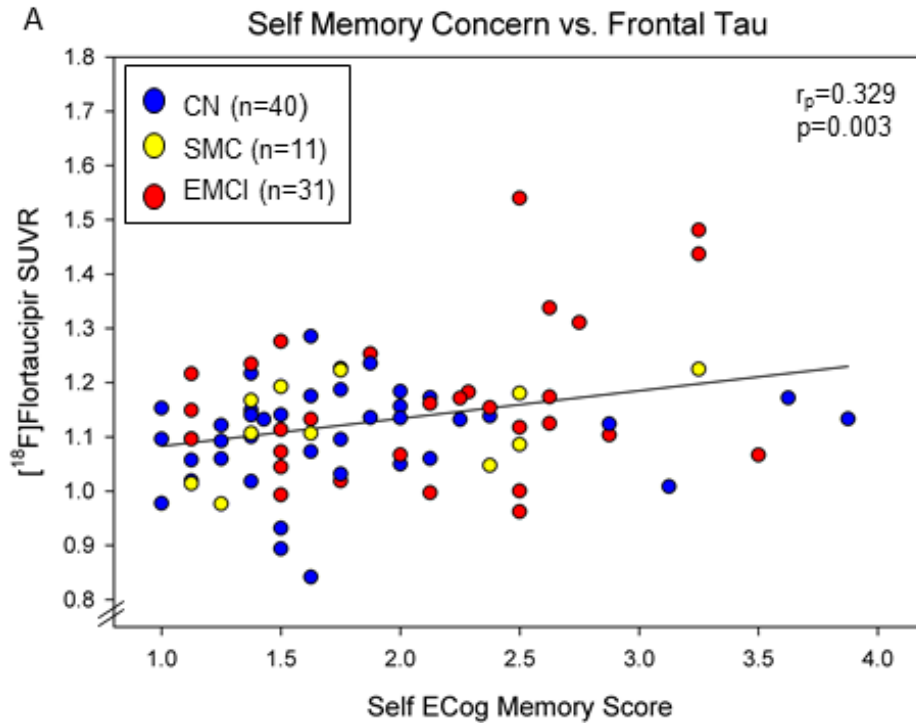
Future studies with larger sample sizes and longitudinal data will help to further elucidate which measures of perceived cognitive decline and which patterns of tau aggregation are most accurate at predicting progression to AD.

Table 22. Demographic and clinical variables of full sample by diagnostic group. Abbreviations can be found in the List of Abbreviations (p. xii).

Variable	CN (n = 40)	SMC (n = 11)	EMCI (n = 31)	p-value	Significant Pair Comparisons*
Age (years)	76.48 (7.21)	71.55 (5.11)	75.32 (7.29)	0.125	None
Education (years)	16.03 (2.37)	16.00 (2.49)	17.03 (2.39)	0.184	None
Sex (M,F)	17, 23	5, 6	22, 9	0.049	N/A
<i>APOE</i> ε4 positivity (%)	42.5	45.5	25.8	0.256	N/A
Amyloid positivity (%)	37.5	36.4	54.8	0.297	N/A
Memory Composite	1.23 (0.67)	1.20 (0.63)	0.73 (0.69)	0.007	EMCI < CN
GDS total	1.21 (1.59)	0.91 (0.83)	1.52 (1.88)	0.527	None
Self ECog Memory	1.77 (0.66)	1.88 (0.68)	2.11 (0.68)	0.114	None
Informant ECog Memory	1.41 (0.48)	1.52 (0.50)	2.02 (0.77)	<0.001	EMCI > CN

Table 23. Demographic and clinical variables of amyloid-positive subset by diagnostic group. Abbreviations can be found in the List of Abbreviations (p. xii).

	CN (n=15)	SMC (n=4)	EMCI (n=17)	p-value	Significant Pair Comparisons*
Age (years)	75.93 (5.56)	71.25 (7.18)	75.71 (8.19)	0.485	None
Education (years)	16.67 (1.54)	16.50 (1.73)	16.18 (2.68)	0.816	None
Sex (M,F)	5, 10	1, 3	12, 5	0.062	N/A
<i>APOE</i> ε4 positivity (%)	46.7%	100%	41.2%	0.1	N/A
Memory Composite	1.39 (0.49)	1.02 (0.91)	0.75 (0.81)	0.05	EMCI < CN
GDS total	0.93 (1.10)	1.00 (0.82)	1.18 (1.94)	0.904	None
Self ECog Memory	1.88 (0.89)	1.97 (0.66)	2.24 (0.60)	0.403	None
Informant ECog Memory	1.38 (0.50)	1.53 (0.57)	2.13 (0.91)	0.02	EMCI > CN



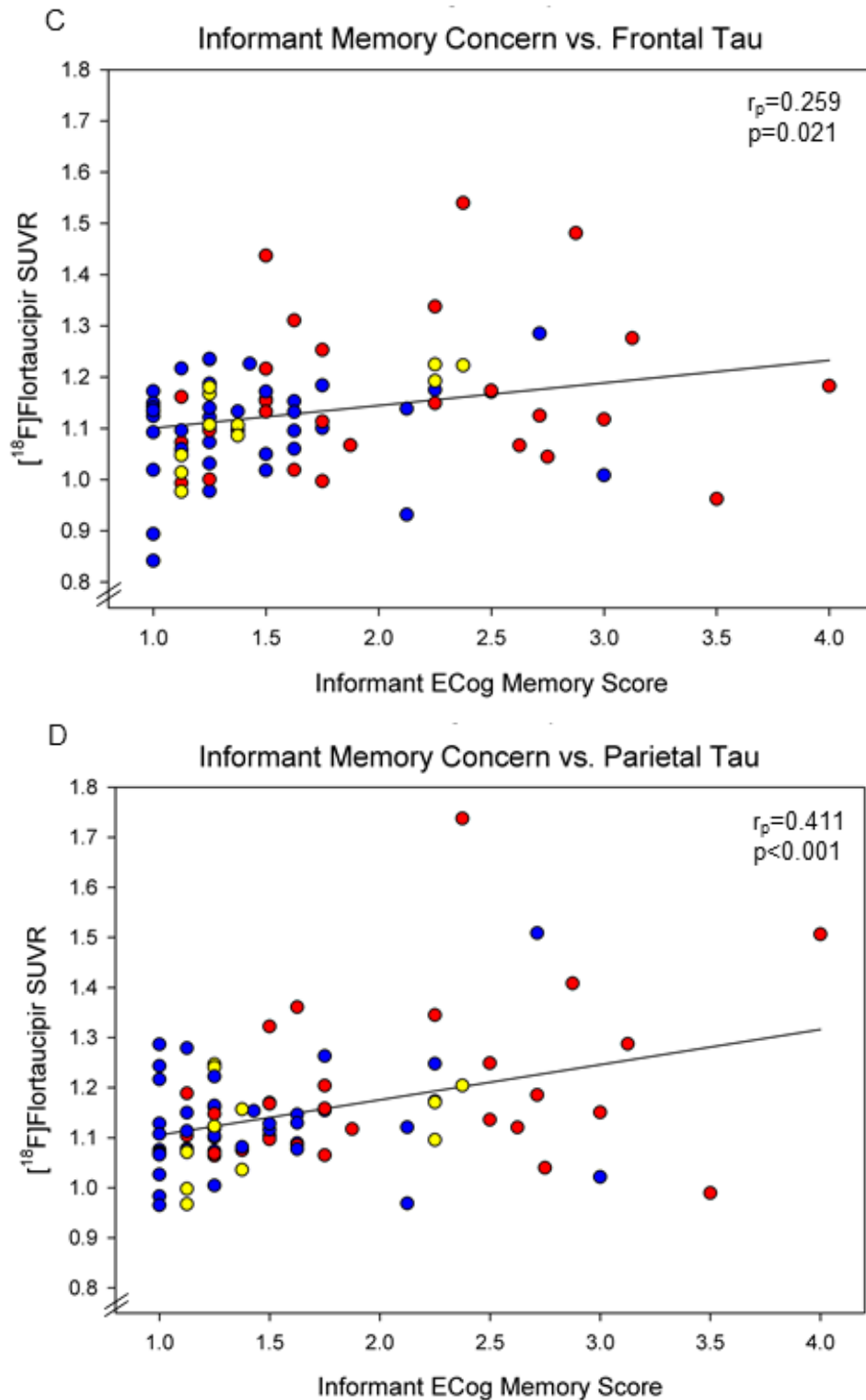
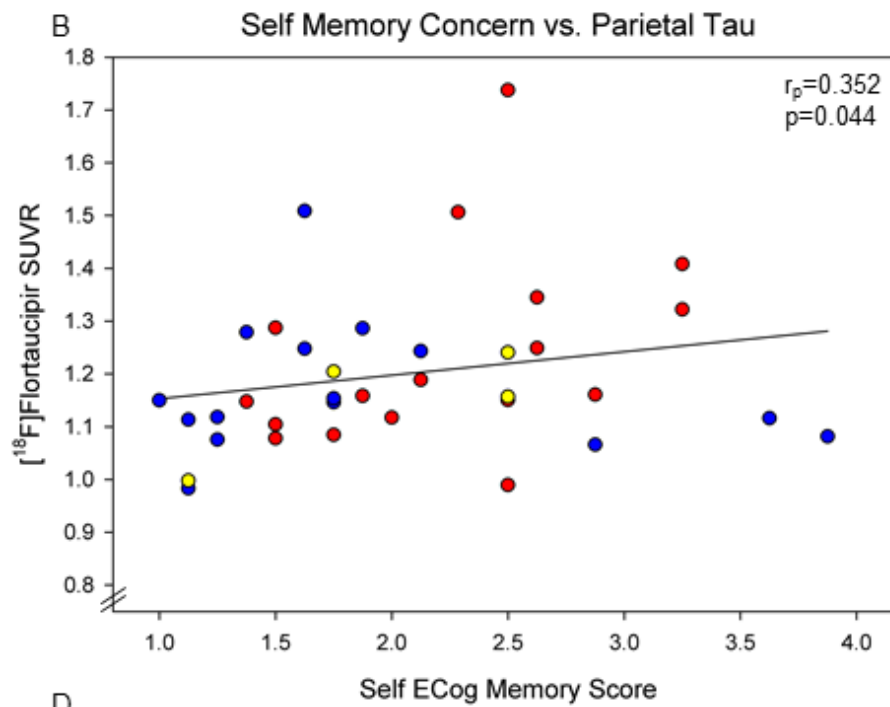
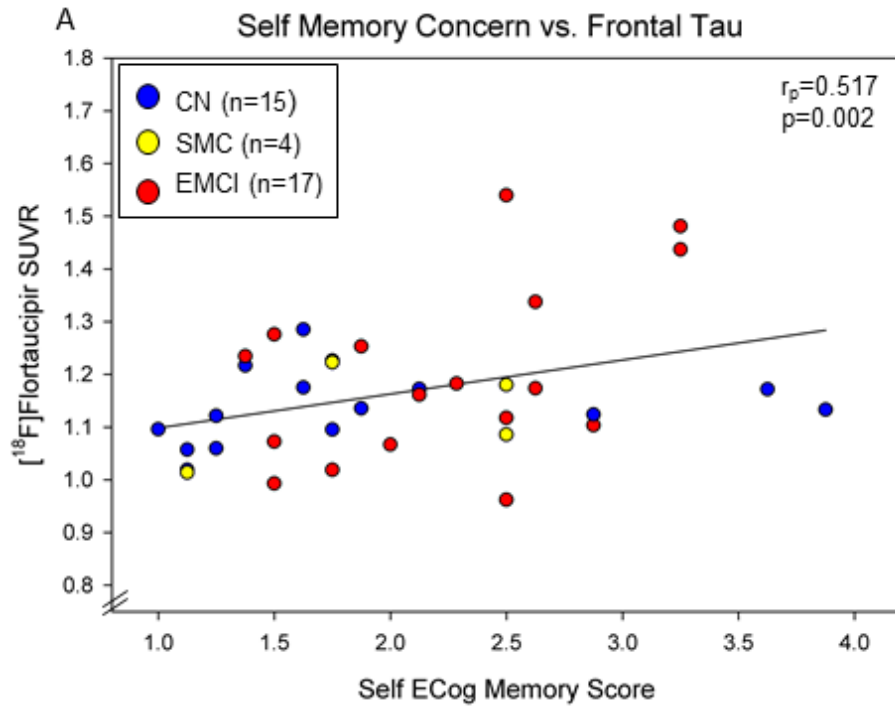


Figure 35. Relationships between self and informant memory concerns with frontal and parietal tau in the full sample. Both self and informant ECog scores were positively associated with frontal and parietal tau aggregation. Informant scores were most strongly associated with tau aggregation in the parietal lobe.



D

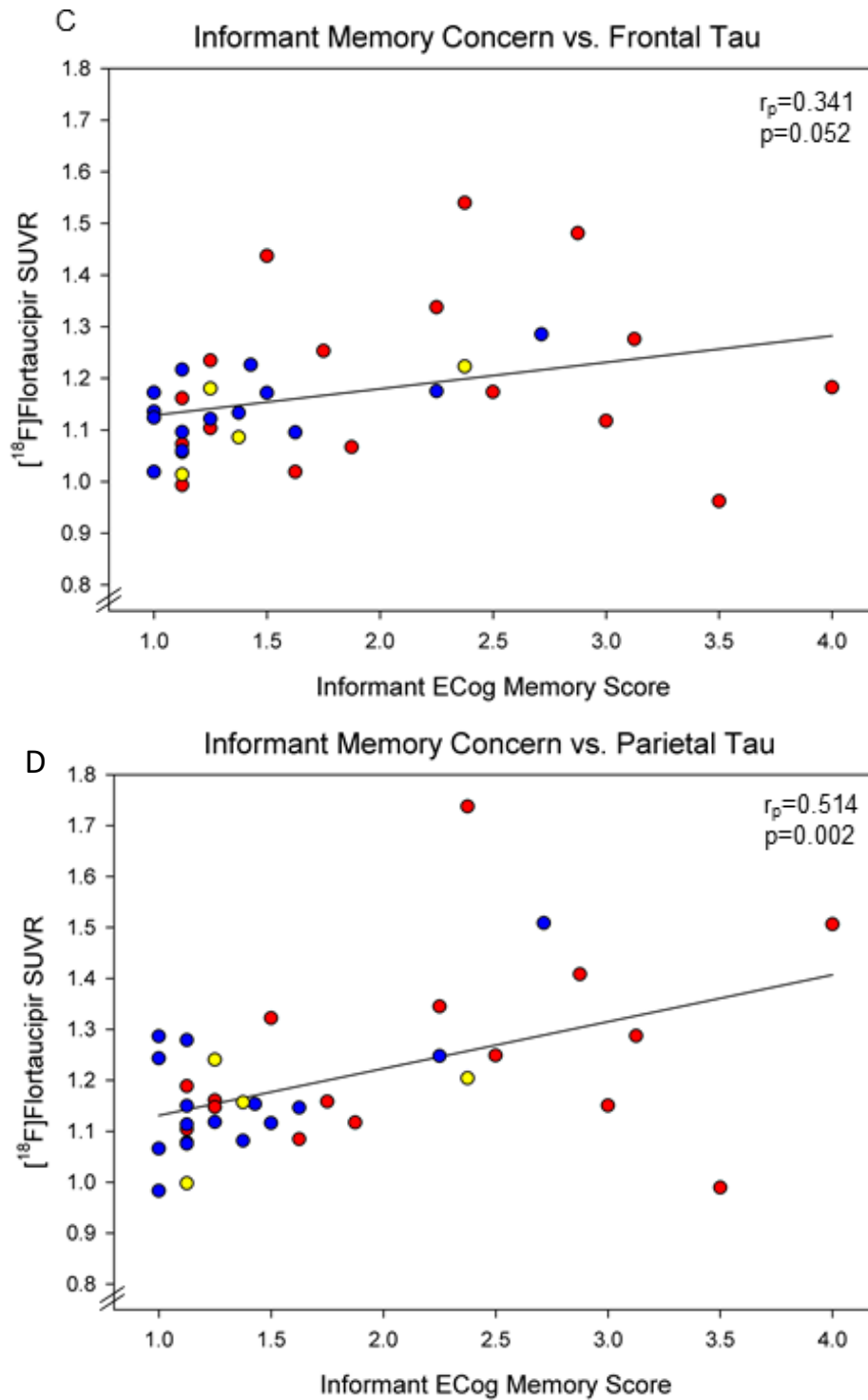


Figure 36. Relationships between self and informant memory concerns with frontal and parietal tau in the amyloid-positive subset. In amyloid-positive individuals, self ECog scores were positively associated with frontal and parietal tau aggregation, with the strongest association in the frontal lobe. Informant ECog scores were positively associated with tau aggregation in the parietal lobe, but the association did not reach statistical significance in the frontal lobe.

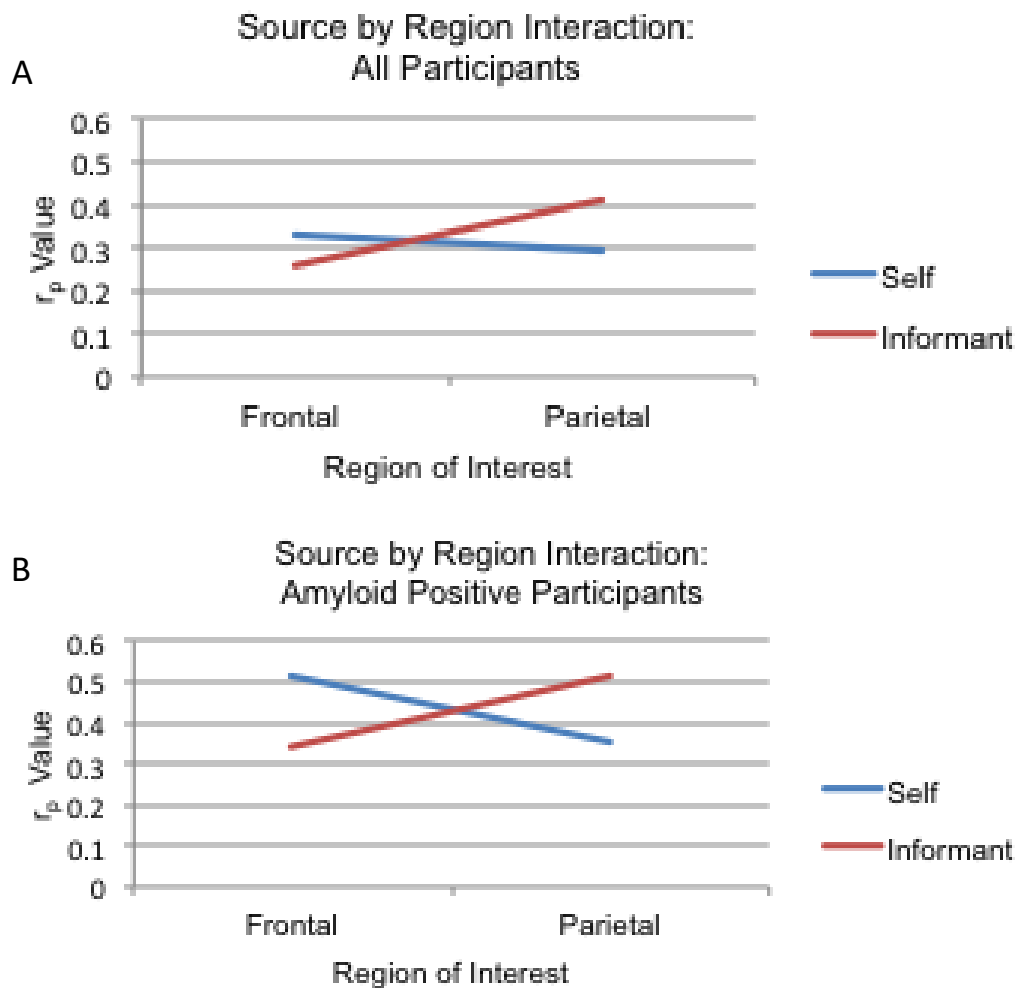


Figure 37. Memory concern source by tau location interaction in the full sample (A) and in the amyloid-positive subset (B). In both the full sample and the amyloid-positive subset, there was an interaction of memory concern source and tau aggregation region such that self ECog scores were preferentially associated with frontal lobe tau aggregation and informant ECog scores were preferentially associated with parietal lobe tau aggregation.

Table 24. Positive correlations between self-ECog memory scores and voxel-wise tau aggregation in the full sample.  $p < 0.05$  with family-wise error correction.

FWE p	Cluster Size (k)	T-value	Z-value	Cluster p (unc.)	Voxel p (unc.)	MNI Coordinates			Nearest Gray Matter Region
						X	Y	Z	
0.017	844	4.36	4.11	0.001	<0.001	-26	46	14	Left Medial Frontal Gyrus (BA 9)

		3.92	3.73	0.001	<0.001	-36	38	28	
		2.96	2.87	0.001	0.002	-12	54	6	Left Medial Frontal Gyrus (BA 10)
		2.69	2.62	0.001	0.004	-18	52	14	
		3.67	3.52	0.001	<0.001	-30	50	-4	Left Frontal Sub-gyral
		3.32	3.2	0.001	0.001	-38	50	-4	
		3.41	3.28	0.001	0.001	-20	56	-2	Left Superior Frontal Gyrus (BA 10)
		2.86	2.78	0.001	0.003	-32	40	-8	Left Middle Frontal Gyrus (BA 47)
		3.34	3.21	0.001	0.001	-38	26	36	Left Middle Frontal Gyrus (BA 9)
		3.29	3.17	0.001	0.001	-42	30	28	
		3.15	3.05	0.001	0.001	-30	40	20	Left Middle Frontal Gyrus (BA 10)
		3.14	3.04	0.001	0.001	-42	40	0	Left Inferior Frontal Gyrus (BA 47)
		2.83	2.75	0.001	0.003	-44	36	-8	
		2.83	2.75	0.001	0.003	-16	50	-10	Left Anterior Cingulate (BA 32)
<0.001	5889	4.02	3.82	<0.001	<0.001	-2	-24	36	Left Cingulate Gyrus (BA 23)
		3.45	3.32	<0.001	<0.001	-4	-42	26	Left Posterior Cingulate (BA 30)
		3.47	3.33	<0.001	<0.001	42	44	8	Right Middle Frontal Gyrus (BA 10)
		3.44	3.3	<0.001	<0.001	52	26	24	Right Middle Frontal Gyrus (BA 46)
		4.12	3.91	<0.001	<0.001	26	28	38	Right Middle Frontal Gyrus (BA 8)
		3.96	3.77	<0.001	<0.001	28	36	40	
		3.93	3.74	<0.001	<0.001	30	38	-20	Right Middle Frontal Gyrus (BA 11)
		3.8	3.63	<0.001	<0.001	40	32	38	Right Middle Frontal Gyrus (BA 9)
		3.85	3.67	<0.001	<0.001	28	32	32	Right Medial Frontal Gyrus (BA 9)
		3.74	3.58	<0.001	<0.001	12	54	24	
		3.69	3.53	<0.001	<0.001	16	42	32	
		3.68	3.52	<0.001	<0.001	14	14	50	Right Medial Frontal Gyrus (BA 32)
		3.8	3.63	<0.001	<0.001	14	36	50	Right Superior Frontal Gyrus (BA 8)
		3.64	3.48	<0.001	<0.001	24	52	14	Right Superior Frontal Gyrus (BA 10)
		3.73	3.57	<0.001	<0.001	20	28	-20	Right Inferior Frontal Gyrus (BA 47)

		3.57	3.42	<0.001	<0.001	58	0	14	Right Precentral Gyrus (BA 6)
		3.67	3.51	<0.001	<0.001	16	-38	54	Right Precuneus (BA 7)
		3.7	3.53	<0.001	<0.001	14	-58	44	
		3.67	3.51	<0.001	<0.001	16	-38	54	
		3.8	3.62	<0.001	<0.001	14	4	58	Right Cingulate Gyrus (BA 24)
		4.04	3.83	<0.001	<0.001	4	2	32	
		3.66	3.5	<0.001	<0.001	10	-10	48	
		3.68	3.52	<0.001	<0.001	10	14	44	Right Cingulate Gyrus (BA 32)
		3.57	3.42	<0.001	<0.001	8	20	42	
		3.44	3.3	<0.001	<0.001	10	36	28	
		3.43	3.29	<0.001	<0.001	8	-34	40	Right Cingulate Gyrus (BA 31)
		3.59	3.44	<0.001	<0.001	12	-42	54	
		3.46	3.32	<0.001	<0.001	6	-46	24	Right Posterior Cingulate (BA 30)
		3.45	3.32	<0.001	<0.001	22	52	-2	Right Anterior Cingulate (BA 10)
		3.56	3.41	<0.001	<0.001	50	12	18	Right Insula (BA 13)
		3.47	3.33	<0.001	<0.001	44	10	22	
		3.46	3.32	<0.001	<0.001	6	-46	24	Right Posterior Cingulate (BA 30)
		3.45	3.32	<0.001	<0.001	22	52	-2	Right Anterior Cingulate (BA 10)
		3.65	3.5	<0.001	<0.001	10	-50	8	Right Cerebellum Anterior Lobe
0.002	1288	4.29	4.05	<0.001	<0.001	54	-2	-24	Right Fusiform Gyrus (BA 20)
		3.77	3.6	<0.001	<0.001	60	-12	-18	Right Middle Temporal Gyrus (BA 21)
		3.64	3.49	<0.001	<0.001	48	4	-32	
		3.4	3.27	<0.001	0.001	56	6	-6	Right Superior Temporal Gyrus (BA 22)
		3.37	3.24	<0.001	0.001	58	0	-6	Right Superior Temporal Gyrus (BA 38)
		3.32	3.2	<0.001	0.001	60	-2	0	Right Superior Temporal Gyrus (BA 22)
		3.2	3.1	<0.001	0.001	52	12	-16	Right Superior Temporal Gyrus (BA 38)
		3.85	3.67	<0.001	<0.001	50	-20	-28	Right Inferior Temporal Gyrus (BA 20)
		3.49	3.35	<0.001	<0.001	46	-8	-34	
		3.71	3.55	<0.001	<0.001	46	-26	-24	Right Parahippocampal Gyrus (BA 36)
		3.59	3.45	<0.001	<0.001	28	2	-	Right Uncus (BA 28)

								30	
		3.58	3.43	<0.001	<0.001	40	2	-34	Right Uncus (BA 36)
		3.18	3.07	<0.001	0.001	52	-14	-20	Right Temporal Sub-gyral (BA 20)
		3.87	3.69	0.001	<0.001	-34	0	32	No Gray Matter Found
0.029	756	3.8	3.63	0.001	<0.001	-36	6	50	Left Middle Frontal Gyrus (BA 6)
		3.6	3.45	0.001	<0.001	-24	0	46	
		3.49	3.35	0.001	<0.001	-46	8	46	
		3.01	2.92	0.001	0.002	-34	8	60	
		3.01	2.91	0.001	0.002	-28	14	60	
		3.07	2.97	0.001	0.001	-28	14	40	Left Middle Frontal Gyrus (BA 8)
		2.74	2.67	0.001	0.004	-30	22	56	
		3.01	2.92	0.001	0.002	-48	2	28	Left Inferior Frontal Gyrus (BA 9)
		3.35	3.22	0.001	0.001	-56	2	26	Left Precentral Gyrus (BA 6)
		3.23	3.11	0.001	0.001	-56	-2	20	
		2.92	2.84	0.001	0.002	-50	6	32	
		3.1	3	0.001	0.001	-40	8	38	Left Precentral Gyrus (BA 9)
		3.32	3.2	0.001	0.001	-60	-14	22	Left Postcentral Gyrus (BA 43)
		3.53	3.39	0.001	<0.001	-22	10	44	Left Cingulate Gyrus (BA 32)
		2.92	2.84	0.001	0.002	-30	-6	42	No Gray Matter Found

Table 25. Positive correlations between informant ECog memory scores and voxel-wise tau aggregation in the full sample.  $p < 0.05$  with family-wise error correction

FWE p	Cluster Size (k)	T-value	Z-value	Cluster p (unc.)	Voxel p (unc.)	MNI Coordinates			Nearest Gray Matter Region
						X	Y	Z	
<0.001	16758	4.56	4.28	<0.001	<0.001	-44	-70	32	Left Middle Temporal Gyrus (BA 39)
		4.56	4.28	<0.001	<0.001	-44	-70	32	
		4.24	4.01	<0.001	<0.001	-52	-62	22	Left Middle Temporal Gyrus (BA 19)
		4.74	4.43	<0.001	<0.001	-48	-	40	Left Superior Temporal

							56		Gyrus (BA 39)
		4.81	4.49	<0.001	<0.001	-4	-58	32	Left Posterior Cingulate (BA 31)
		4.66	4.36	<0.001	<0.001	-6	-46	32	Left Posterior Cingulate (BA 23)
		4.6	4.31	<0.001	<0.001	-8	-64	34	Left Precuneus (BA 31)
		4.31	4.07	<0.001	<0.001	-30	-66	48	Left Precuneus (BA 7)
		5.2	4.8	<0.001	<0.001	-14	-74	40	Left Cuneus (BA 7)
		4.33	4.09	<0.001	<0.001	48	-60	34	Right Middle Temporal Gyrus (BA 39)
		4.87	4.53	<0.001	<0.001	50	-70	16	
		4.73	4.41	<0.001	<0.001	42	-78	-10	Right Fusiform Gyrus (BA 19)
		4.94	4.59	<0.001	<0.001	4	-54	34	Right Cingulate Gyrus (BA 31)
		5.13	4.74	<0.001	<0.001	4	-46	24	Right Posterior Cingulate (BA 30)
		5.06	4.68	<0.001	<0.001	4	-44	28	Right Posterior Cingulate (BA 23)
		4.61	4.32	<0.001	<0.001	8	-52	28	Right Posterior Cingulate (BA 31)
		4.45	4.19	<0.001	<0.001	60	-48	24	Right Supramarginal Gyrus (BA 40)
		4.29	4.05	<0.001	<0.001	62	-44	44	
		4.44	4.18	<0.001	<0.001	40	-56	54	Right Inferior Parietal Lobule (BA 7)
		4.22	3.99	<0.001	<0.001	46	-54	48	Right Inferior Parietal Lobule (BA 40)
		4.21	3.98	<0.001	<0.001	42	-72	34	Right Superior Occipital Gyrus (BA 19)
		4.6	4.31	<0.001	<0.001	44	-80	-4	Right Middle Occipital Gyrus (BA 18)
		4.35	4.1	<0.001	<0.001	24	-50	64	Right Precuneus (BA 7)
		4.2	3.98	<0.001	<0.001	32	-46	62	
		5.15	4.76	<0.001	<0.001	22	-68	40	
		4.79	4.47	<0.001	<0.001	28	-50	48	
		4.15	3.93	<0.001	<0.001	6	-70	36	Right Precuneus (BA 31)
		4.38	4.12	<0.001	<0.001	28	-76	38	
		4.54	4.26	<0.001	<0.001	62	-30	26	Right Insula (BA 13)
		4.32	4.08	<0.001	<0.001	36	-66	-18	Right Cerebellum Posterior Lobe
		4.27	4.03	<0.001	<0.001	52	-	34	No Grey Matter Found

							42		
<0.001	4893	5.26	4.84	<0.001	<0.001	20	46	32	Right Superior Frontal Gyrus (BA 9)
		4.95	4.6	<0.001	<0.001	28	32	48	Right Superior Frontal Gyrus (BA 8)
		3.5	3.36	<0.001	<0.001	16	16	56	Right Superior Frontal Gyrus (BA 6)
		3.4	3.27	<0.001	0.001	24	52	16	
		3.38	3.25	<0.001	0.001	10	12	60	
		3.29	3.17	<0.001	0.001	14	20	60	
		5.15	4.76	<0.001	<0.001	26	34	38	Right Middle Frontal Gyrus (BA 8)
		4.89	4.55	<0.001	<0.001	30	28	50	
		4.21	3.98	<0.001	<0.001	32	20	56	
		3.72	3.56	<0.001	<0.001	32	18	44	Right Middle Frontal Gyrus (BA 9)
		3.99	3.8	<0.001	<0.001	38	30	40	
		4.38	4.13	<0.001	<0.001	40	36	30	Right Middle Frontal Gyrus (BA 9)
		4.13	3.91	<0.001	<0.001	28	4	52	Right Middle Frontal Gyrus (BA 6)
		3.51	3.37	<0.001	<0.001	42	0	54	Right Middle Frontal Gyrus (BA 6)
		3.01	2.91	<0.001	0.002	44	46	14	Right Middle Frontal Gyrus (BA 10)
		4.32	4.07	<0.001	<0.001	14	40	44	Right Medial Frontal Gyrus (BA 8)
		4.1	3.89	<0.001	<0.001	12	34	48	
		4.1	3.88	<0.001	<0.001	10	50	40	
		3.38	3.25	<0.001	0.001	28	52	8	Right Medial Frontal Gyrus (BA 10)
		3.34	3.21	<0.001	0.001	10	62	14	
		3	2.91	<0.001	0.002	16	64	6	Right Medial Frontal Gyrus (BA 10)
		2.99	2.9	<0.001	0.002	12	2	62	Right Medial Frontal Gyrus (BA 6)
		3.94	3.75	<0.001	<0.001	46	6	36	Right Precentral Gyrus (BA 6)
		3.89	3.71	<0.001	<0.001	34	-8	58	
		3.52	3.38	<0.001	<0.001	56	4	36	
		3.39	3.26	<0.001	0.001	38	10	30	
		3.74	3.57	<0.001	<0.001	40	14	42	Right Precentral Gyrus (BA 9)
		2.95	2.86	<0.001	0.002	56	8	8	Right Precentral Gyrus (BA 44)
		3.33	3.21	<0.001	0.001	8	20	44	Right Cingulate Gyrus (BA 32)
		3.25	3.14	<0.001	0.001	22	12	50	Right Cingulate Gyrus (BA 24)
		3.16	3.06	<0.001	0.001	46	14	22	Right Insula (BA 13)
		3.18	3.08	<0.001	0.001	24	-2	60	Right Frontal Sub-gyral (BA 6)
<0.001	1702	5.04	4.67	<0.001	<0.001	-38	6	54	Left Middle Frontal Gyrus (BA 6)
		4.92	4.57	<0.001	<0.001	-22	28	44	Left Middle Frontal Gyrus (BA 8)
		3.97	3.77	<0.001	<0.001	-20	38	46	Left Middle Frontal Gyrus (BA 9)
		3.83	3.65	<0.001	<0.001	-36	42	28	

		3.42	3.29	<0.001	<0.001	-30	40	38	
		2.84	2.76	<0.001	0.003	-42	20	34	
		4.78	4.46	<0.001	<0.001	-24	16	50	Left Medial Frontal Gyrus (BA 32)
		3.7	3.54	<0.001	<0.001	-10	46	40	Left Medial Frontal Gyrus (BA 8)
		3.03	2.93	<0.001	0.002	-8	30	48	
		4.36	4.11	<0.001	<0.001	-14	16	62	Left Superior Frontal Gyrus (BA 6)
		3.08	2.98	<0.001	0.001	-38	24	42	Left Precentral Gyrus (BA 9)
		2.95	2.86	<0.001	0.002	-44	2	40	
		4.14	3.93	<0.001	<0.001	-14	54	28	Left Superior Frontal Gyrus (BA 9)
		3.24	3.13	<0.001	0.001	-10	22	50	Left Cingulate Gyrus (BA 32)
0.008	978	4.5	4.22	<0.001	<0.001	48	10	-38	Right Middle Temporal Gyrus (BA 21)
		4.4	4.15	<0.001	<0.001	64	-12	-20	
		3.61	3.46	<0.001	<0.001	58	-6	-34	Right Inferior Temporal Gyrus (BA 20)
<0.001	1890	4.33	4.09	<0.001	<0.001	-60	-52	-4	Left Middle Temporal Gyrus (BA 37)
		3.6	3.45	<0.001	<0.001	-62	-38	-14	Left Middle Temporal Gyrus (BA 20)
		3.78	3.61	<0.001	<0.001	-58	-60	2	Left Inferior Temporal Gyrus (BA 19)
		3.71	3.55	<0.001	<0.001	-42	-84	-8	Left Inferior Occipital Gyrus (BA 18)
		3.58	3.43	<0.001	<0.001	-54	-64	-10	Left Fusiform Gyrus (BA 19)
		3.4	3.27	<0.001	0.001	-58	-56	-14	Left Fusiform Gyrus (BA 37)
		3.26	3.15	<0.001	0.001	-30	-90	-14	Left Fusiform Gyrus (BA 18)
		3.98	3.78	<0.001	<0.001	-22	-64	-10	Left Cerebellum Posterior Lobe
		3.87	3.69	<0.001	<0.001	-36	-80	-16	
		3.54	3.4	<0.001	<0.001	-26	-50	-10	
		3.24	3.12	<0.001	0.001	-26	-22	-30	Left Cerebellum Anterior Lobe
		2.88	2.8	<0.001	0.003	-26	-32	-24	
		2.75	2.67	<0.001	0.004	-22	-36	-18	
		2.67	2.6	<0.001	0.005	-16	-42	-12	

Table 26. Positive correlations between self-ECog memory scores and voxel-wise tau aggregation in the amyloid-positive subset.  $p < 0.05$  with family-wise error correction.

FWE p	Cluster Size (k)	T-value	Z-value	Cluster p (unc.)	Voxel p (unc.)	MNI Coordinates			Nearest Gray Matter Region
						X	Y	Z	
<0.001	8947	4.76	4.09	<0.001	<0.001	-22	30	-20	Left Middle Frontal Gyrus (BA 11)
		4.32	3.79	<0.001	<0.001	-44	28	30	Left Middle Frontal Gyrus (BA 9)
		3.82	3.43	<0.001	<0.001	-36	34	38	Left Middle Frontal Gyrus (BA 9)
		3.77	3.4	<0.001	<0.001	-38	28	44	Left Middle Frontal Gyrus (BA 8)
		3.91	3.5	<0.001	<0.001	0	30	-22	Left Medial Frontal Gyrus (BA 25)
		3.86	3.46	<0.001	<0.001	-12	56	2	Left Medial Frontal Gyrus (BA 10)
		4.07	3.61	<0.001	<0.001	-46	20	14	Left Inferior Frontal Gyrus (BA 44)
		3.88	3.48	<0.001	<0.001	-40	40	-4	Left Inferior Frontal Gyrus (BA 47)
		3.77	3.39	<0.001	<0.001	-34	38	-8	Left Inferior Frontal Gyrus (BA 47)
		3.74	3.37	<0.001	<0.001	-6	28	-14	Left Subcallosal Gyrus (BA 25)
		3.83	3.44	<0.001	<0.001	-10	42	10	Left Anterior Cingulate (BA 32)
		3.83	3.44	<0.001	<0.001	42	28	32	Right Middle Frontal Gyrus (BA 9)
		3.96	3.53	<0.001	<0.001	44	44	8	Right Middle Frontal Gyrus (BA 10)
		4.83	4.14	<0.001	<0.001	24	30	-20	Right Middle Frontal Gyrus (BA 11)
		4.01	3.57	<0.001	<0.001	30	38	-18	Right Middle Frontal Gyrus (BA 11)
		4.08	3.62	<0.001	<0.001	48	30	10	Right Inferior Frontal Gyrus (BA 13)
		4.88	4.17	<0.001	<0.001	50	34	2	Right Inferior Frontal Gyrus (BA 13)
		4.86	4.16	<0.001	<0.001	56	-2	-22	Right Middle Temporal Gyrus (BA 21)
		4.74	4.08	<0.001	<0.001	40	6	-34	Right Middle Temporal Gyrus (BA 21)
		4.67	4.03	<0.001	<0.001	44	-6	-30	Right Middle Temporal Gyrus (BA 21)
		4.04	3.59	<0.001	<0.001	50	-20	-28	Right Inferior Temporal Gyrus (BA 20)
		4.42	3.86	<0.001	<0.001	40	12	40	Right Precentral Gyrus (BA 9)
		4.37	3.82	<0.001	<0.001	36	10	36	Right Precentral Gyrus (BA 6)
		3.94	3.52	<0.001	<0.001	6	24	-16	Right Subcallosal Gyrus (BA 25)
		3.75	3.38	<0.001	<0.001	8	36	8	Right Anterior Cingulate (BA 24)
		3.89	3.48	<0.001	<0.001	30	4	-34	Right Uncus (BA 36)
		3.75	3.38	<0.001	<0.001	52	10	16	Right Insula (BA 13)
		4.35	3.81	<0.001	<0.001	28	12	-	Right Putamen

								12	
		4.08	3.62	<0.001	<0.001	24	18	-10	
		3.74	3.37	<0.001	<0.001	36	-8	-6	
		4.19	3.7	<0.001	<0.001	26	-22	-24	Right Cerebellum Anterior Lobe

Table 27. Positive correlations between informant ECog memory scores and voxel-wise tau aggregation in the amyloid-positive subset.  $p < 0.05$  with family-wise error correction.

FWE p	Cluster Size (k)	T-value	Z-value	Cluster p (unc.)	Voxel p (unc.)	MNI Coordinates			Nearest Gray Matter Region
						X	Y	Z	
<0.001	2106	5.92	4.81	<0.001	<0.001	-22	36	46	Left Middle Frontal Gyrus (BA 8)
		4.18	3.69	<0.001	<0.001	-36	28	44	
		4.7	4.05	<0.001	<0.001	-36	20	34	Left Middle Frontal Gyrus (BA 9)
		3.64	3.29	<0.001	<0.001	-36	44	28	
		4.15	3.67	<0.001	<0.001	-40	4	52	Left Middle Frontal Gyrus (BA 6)
		4.47	3.9	<0.001	<0.001	-20	10	56	Left Medial Frontal Gyrus (BA 6)
		3.3	3.03	<0.001	0.001	-12	44	40	Left Medial Frontal Gyrus (BA 8)
		4.27	3.76	<0.001	<0.001	-22	18	48	Left Superior Frontal Gyrus (BA 8)
		3.92	3.5	<0.001	<0.001	-6	36	48	
		3.9	3.49	<0.001	<0.001	-14	16	60	Left Superior Frontal Gyrus (BA 6)
		3.55	3.22	<0.001	0.001	-16	52	30	Left Superior Frontal Gyrus (BA 9)
		3.52	3.2	<0.001	0.001	-18	52	24	
		3.53	3.21	<0.001	0.001	-42	10	34	Left Inferior Frontal Gyrus (BA 9)
		3.8	3.42	<0.001	<0.001	-26	6	60	Left Frontal Sub-Gyral (BA 6)
		3.59	3.26	<0.001	0.001	-20	8	62	
		3.8	3.42	<0.001	<0.001	-44	-2	48	Left Precentral Gyrus (BA 6)
		3.46	3.16	<0.001	0.001	-36	4	30	
		3.39	3.11	<0.001	0.001	-38	8	32	
		3.1	2.87	<0.001	0.002	-46	0	40	
		3.09	2.86	<0.001	0.002	-50	4	36	
		3.23	2.97	<0.001	0.001	-8	26	44	Left Cingulate Gyrus (BA 32)
<0.001	11032	4.22	3.72	<0.001	<0.001	-42	-70	32	Left Middle Temporal Gyrus (BA 39)
		3.94	3.52	<0.001	<0.001	-48	-66	30	
		3.86	3.46	<0.001	<0.001	-36	-60	38	
		4.88	4.17	<0.001	<0.001	-48	-58	38	Left Superior Temporal Gyrus (BA 39)
		3.94	3.52	<0.001	<0.001	-4	-22	28	Left Cingulate Gyrus (BA 23)
		4.25	3.75	<0.001	<0.001	-6	-54	18	Left Posterior Cingulate (BA 29)
		4.22	3.72	<0.001	<0.001	-8	-46	32	Left Posterior Cingulate (BA 23)

		4	3.57	<0.001	<0.001	-14	-60	20	Left Posterior Cingulate (BA 30)
		5.12	4.32	<0.001	<0.001	-4	-60	32	Left Precuneus (BA 31)
		3.83	3.44	<0.001	<0.001	-20	-70	30	
		4.95	4.22	<0.001	<0.001	14	-62	62	Left Precuneus (BA 7)
		4.25	3.74	<0.001	<0.001	-22	-60	58	
		5.58	4.61	<0.001	<0.001	-12	-70	42	Left Cuneus (BA 7)
		4.82	4.13	<0.001	<0.001	-12	-78	38	Left Cuneus (BA 19)
		4.59	3.98	<0.001	<0.001	50	-68	16	Right Middle Temporal Gyrus (BA 39)
		4.03	3.58	<0.001	<0.001	50	-60	36	
		4.41	3.86	<0.001	<0.001	58	-48	28	Right Supramarginal Gyrus (BA 40)
		3.94	3.52	<0.001	<0.001	58	-48	38	
		4.02	3.58	<0.001	<0.001	56	-22	40	Right Postcentral Gyrus (BA 2)
		4.01	3.57	<0.001	<0.001	46	-26	58	Right Postcentral Gyrus (BA 3)
		3.97	3.54	<0.001	<0.001	50	-20	48	
		4.31	3.78	<0.001	<0.001	6	-54	36	Right Cingulate Gyrus (BA 31)
		4.87	4.16	<0.001	<0.001	4	-58	22	Right Posterior Cingulate (BA 23)
		4.37	3.82	<0.001	<0.001	6	-46	22	Right Posterior Cingulate (BA 30)
		3.89	3.48	<0.001	<0.001	8	-26	28	
		4.02	3.58	<0.001	<0.001	12	-50	32	Right Posterior Cingulate (BA 31)
		4.85	4.15	<0.001	<0.001	16	-64	36	Right Precuneus (BA 31)
		4.76	4.09	<0.001	<0.001	34	-46	62	Right Precuneus (BA 7)
		4.56	3.96	<0.001	<0.001	22	-52	66	
		4.04	3.59	<0.001	<0.001	28	-50	48	
		3.98	3.55	<0.001	<0.001	60	-28	22	Right Insula (BA 13)
		4.42	3.86	<0.001	<0.001	40	-78	-12	Right Cerebellum Posterior Lobe
<0.001	3884	5.48	4.55	<0.001	<0.001	34	22	54	Right Middle Frontal Gyrus (BA 8)
		4.52	3.93	<0.001	<0.001	26	34	48	
		4.78	4.1	<0.001	<0.001	42	24	36	Right Middle Frontal Gyrus (BA 9)
		4.61	3.99	<0.001	<0.001	40	20	38	
		3.49	3.18	<0.001	0.001	40	38	28	
		3.17	2.93	<0.001	0.002	34	38	32	Right Middle Frontal Gyrus (BA 6)
		4.35	3.81	<0.001	<0.001	42	0	52	
		3.75	3.38	<0.001	<0.001	36	8	46	
		3.14	2.91	<0.001	0.002	26	2	52	
		3.12	2.89	<0.001	0.002	34	-4	48	Right Middle Frontal Gyrus (BA 46)
		3.33	3.05	<0.001	0.001	48	18	22	
		4.84	4.15	<0.001	<0.001	20	36	46	Right Medial Frontal Gyrus (BA 8)
		4.18	3.69	<0.001	<0.001	8	48	42	
		3.31	3.04	<0.001	0.001	8	30	52	Right Medial Frontal Gyrus (BA 6)
		4.68	4.04	<0.001	<0.001	24	34	38	
		3.22	2.97	<0.001	0.001	14	16	54	Right Medial Frontal Gyrus (BA 32)
		4.8	4.12	<0.001	<0.001	20	46	34	Right Superior Frontal Gyrus (BA 9)
		3.12	2.88	<0.001	0.002	12	56	30	
		4.63	4	<0.001	<0.001	24	26	50	Right Superior Frontal

									Gyrus (BA 8)
		3.72	3.36	<0.001	<0.001	14	22	62	Right Superior Frontal Gyrus (BA 6)
		4.68	4.04	<0.001	<0.001	52	6	30	Right Inferior Frontal Gyrus (BA 9)
		4.5	3.92	<0.001	<0.001	28	0	66	Right Frontal Sub-Gyral (BA 6)
		4.26	3.75	<0.001	<0.001	36	-6	62	Right Precentral Gyrus (BA 6)
		3.94	3.52	<0.001	<0.001	34	-12	68	Right Precentral Gyrus (BA 6)
		2.78	2.61	<0.001	0.005	42	-14	64	Right Precentral Gyrus (BA 4)
		2.78	2.61	<0.001	0.005	44	-18	64	Right Precentral Gyrus (BA 4)
		4.78	4.1	<0.001	<0.001	44	20	42	Right Precentral Gyrus (BA 9)
		3.56	3.24	<0.001	0.001	26	12	48	Right Cingulate Gyrus (BA 32)
		2.84	2.66	<0.001	0.004	54	12	20	Right Insula (BA 13)

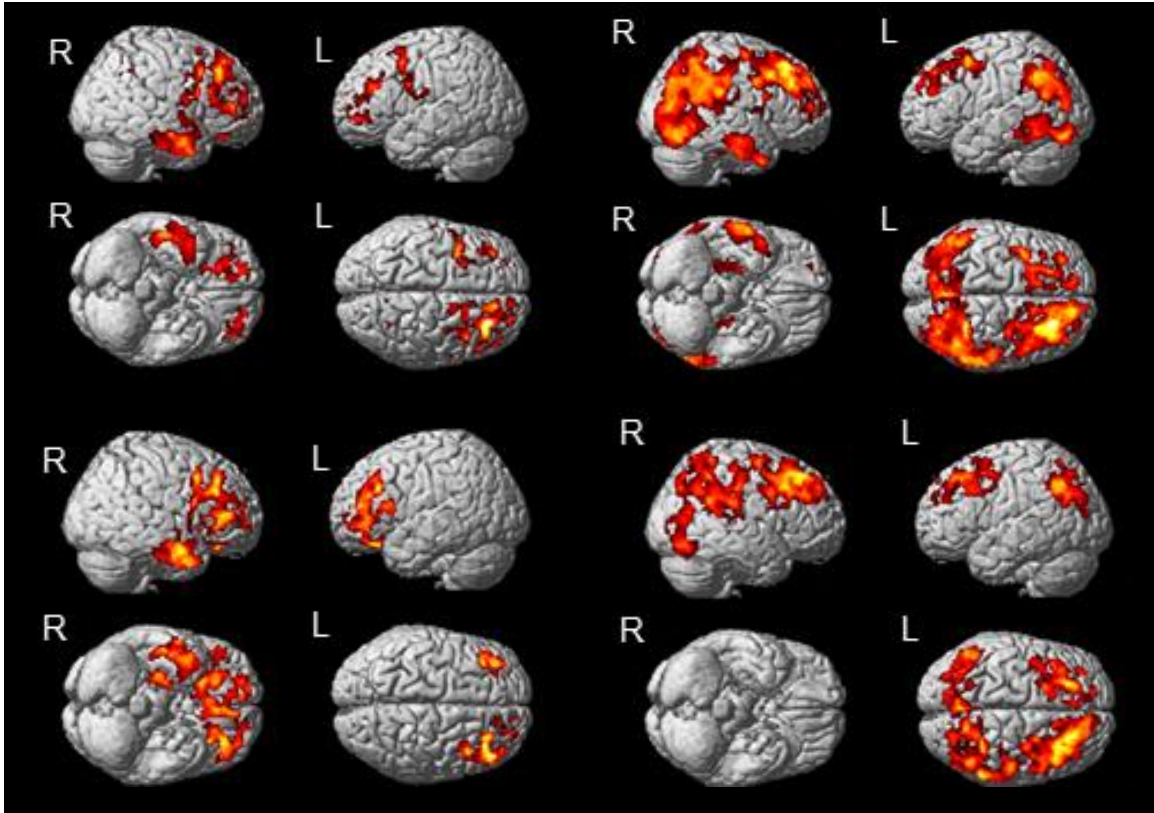


Figure 38. Visualization of positive correlations between self-ECog (A&C) and informant (B&D) ECog scores with voxel-wise tau aggregation in the full sample (A&B) and the amyloid-positive subset (C&D). In the full sample, self ECog scores were positively associated with tau aggregation in frontal, temporal, cingulate, and parahippocampal regions, precuneus, insula, uncus, and cerebellum (A). Informant ECog scores were positively associated with tau aggregation in frontal, temporal, temporoparietal, parietal, occipital, and cingulate regions, insula and cerebellum (B). In the amyloid-positive subset, self ECog scores were positively associated with tau aggregation in frontal, temporal, and cingulate regions, putamen, uncus, insula, and cerebellum (C). Informant ECog scores were positively associated with tau aggregation in frontal, temporal, cingulate, and parietal regions, precuneus, cuneus, insula, and cerebellum (D).

## Chapter 5: Implications of Findings and Future Directions

In this dissertation, I present our work investigating the relationships between CBF, known and potential AD risk factors, AD pathologies, and cognitive function in nondemented older adults. We found that CBF is affected by hypertension, self-identified race, *APOE*  $\epsilon 4$  positivity, and amyloid beta and tau aggregation. We also suggest that each of these relationships may be affected by the other factors. These relationships and their interactions will be critical to thoroughly understand for the use of CBF as an early biomarker for AD.

Our systematic review of published literature (Chapter 1) showed that CBF is generally decreased but can sometimes be increased in certain brain regions in AD, and especially in early stages such as MCI. This review also highlighted that more characterizations of CBF in early stages of AD are needed and that potential confounding factors should be included in these analyses. In our original work, we found that hypertension is associated with decreased CBF especially in anterior brain regions (Chapter 2), and that African Americans have regions of both decreased CBF and increased CBF compared to non-Hispanic white Americans that is not explained by the greater prevalence of hypertension in African Americans (Chapter 2). Similar results with respect to the overall spatial patterns of decreased and increased CBF in African Americans were found in an independent sample. CBF in the fusiform, one region with decreased CBF in African Americans, was positively correlated with delayed memory function, suggesting that decreased CBF in this region is related to cognitive decline (Chapter 2). Additionally, we found that CBF is negatively correlated with both global cortical amyloid and medial temporal lobe tau measured by PET, and that both

hypertension and *APOE*  $\epsilon 4$  may affect these correlations (Chapter 3). The clearest effect was of hypertension on the relationship between CBF and global cortical amyloid. There was a positive association between CBF and amyloid in hypertensive individuals and a negative association between CBF and amyloid in normotensive individuals (Chapter 3). Finally, we found that the spatial distribution of tau is related to subjective memory concerns. Self-concern was related to tau in frontal brain regions, while informant concern was related to tau in parietal brain regions (Chapter 4). Together, our findings provide evidence of complex and potentially interacting relationships between CBF and AD risks, pathologies, and symptoms that warrant further investigation so that CBF can be utilized as an effective early biomarker of AD.

In Chapter 2, we report an association between hypertension and decreased CBF in all of our *a priori* hypertension-related regions chosen from previous literature and in widespread frontotemporal regions and a region of the occipital lobe in voxel-wise analyses in a diverse sample of older adults without dementia. Although the number of African Americans in our sample was relatively small, this suggests that hypertension's effect on CBF is similar in African Americans and non-Hispanic white Americans. We also found that hypertension did not fully explain the difference in CBF between African Americans and white Americans, even though there was a higher prevalence of hypertension in the African American group. This is in agreement with Clark et al<sup>68</sup> and was true for both independent samples studied. In Chapter 3, we report negative correlations between CBF and medial temporal lobe tau pathology, and a nonsignificant trend of negative associations between CBF and global cortical amyloid in older adults without dementia. While both positive and negative correlations have previously been

reported in this population, the overall pattern of correlations between CBF and AD pathology is not yet conclusive in preclinical stages of AD. CBF in medial temporal regions was negatively correlated with medial temporal lobe tau, and CBF in similar regions was negatively associated with global cortical amyloid. In AD, tau pathology begins in the medial temporal lobe, and this corresponds with memory problems often being the first symptoms to appear in AD. Our findings also conceptually align with previous evidence that tau pathology more closely tracks both spatially and temporally with cognitive symptoms than amyloid beta pathology does in AD.

We also reported an interaction effect of global cortical amyloid and hypertension on CBF; amyloid pathology and CBF positively correlated in individuals with hypertension and negatively correlated in individuals without hypertension. To our knowledge, this interaction has not been previously reported. This suggests that hypertension status must be taken into account when utilizing altered CBF as a biomarker and that cerebral vascular function is differentially affected by AD pathology in older adults depending on whether their cardiovascular risk factors during preclinical stages of disease. We expected that hypertension would exacerbate the decreased CBF in individuals with amyloid pathology; future studies are needed to better understand this interaction effect. There were weaker interactions of *APOE*  $\epsilon$ 4 and amyloid beta and tau pathology, as well as of hypertension and tau pathology, on CBF. Future studies with larger sample sizes are needed to determine whether these interactions have meaningful effects on CBF in this population.

The original research reported in Chapter 2 is the first to directly compare CBF between African Americans and non-Hispanic white Americans in two independent

samples and to report both regional increases and regional decreases in CBF in African Americans relative to white Americans. This new information is important alongside previous reports of decreased global CBF in African Americans; certain brain regions might be more affected than others, and CBF in some brain regions might be preserved or even increased. This is important because CBF in different brain regions will have different effects on cognition, which could lead to distinct presentations of AD in African Americans. It also means that the classical pattern of hypoperfusion attributed to AD might be specific to those of European descent. At the same time, sociological and environmental factors likely contribute to these differences, so brain regions with more greatly reduced CBF may be those most susceptible to the effects of these stressors. The concept of the Weathering Hypothesis<sup>100</sup> previously mentioned may not be as simple as a brain that uniformly ages more quickly, but perhaps some brain regions age prematurely while compensatory mechanisms are active in other brain regions.

To our knowledge, no previous studies have compared the relationships between tau PET and self-based and informant memory concerns. We found that self-based memory concerns were most strongly correlated with frontal lobe tau, while informant memory concerns were most strongly correlated with parietal lobe tau. These discrepancies may indicate the degree to which different brain regions are related to insight, or they may represent spatial patterns of tau pathology that correspond to AD subtypes. Either way, the concept that the location of tau pathology relates to one's perception of their own cognitive functioning further relates tau pathology to cognition in the earliest preclinical stages of the AD. While we report a correlation between medial temporal lobe tau and CBF in Chapter 3, Chapter 4 suggests that the spatial distribution

of tau will also be critical to consider when assessing the prognosis of early stage AD using CBF as a biomarker.

Of course, many scientific questions remain. It will be important to continue to elucidate the prognostic and mechanistic role that hypertension plays in AD risk, both in the context of better understanding AD etiology and in better understanding AD biomarkers and disease trajectories in those with hypertension compared to those without. CBF may be an especially sensitive marker to hypertension-related vascular damage and may thus help to identify hypertension-dependent subtypes of AD in the future. For example, it may be the case that individuals with hypertension have a distinct pattern of pathology related to brain regions' relative vulnerabilities to hypertension-related damage. The relationships between CBF, amyloid and tau pathology, genetic, demographic, and environmental risk factors, and presentation of cognitive decline add further complexity to the potentially many subtypes of AD. With better understanding of these relationships, especially in preclinical disease stages, early biomarkers such as CBF may be able to categorize cases based on how these risk factors and pathologies interact with one another. It may be that each case of AD is biologically unique. As more medical fields move towards precision medicine, it becomes reasonable to consider that in the future, individualized treatments based on one's specific presentation of AD may become available. It will be important to disentangle the reason(s) for differences in CBF between African Americans and non-Hispanic white Americans that has been previously reported and is reported here. Whether genetic, socioeconomic, cultural, stress-related, cardiovascular factors or a combination of some or all of these causes these differences,

we may be able to model “typical AD” patterns of altered CBF that are more accurate for individuals or groups of people based on their presence or absence of those factors.

Finally, the focus on early stages of AD should be broken down into subphases as there are brain regions with increases and regions with decreases in CBF during that time, and changes may occur quickly. It will be important to study individuals longitudinally and to measure CBF frequently over that time, as well as to find which factors can predict how CBF will change.

In order to begin to answer these remaining questions, larger and more diverse samples are required, and longitudinal studies will be best. Larger and more diverse samples will allow for individuals to be grouped into more specific categories based on multiple factors so that CBF can be compared between and among them. Studies comparing various ethn racial groups likewise must be large enough to take into account individual differences in socioeconomic status, quality of education, stress experienced in various life stages, health risks, and specific ancestry based on genetics rather than self-reported race alone. Hypertension should likewise be more specifically defined, including factors like age at and duration of hypertension, as well as level of pharmacological or lifestyle-based control of blood pressure during that time. Methodologically, the use of tau PET and amyloid PET alongside ASL MRI would be ideal to retain the spatial information of all three modalities to see where in the brain these pathologies overlap and where they are distinct. This may result in a finite number of spatial patterns across individuals that can would potentially although us to predict spatial patterns of amyloid and tau pathology from the spatial pattern of altered CBF.

Overall, the relationships between CBF and AD risk factors, pathologies and symptoms are complex. Due to various demographic, clinical, and environmental factors, these relationships will most likely differ between individuals or groups of people. Future studies to characterize CBF in relationship to these factors could allow us to quickly and noninvasively determine which AD pattern or subtype an individual has using ASL MRI. This method will also allow for frequent assessment of CBF so that we can determine how it changes in relation to other pathologies and factors over time and thus eventually determine who is most in need of preventative care. Additionally, CBF as an early biomarker for AD could be used to choose participants for targeted clinical trials, to track the prognosis of the disease over time, and to measure treatment efficacy. CBF may even be a modifiable target for treatment; maintaining CBF may slow the onset or progression of AD. In conclusion, further characterization of CBF as an early biomarker of AD is warranted and could potentially help to develop effective treatments for AD in the near future.

## References

1. 2021 Alzheimer's disease facts and figures. *Alzheimers Dement.* 2021;17(3):327-406. doi: 10.1002/alz.12328. PubMed PMID: 33756057.
2. Zhu CC, Fu SY, Chen YX, et al. Advances in Drug Therapy for Alzheimer's Disease. *Curr Med Sci.* Dec 2020;40(6):999-1008. doi:10.1007/s11596-020-2281-2
3. Blennow K, Zetterberg H. The Past and the Future of Alzheimer's Disease Fluid Biomarkers. *J Alzheimers Dis.* 2018;62(3):1125-1140. doi:10.3233/JAD-170773
4. Counts SE, Ikonovic MD, Mercado N, Vega IE, Mufson EJ. Biomarkers for the Early Detection and Progression of Alzheimer's Disease. *Neurotherapeutics.* Jan 2017;14(1):35-53. doi:10.1007/s13311-016-0481-z
5. Petersen RC, Smith GE, Waring SC, Ivnik RJ, Tangalos EG, Kokmen E. Mild cognitive impairment: clinical characterization and outcome. *Arch Neurol.* Mar 1999;56(3):303-8. doi:10.1001/archneur.56.3.303
6. Petersen RC. Mild Cognitive Impairment. *Continuum (Minneap Minn).* Apr 2016;22(2 Dementia):404-18. doi:10.1212/CON.0000000000000313
7. Jessen F, Amariglio RE, van Boxtel M, et al. A conceptual framework for research on subjective cognitive decline in preclinical Alzheimer's disease. *Alzheimers Dement.* Nov 2014;10(6):844-52. doi:10.1016/j.jalz.2014.01.001
8. Jessen F, Amariglio RE, Buckley RF, et al. The characterisation of subjective cognitive decline. *Lancet Neurol.* Mar 2020;19(3):271-278. doi:10.1016/S1474-4422(19)30368-0
9. Culpepper L, Lam RW, McIntyre RS. Cognitive Impairment in Patients With Depression: Awareness, Assessment, and Management. *J Clin Psychiatry.* Nov/Dec 2017;78(9):1383-1394. doi:10.4088/JCP.tk16043ah5c
10. Vavilala MS, Lee LA, Lam AM. Cerebral blood flow and vascular physiology. *Anesthesiol Clin North Am.* Jun 2002;20(2):247-64. v. doi:10.1016/s0889-8537(01)00012-8
11. Iadecola C, Gottesman RF. Neurovascular and Cognitive Dysfunction in Hypertension. *Circ Res.* Mar 29 2019;124(7):1025-1044. doi:10.1161/CIRCRESAHA.118.313260
12. Hardy JA, Higgins GA. Alzheimer's disease: the amyloid cascade hypothesis. *Science.* Apr 10 1992;256(5054):184-5. doi:10.1126/science.1566067
13. Zlokovic BV. Neurovascular pathways to neurodegeneration in Alzheimer's disease and other disorders. *Nat Rev Neurosci.* Nov 3 2011;12(12):723-38. doi:10.1038/nrn3114
14. Duan W, Zhou GD, Balachandrasekaran A, et al. Cerebral Blood Flow Predicts Conversion of Mild Cognitive Impairment into Alzheimer's Disease and Cognitive Decline: An Arterial Spin Labeling Follow-up Study. *J Alzheimers Dis.* 2021;82(1):293-305. doi:10.3233/JAD-210199
15. Kety SS, Schmidt CF. The Nitrous Oxide Method for the Quantitative Determination of Cerebral Blood Flow in Man: Theory, Procedure and Normal Values. *J Clin Invest.* Jul 1948;27(4):476-83. doi:10.1172/JCI101994
16. Lassen NA, Ingvar DH. The blood flow of the cerebral cortex determined by radioactive krypton. *Experientia.* Jan 15 1961;17:42-3. doi:10.1007/BF02157946

17. Lassen NA, Hoedt-Rasmussen K, Sorensen SC, et al. Regional Cerebral Blood Flow in Man Determined by Krypton. *Neurology*. Sep 1963;13:719-27. doi:10.1212/wnl.13.9.719
18. Jones T, Chesler DA, Ter-Pogossian MM. The continuous inhalation of oxygen-15 for assessing regional oxygen extraction in the brain of man. *Br J Radiol*. Apr 1976;49(580):339-43. doi:10.1259/0007-1285-49-580-339
19. Edelman RR, Mattle HP, Atkinson DJ, et al. Cerebral blood flow: assessment with dynamic contrast-enhanced T2\*-weighted MR imaging at 1.5 T. *Radiology*. Jul 1990;176(1):211-20. doi:10.1148/radiology.176.1.2353094
20. Rempp KA, Brix G, Wenz F, Becker CR, Guckel F, Lorenz WJ. Quantification of regional cerebral blood flow and volume with dynamic susceptibility contrast-enhanced MR imaging. *Radiology*. Dec 1994;193(3):637-41. doi:10.1148/radiology.193.3.7972800
21. Warwick JM. Imaging of brain function using SPECT. *Metab Brain Dis*. Jun 2004;19(1-2):113-23. doi:10.1023/b:mebr.0000027422.48744.a3
22. Detre JA, Rao H, Wang DJ, Chen YF, Wang Z. Applications of arterial spin labeled MRI in the brain. *J Magn Reson Imaging*. May 2012;35(5):1026-37. doi:10.1002/jmri.23581
23. Zhang H, Wang Y, Lyu D, et al. Cerebral blood flow in mild cognitive impairment and Alzheimer's disease: A systematic review and meta-analysis. *Ageing Res Rev*. Nov 2021;71:101450. doi:10.1016/j.arr.2021.101450
24. Iturria-Medina Y, Carbonell FM, Sotero RC, Chouinard-Decorte F, Evans AC, Alzheimer's Disease Neuroimaging I. Multifactorial causal model of brain (dis)organization and therapeutic intervention: Application to Alzheimer's disease. *Neuroimage*. May 15 2017;152:60-77. doi:10.1016/j.neuroimage.2017.02.058
25. Moretti DV. Electroencephalography-driven approach to prodromal Alzheimer's disease diagnosis: from biomarker integration to network-level comprehension. *Clin Interv Aging*. 2016;11:897-912. doi:10.2147/CIA.S103313
26. Vogel A, Hasselbalch SG, Gade A, Ziebell M, Waldemar G. Cognitive and functional neuroimaging correlate for anosognosia in mild cognitive impairment and Alzheimer's disease. *Int J Geriatr Psychiatry*. Mar 2005;20(3):238-46. doi:10.1002/gps.1272
27. Jagust WJ, Reed BR, Seab JP, Budinger TF. Alzheimer's disease. Age at onset and single-photon emission computed tomographic patterns of regional cerebral blood flow. *Arch Neurol*. Jun 1990;47(6):628-33. doi:10.1001/archneur.1990.00530060036013
28. Dougall N, Nobili F, Ebmeier KP. Predicting the accuracy of a diagnosis of Alzheimer's disease with 99mTc HMPAO single photon emission computed tomography. *Psychiatry Res*. Jul 30 2004;131(2):157-68. doi:10.1016/j.psychresns.2003.11.001
29. Starkstein SE, Migliorelli R, Teson A, et al. Specificity of changes in cerebral blood flow in patients with frontal lobe dementia. *J Neurol Neurosurg Psychiatry*. Jul 1994;57(7):790-6. doi:10.1136/jnnp.57.7.790
30. Cho H, Kwon JH, Seo HJ, Kim JS. The short-term effect of acetylcholinesterase inhibitor on the regional cerebral blood flow of Alzheimer's disease. *Arch Gerontol Geriatr*. Mar-Apr 2010;50(2):222-6. doi:10.1016/j.archger.2009.03.013

31. De Reuck J, Decoo D, Van Aken J, Strijckmans K, Lemahieu I, Vermeulen A. Positron emission tomography study of the human hypothalamus during normal ageing and in ischemic and degenerative disorders. *Clin Neurol Neurosurg.* 1992;94(2):113-8. doi:10.1016/0303-8467(92)90067-d
32. Hanyu H, Shimuzu T, Tanaka Y, Takasaki M, Koizumi K, Abe K. Effect of age on regional cerebral blood flow patterns in Alzheimer's disease patients. *J Neurol Sci.* May 15 2003;209(1-2):25-30. doi:10.1016/s0022-510x(02)00456-2
33. Hanyu H, Shimizu S, Tanaka Y, Takasaki M, Koizumi K, Abe K. Differences in regional cerebral blood flow patterns in male versus female patients with Alzheimer disease. *AJNR Am J Neuroradiol.* Aug 2004;25(7):1199-204.
34. Haji M, Kimura N, Hanaoka T, et al. Evaluation of regional cerebral blood flow in Alzheimer's disease patients with subclinical hypothyroidism. *Dement Geriatr Cogn Disord.* 2015;39(5-6):360-7. doi:10.1159/000375298
35. Kimura N, Kumamoto T, Masuda H, et al. Relationship between thyroid hormone levels and regional cerebral blood flow in Alzheimer disease. *Alzheimer Dis Assoc Disord.* Apr-Jun 2011;25(2):138-43. doi:10.1097/WAD.0b013e3181f9aff2
36. Brown DR, Wyper DJ, Owens J, et al. 123Iodo-MK-801: a spect agent for imaging the pattern and extent of glutamate (NMDA) receptor activation in Alzheimer's disease. *J Psychiatr Res.* Nov-Dec 1997;31(6):605-19. doi:10.1016/s0022-3956(97)00031-9
37. Brown DR, Hunter R, Wyper DJ, et al. Longitudinal changes in cognitive function and regional cerebral function in Alzheimer's disease: a SPECT blood flow study. *J Psychiatr Res.* Mar-Apr 1996;30(2):109-26. doi:10.1016/0022-3956(95)00032-1
38. Colloby SJ, Fenwick JD, Williams ED, et al. A comparison of (99m)Tc-HMPAO SPET changes in dementia with Lewy bodies and Alzheimer's disease using statistical parametric mapping. *Eur J Nucl Med Mol Imaging.* May 2002;29(5):615-22. doi:10.1007/s00259-002-0778-5
39. Firbank MJ, He J, Blamire AM, et al. Cerebral blood flow by arterial spin labeling in poststroke dementia. *Neurology.* Apr 26 2011;76(17):1478-84. doi:10.1212/WNL.0b013e318217e76a
40. Kawamura J, Meyer JS, Terayama Y, Weathers S. Cerebral white matter perfusion in dementia of Alzheimer type. *Alzheimer Dis Assoc Disord.* Winter 1991;5(4):231-9. doi:10.1097/00002093-199100540-00002
41. Mortel KF, Pavol MA, Wood S, et al. Prospective studies of cerebral perfusion and cognitive testing among elderly normal volunteers and patients with ischemic vascular dementia and Alzheimer's disease. *Angiology.* Mar 1994;45(3):171-80. doi:10.1177/000331979404500301
42. Obara K, Meyer JS, Mortel KF, Muramatsu K. Cognitive declines correlate with decreased cortical volume and perfusion in dementia of Alzheimer type. *J Neurol Sci.* Dec 1 1994;127(1):96-102. doi:10.1016/0022-510x(94)90141-4
43. Pearlson GD, Harris GJ, Powers RE, et al. Quantitative changes in mesial temporal volume, regional cerebral blood flow, and cognition in Alzheimer's disease. *Arch Gen Psychiatry.* May 1992;49(5):402-8. doi:10.1001/archpsyc.1992.01820050066012

44. Harris GJ, Links JM, Pearlson GD, Camargo EE. Cortical circumferential profile of SPECT cerebral perfusion in Alzheimer's disease. *Psychiatry Res.* Nov 1991;40(3):167-80. doi:10.1016/0925-4927(91)90008-e
45. Alegret M, Vinyes-Junque G, Boada M, et al. Brain perfusion correlates of visuoperceptual deficits in mild cognitive impairment and mild Alzheimer's disease. *J Alzheimers Dis.* 2010;21(2):557-67. doi:10.3233/JAD-2010-091069
46. Benoit M, Koulibaly PM, Migneco O, Darcourt J, Pringuey DJ, Robert PH. Brain perfusion in Alzheimer's disease with and without apathy: a SPECT study with statistical parametric mapping analysis. *Psychiatry Res.* Jun 15 2002;114(2):103-11. doi:10.1016/s0925-4927(02)00003-3
47. Claus JJ, van Harskamp F, Breteler MM, et al. Assessment of cerebral perfusion with single-photon emission tomography in normal subjects and in patients with Alzheimer's disease: effects of region of interest selection. *Eur J Nucl Med.* Oct 1994;21(10):1044-51. doi:10.1007/BF00181058
48. Dai W, Lopez OL, Carmichael OT, Becker JT, Kuller LH, Gach HM. Mild cognitive impairment and alzheimer disease: patterns of altered cerebral blood flow at MR imaging. *Radiology.* Mar 2009;250(3):856-66. doi:10.1148/radiol.2503080751
49. Ding B, Ling HW, Zhang Y, et al. Pattern of cerebral hyperperfusion in Alzheimer's disease and amnesic mild cognitive impairment using voxel-based analysis of 3D arterial spin-labeling imaging: initial experience. *Clin Interv Aging.* 2014;9:493-500. doi:10.2147/CIA.S58879
50. Encinas M, De Juan R, Marcos A, et al. Regional cerebral blood flow assessed with 99mTc-ECD SPET as a marker of progression of mild cognitive impairment to Alzheimer's disease. *Eur J Nucl Med Mol Imaging.* Nov 2003;30(11):1473-80. doi:10.1007/s00259-003-1277-z
51. Hanyu H, Sato T, Shimizu S, Kanetaka H, Iwamoto T, Koizumi K. The effect of education on rCBF changes in Alzheimer's disease: a longitudinal SPECT study. *Eur J Nucl Med Mol Imaging.* Dec 2008;35(12):2182-90. doi:10.1007/s00259-008-0848-4
52. Iizuka T, Kameyama M. Cholinergic enhancement increases regional cerebral blood flow to the posterior cingulate cortex in mild Alzheimer's disease. *Geriatr Gerontol Int.* Jun 2017;17(6):951-958. doi:10.1111/ggi.12818
53. Jagust WJ, Budinger TF, Reed BR. The diagnosis of dementia with single photon emission computed tomography. *Arch Neurol.* Mar 1987;44(3):258-62. doi:10.1001/archneur.1987.00520150014011
54. Johnson KA, Moran EK, Becker JA, Blacker D, Fischman AJ, Albert MS. Single photon emission computed tomography perfusion differences in mild cognitive impairment. *J Neurol Neurosurg Psychiatry.* Mar 2007;78(3):240-7. doi:10.1136/jnnp.2006.096800
55. Lacalle-Aurioles M, Aleman-Gomez Y, Guzman-De-Villoria JA, et al. Is the cerebellum the optimal reference region for intensity normalization of perfusion MR studies in early Alzheimer's disease? *PLoS One.* 2013;8(12):e81548. doi:10.1371/journal.pone.0081548
56. Lee YC, Liu RS, Liao YC, et al. Statistical parametric mapping of brain SPECT perfusion abnormalities in patients with Alzheimer's disease. *Eur Neurol.* 2003;49(3):142-5. doi:10.1159/000069086

57. Mubrin Z, Knezevic S, Spilich G, et al. Normalization of rCBF pattern in senile dementia of the Alzheimer's type. *Psychiatry Res.* Sep 1989;29(3):303-6. doi:10.1016/0165-1781(89)90072-3
58. Nagahama Y, Nabatame H, Okina T, et al. Cerebral correlates of the progression rate of the cognitive decline in probable Alzheimer's disease. *Eur Neurol.* 2003;50(1):1-9. doi:10.1159/000070851
59. Sase S, Yamamoto H, Kawashima E, Tan X, Sawa Y. Discrimination Between Patients With Alzheimer Disease and Healthy Subjects Using Layer Analysis of Cerebral Blood Flow and Xenon Solubility Coefficient in Xenon-Enhanced Computed Tomography. *J Comput Assist Tomogr.* May/Jun 2017;41(3):477-483. doi:10.1097/RCT.0000000000000525
60. Schuff N, Matsumoto S, Kmiecik J, et al. Cerebral blood flow in ischemic vascular dementia and Alzheimer's disease, measured by arterial spin-labeling magnetic resonance imaging. *Alzheimers Dement.* Nov 2009;5(6):454-62. doi:10.1016/j.jalz.2009.04.1233
61. Shimizu S, Hanyu H, Kanetaka H, Iwamoto T, Koizumi K, Abe K. Differentiation of dementia with Lewy bodies from Alzheimer's disease using brain SPECT. *Dement Geriatr Cogn Disord.* 2005;20(1):25-30. doi:10.1159/000085070
62. Sundstrom T, Elgh E, Larsson A, Nasman B, Nyberg L, Riklund KA. Memory-provoked rCBF-SPECT as a diagnostic tool in Alzheimer's disease? *Eur J Nucl Med Mol Imaging.* Jan 2006;33(1):73-80. doi:10.1007/s00259-005-1874-0
63. Takahashi M, Sato A, Nakajima K, et al. Poor performance in Clock-Drawing Test associated with visual memory deficit and reduced bilateral hippocampal and left temporoparietal regional blood flows in Alzheimer's disease patients. *Psychiatry Clin Neurosci.* Apr 2008;62(2):167-73. doi:10.1111/j.1440-1819.2008.01750.x
64. Tateno M, Kobayashi S, Shirasaka T, et al. Comparison of the usefulness of brain perfusion SPECT and MIBG myocardial scintigraphy for the diagnosis of dementia with Lewy bodies. *Dement Geriatr Cogn Disord.* 2008;26(5):453-7. doi:10.1159/000165918
65. van de Haar HJ, Jansen JFA, van Osch MJP, et al. Neurovascular unit impairment in early Alzheimer's disease measured with magnetic resonance imaging. *Neurobiol Aging.* Sep 2016;45:190-196. doi:10.1016/j.neurobiolaging.2016.06.006
66. Yew B, Nation DA, Alzheimer's Disease Neuroimaging I. Cerebrovascular resistance: effects on cognitive decline, cortical atrophy, and progression to dementia. *Brain.* Jul 1 2017;140(7):1987-2001. doi:10.1093/brain/awx112
67. Yoshida T, Kazui H, Tokunaga H, et al. Protein synthesis in the posterior cingulate cortex in Alzheimer's disease. *Psychogeriatrics.* Mar 2011;11(1):40-5. doi:10.1111/j.1479-8301.2010.00350.x
68. Clark LR, Zuelsdorff M, Norton D, et al. Association of Cardiovascular Risk Factors with Cerebral Perfusion in Whites and African Americans. *J Alzheimers Dis.* 2020;75(2):649-660. doi:10.3233/JAD-190360
69. Race, education and prevalence of hypertension. *Am J Epidemiol.* Nov 1977;106(5):351-61.
70. Entwisle G, Apostolides AY, Hebel JR, Henderson MM. Target organ damage in black hypertensives. *Circulation.* May 1977;55(5):792-6. doi:10.1161/01.cir.55.5.792

71. Iturria-Medina Y, Sotero RC, Toussaint PJ, Mateos-Perez JM, Evans AC, Alzheimer's Disease Neuroimaging I. Early role of vascular dysregulation on late-onset Alzheimer's disease based on multifactorial data-driven analysis. *Nat Commun.* Jun 21 2016;7:11934. doi:10.1038/ncomms11934
72. Clark LR, Norton D, Berman SE, et al. Association of Cardiovascular and Alzheimer's Disease Risk Factors with Intracranial Arterial Blood Flow in Whites and African Americans. *J Alzheimers Dis.* 2019;72(3):919-929. doi:10.3233/JAD-190645
73. Hurr C, Kim K, Harrison ML, Brothers RM. Attenuated cerebral vasodilatory capacity in response to hypercapnia in college-aged African Americans. *Exp Physiol.* Jan 2015;100(1):35-43. doi:10.1113/expphysiol.2014.082362
74. Thayer JF, Koenig J. Resting Cerebral Blood Flow and Ethnic Differences in Heart Rate Variability: Links to Self-Reports of Affect and Affect Regulation. *Neuroimage.* Nov 15 2019;202:116154. doi:10.1016/j.neuroimage.2019.116154
75. Allen B, Jennings JR, Gianaros PJ, Thayer JF, Manuck SB. Resting high-frequency heart rate variability is related to resting brain perfusion. *Psychophysiology.* Feb 2015;52(2):277-87. doi:10.1111/psyp.12321
76. Saykin AJ, Wishart HA, Rabin LA, et al. Older adults with cognitive complaints show brain atrophy similar to that of amnesic MCI. *Neurology.* Sep 12 2006;67(5):834-42. doi:10.1212/01.wnl.0000234032.77541.a2
77. Butcher TJ, Chumin EJ, West JD, Dziedzic M, Yoder KK. Cerebral Blood Flow in the Salience Network of Individuals with Alcohol Use Disorder. *Alcohol Alcohol.* Sep 17 2021;doi:10.1093/alcalc/agab062
78. Wong EC, Buxton RB, Frank LR. Implementation of quantitative perfusion imaging techniques for functional brain mapping using pulsed arterial spin labeling. *NMR Biomed.* Jun-Aug 1997;10(4-5):237-49. doi:10.1002/(sici)1099-1492(199706/08)10:4/5<237::aid-nbm475>3.0.co;2-x
79. Luh WM, Wong EC, Bandettini PA, Hyde JS. QUIPSS II with thin-slice T11 periodic saturation: a method for improving accuracy of quantitative perfusion imaging using pulsed arterial spin labeling. *Magn Reson Med.* Jun 1999;41(6):1246-54. doi:10.1002/(sici)1522-2594(199906)41:6<1246::aid-mrm22>3.0.co;2-n
80. Beason-Held LL, Moghekar A, Zonderman AB, Kraut MA, Resnick SM. Longitudinal changes in cerebral blood flow in the older hypertensive brain. *Stroke.* Jun 2007;38(6):1766-73. doi:10.1161/STROKEAHA.106.477109
81. Rodriguez G, Arvigo F, Marengo S, et al. Regional cerebral blood flow in essential hypertension: data evaluation by a mapping system. *Stroke.* Jan-Feb 1987;18(1):13-20. doi:10.1161/01.str.18.1.13
82. Nobili F, Rodriguez G, Marengo S, et al. Regional cerebral blood flow in chronic hypertension. A correlative study. *Stroke.* Aug 1993;24(8):1148-53. doi:10.1161/01.str.24.8.1148
83. Fujii K, Sadoshima S, Okada Y, et al. Cerebral blood flow and metabolism in normotensive and hypertensive patients with transient neurologic deficits. *Stroke.* Feb 1990;21(2):283-90. doi:10.1161/01.str.21.2.283
84. Kume K, Hanyu H, Sakurai H, Takada Y, Onuma T, Iwamoto T. Effects of telmisartan on cognition and regional cerebral blood flow in hypertensive patients

- with Alzheimer's disease. *Geriatr Gerontol Int*. Apr 2012;12(2):207-14.  
doi:10.1111/j.1447-0594.2011.00746.x
85. Moody DM, Brown WR, Challa VR, Ghazi-Birry HS, Reboussin DM. Cerebral microvascular alterations in aging, leukoaraiosis, and Alzheimer's disease. *Ann N Y Acad Sci*. Sep 26 1997;826:103-16. doi:10.1111/j.1749-6632.1997.tb48464.x
  86. Gasecki D, Kwarciany M, Nyka W, Narkiewicz K. Hypertension, brain damage and cognitive decline. *Curr Hypertens Rep*. Dec 2013;15(6):547-58.  
doi:10.1007/s11906-013-0398-4
  87. Juergenson I, Mazzucco S, Tinazzi M. A typical example of cerebral watershed infarct. *Clin Pract*. Sep 28 2011;1(4):e114. doi:10.4081/cp.2011.e114
  88. Caruso P, Signori R, Moretti R. Small vessel disease to subcortical dementia: a dynamic model, which interfaces aging, cholinergic dysregulation and the neurovascular unit. *Vasc Health Risk Manag*. 2019;15:259-281.  
doi:10.2147/VHRM.S190470
  89. Efimova IY, Efimova NY, Triss SV, Lishmanov YB. Brain perfusion and cognitive function changes in hypertensive patients. *Hypertens Res*. Apr 2008;31(4):673-8.  
doi:10.1291/hypres.31.673
  90. Dai W, Lopez OL, Carmichael OT, Becker JT, Kuller LH, Gach HM. Abnormal regional cerebral blood flow in cognitively normal elderly subjects with hypertension. *Stroke*. Feb 2008;39(2):349-54.  
doi:10.1161/STROKEAHA.107.495457
  91. Copenhagen BR, Hsia AW, Merino JG, et al. Racial differences in microbleed prevalence in primary intracerebral hemorrhage. *Neurology*. Oct 7 2008;71(15):1176-82. doi:10.1212/01.wnl.0000327524.16575.ca
  92. Caughey MC, Qiao Y, Windham BG, Gottesman RF, Mosley TH, Wasserman BA. Carotid Intima-Media Thickness and Silent Brain Infarctions in a Biracial Cohort: The Atherosclerosis Risk in Communities (ARIC) Study. *Am J Hypertens*. Jul 16 2018;31(8):869-875. doi:10.1093/ajh/hpy022
  93. Yang D, Cabral D, Gaspard EN, Lipton RB, Rundek T, Derby CA. Cerebral Hemodynamics in the Elderly: A Transcranial Doppler Study in the Einstein Aging Study Cohort. *J Ultrasound Med*. Sep 2016;35(9):1907-14.  
doi:10.7863/ultra.15.10040
  94. Patik JC, Curtis BM, Nasirian A, Vranish JR, Fadel PJ, Brothers RM. Sex differences in the mechanisms mediating blunted cutaneous microvascular function in young black men and women. *Am J Physiol Heart Circ Physiol*. Oct 1 2018;315(4):H1063-H1071. doi:10.1152/ajpheart.00142.2018
  95. Howell JC, Watts KD, Parker MW, et al. Race modifies the relationship between cognition and Alzheimer's disease cerebrospinal fluid biomarkers. *Alzheimers Res Ther*. Nov 2 2017;9(1):88. doi:10.1186/s13195-017-0315-1
  96. Weiner KS, Zilles K. The anatomical and functional specialization of the fusiform gyrus. *Neuropsychologia*. Mar 2016;83:48-62.  
doi:10.1016/j.neuropsychologia.2015.06.033
  97. Brunye TT, Moran JM, Holmes A, Mahoney CR, Taylor HA. Non-invasive brain stimulation targeting the right fusiform gyrus selectively increases working memory for faces. *Brain Cogn*. Apr 2017;113:32-39. doi:10.1016/j.bandc.2017.01.006

98. Geiger MJ, O'Gorman Tuura R, Klaver P. Inter-hemispheric connectivity in the fusiform gyrus supports memory consolidation for faces. *Eur J Neurosci*. May 2016;43(9):1137-45. doi:10.1111/ejn.13197
99. Convit A, De Leon MJ, Tarshish C, et al. Specific hippocampal volume reductions in individuals at risk for Alzheimer's disease. *Neurobiol Aging*. Mar-Apr 1997;18(2):131-8. doi:10.1016/s0197-4580(97)00001-8
100. Geronimus AT. The weathering hypothesis and the health of African-American women and infants: evidence and speculations. *Ethn Dis*. Summer 1992;2(3):207-21.
101. McDonough IM. Beta-amyloid and Cortical Thickness Reveal Racial Disparities in Preclinical Alzheimer's Disease. *Neuroimage Clin*. 2017;16:659-667. doi:10.1016/j.nicl.2017.09.014
102. Crous-Bou M, Minguillon C, Gramunt N, Molinuevo JL. Alzheimer's disease prevention: from risk factors to early intervention. *Alzheimers Res Ther*. Sep 12 2017;9(1):71. doi:10.1186/s13195-017-0297-z
103. Lu L, Zheng X, Wang S, et al. Anti-Abeta agents for mild to moderate Alzheimer's disease: systematic review and meta-analysis. *J Neurol Neurosurg Psychiatry*. Dec 2020;91(12):1316-1324. doi:10.1136/jnnp-2020-323497
104. Congdon EE, Sigurdsson EM. Tau-targeting therapies for Alzheimer disease. *Nat Rev Neurol*. Jul 2018;14(7):399-415. doi:10.1038/s41582-018-0013-z
105. Alsop DC, Detre JA, Grossman M. Assessment of cerebral blood flow in Alzheimer's disease by spin-labeled magnetic resonance imaging. *Ann Neurol*. Jan 2000;47(1):93-100.
106. Binnewijzend MA, Kuijter JP, Benedictus MR, et al. Cerebral blood flow measured with 3D pseudocontinuous arterial spin-labeling MR imaging in Alzheimer disease and mild cognitive impairment: a marker for disease severity. *Radiology*. Apr 2013;267(1):221-30. doi:10.1148/radiol.12120928
107. Korte N, Nortley R, Attwell D. Cerebral blood flow decrease as an early pathological mechanism in Alzheimer's disease. *Acta Neuropathol*. Dec 2020;140(6):793-810. doi:10.1007/s00401-020-02215-w
108. Gorelick PB. Risk factors for vascular dementia and Alzheimer disease. *Stroke*. Nov 2004;35(11 Suppl 1):2620-2. doi:10.1161/01.STR.0000143318.70292.47
109. Iadecola C. Neurovascular regulation in the normal brain and in Alzheimer's disease. *Nat Rev Neurosci*. May 2004;5(5):347-60. doi:10.1038/nrn1387
110. Beishon L, Haunton VJ, Panerai RB, Robinson TG. Cerebral Hemodynamics in Mild Cognitive Impairment: A Systematic Review. *J Alzheimers Dis*. 2017;59(1):369-385. doi:10.3233/JAD-170181
111. West JD, Risacher SL, Gandhi PK, et al. Elevated Cerebral Blood Flow in Participants with Subjective Cognitive Decline. *Alzheimers Dement*. 2016;12(7):70-71. doi:10.1016/j.alz.2016.06.121
112. Wierenga CE, Hays CC, Zlatar ZZ. Cerebral blood flow measured by arterial spin labeling MRI as a preclinical marker of Alzheimer's disease. *J Alzheimers Dis*. 2014;42 Suppl 4:S411-9. doi:10.3233/JAD-141467
113. Boles Ponto LL, Magnotta VA, Moser DJ, Duff KM, Schultz SK. Global cerebral blood flow in relation to cognitive performance and reserve in subjects with mild memory deficits. *Mol Imaging Biol*. Nov-Dec 2006;8(6):363-72. doi:10.1007/s11307-006-0066-z

114. Albrecht D, Isenberg AL, Stradford J, et al. Associations between Vascular Function and Tau PET Are Associated with Global Cognition and Amyloid. *J Neurosci*. Oct 28 2020;40(44):8573-8586. doi:10.1523/JNEUROSCI.1230-20.2020
115. Rubinski A, Tosun D, Franzmeier N, et al. Lower cerebral perfusion is associated with tau-PET in the entorhinal cortex across the Alzheimer's continuum. *Neurobiol Aging*. Jun 2021;102:111-118. doi:10.1016/j.neurobiolaging.2021.02.003
116. Visser D, Wolters EE, Verfaillie SCJ, et al. Tau pathology and relative cerebral blood flow are independently associated with cognition in Alzheimer's disease. *Eur J Nucl Med Mol Imaging*. Dec 2020;47(13):3165-3175. doi:10.1007/s00259-020-04831-w
117. Mattsson N, Tosun D, Insel PS, et al. Association of brain amyloid-beta with cerebral perfusion and structure in Alzheimer's disease and mild cognitive impairment. *Brain*. May 2014;137(Pt 5):1550-61. doi:10.1093/brain/awu043
118. Rodell AB, O'Keefe G, Rowe CC, Villemagne VL, Gjedde A. Cerebral Blood Flow and Abeta-Amyloid Estimates by WARM Analysis of [(11)C]PiB Uptake Distinguish among and between Neurodegenerative Disorders and Aging. *Front Aging Neurosci*. 2016;8:321. doi:10.3389/fnagi.2016.00321
119. Tosun D, Schuff N, Jagust W, Weiner MW, Alzheimer's Disease Neuroimaging I. Discriminative Power of Arterial Spin Labeling Magnetic Resonance Imaging and 18F-Fluorodeoxyglucose Positron Emission Tomography Changes for Amyloid-beta-Positive Subjects in the Alzheimer's Disease Continuum. *Neurodegener Dis*. 2016;16(1-2):87-94. doi:10.1159/000439257
120. Codispoti KE, Beason-Held LL, Kraut MA, et al. Longitudinal brain activity changes in asymptomatic Alzheimer disease. *Brain Behav*. May 2012;2(3):221-30. doi:10.1002/brb3.47
121. Stomrud E, Forsberg A, Hagerstrom D, et al. CSF biomarkers correlate with cerebral blood flow on SPECT in healthy elderly. *Dement Geriatr Cogn Disord*. 2012;33(2-3):156-63. doi:10.1159/000338185
122. Fazlollahi A, Calamante F, Liang X, et al. Increased cerebral blood flow with increased amyloid burden in the preclinical phase of alzheimer's disease. *J Magn Reson Imaging*. Feb 2020;51(2):505-513. doi:10.1002/jmri.26810
123. Tosun D, Joshi S, Weiner MW, the Alzheimer's Disease Neuroimaging I. Multimodal MRI-based Imputation of the Abeta+ in Early Mild Cognitive Impairment. *Ann Clin Transl Neurol*. Mar 2014;1(3):160-170. doi:10.1002/acn3.40
124. Sojkova J, Beason-Held L, Zhou Y, et al. Longitudinal cerebral blood flow and amyloid deposition: an emerging pattern? *J Nucl Med*. Sep 2008;49(9):1465-71. doi:10.2967/jnumed.108.051946
125. Solis E, Jr., Hascup KN, Hascup ER. Alzheimer's Disease: The Link Between Amyloid-beta and Neurovascular Dysfunction. *J Alzheimers Dis*. 2020;76(4):1179-1198. doi:10.3233/JAD-200473
126. Bell RD, Winkler EA, Singh I, et al. Apolipoprotein E controls cerebrovascular integrity via cyclophilin A. *Nature*. May 16 2012;485(7399):512-6. doi:10.1038/nature11087
127. Wiesmann M, Zerbi V, Jansen D, et al. A Dietary Treatment Improves Cerebral Blood Flow and Brain Connectivity in Aging apoE4 Mice. *Neural Plast*. 2016;2016:6846721. doi:10.1155/2016/6846721

128. Suwa A, Nishida K, Utsunomiya K, et al. Neuropsychological Evaluation and Cerebral Blood Flow Effects of Apolipoprotein E4 in Alzheimer's Disease Patients after One Year of Treatment: An Exploratory Study. *Dement Geriatr Cogn Dis Extra*. Sep-Dec 2015;5(3):414-23. doi:10.1159/000440714
129. Risacher SL, West JD, Deardorff R, et al. Head injury is associated with tau deposition on PET in MCI and AD patients. *Alzheimers Dement (Amst)*. 2021;13(1):e12230. doi:10.1002/dad2.12230
130. Chan SL, Bishop N, Li Z, Cipolla MJ. Inhibition of PAI (Plasminogen Activator Inhibitor)-1 Improves Brain Collateral Perfusion and Injury After Acute Ischemic Stroke in Aged Hypertensive Rats. *Stroke*. Aug 2018;49(8):1969-1976. doi:10.1161/STROKEAHA.118.022056
131. de la Torre JC, Pappas BA, Prevot V, et al. Hippocampal nitric oxide upregulation precedes memory loss and A beta 1-40 accumulation after chronic brain hypoperfusion in rats. *Neurol Res*. Sep 2003;25(6):635-41. doi:10.1179/016164103101201931
132. Faraco G, Park L, Zhou P, et al. Hypertension enhances Abeta-induced neurovascular dysfunction, promotes beta-secretase activity, and leads to amyloidogenic processing of APP. *J Cereb Blood Flow Metab*. Jan 2016;36(1):241-52. doi:10.1038/jcbfm.2015.79
133. Khan MB, Hoda MN, Vaibhav K, et al. Remote ischemic postconditioning: harnessing endogenous protection in a murine model of vascular cognitive impairment. *Transl Stroke Res*. Feb 2015;6(1):69-77. doi:10.1007/s12975-014-0374-6
134. Liang W, Zhang W, Zhao S, Li Q, Liang H, Ceng R. Altered expression of neurofilament 200 and amyloid-beta peptide (1-40) in a rat model of chronic cerebral hypoperfusion. *Neurol Sci*. May 2015;36(5):707-12. doi:10.1007/s10072-014-2014-z
135. Klohs J, Rudin M, Shimshek DR, Beckmann N. Imaging of cerebrovascular pathology in animal models of Alzheimer's disease. *Front Aging Neurosci*. 2014;6:32. doi:10.3389/fnagi.2014.00032
136. Niwa K, Kazama K, Younkin L, Younkin SG, Carlson GA, Iadecola C. Cerebrovascular autoregulation is profoundly impaired in mice overexpressing amyloid precursor protein. *Am J Physiol Heart Circ Physiol*. Jul 2002;283(1):H315-23. doi:10.1152/ajpheart.00022.2002
137. Niwa K, Carlson GA, Iadecola C. Exogenous A beta1-40 reproduces cerebrovascular alterations resulting from amyloid precursor protein overexpression in mice. *J Cereb Blood Flow Metab*. Dec 2000;20(12):1659-68. doi:10.1097/00004647-200012000-00005
138. Niwa K, Porter VA, Kazama K, Cornfield D, Carlson GA, Iadecola C. A beta-peptides enhance vasoconstriction in cerebral circulation. *Am J Physiol Heart Circ Physiol*. Dec 2001;281(6):H2417-24. doi:10.1152/ajpheart.2001.281.6.H2417
139. Nortley R, Korte N, Izquierdo P, et al. Amyloid beta oligomers constrict human capillaries in Alzheimer's disease via signaling to pericytes. *Science*. Jul 19 2019;365(6450)doi:10.1126/science.aav9518
140. Chen YJ, Rosario BL, Mowrey W, et al. Relative 11C-PiB Delivery as a Proxy of Relative CBF: Quantitative Evaluation Using Single-Session 15O-Water and 11C-PiB PET. *J Nucl Med*. Aug 2015;56(8):1199-205. doi:10.2967/jnumed.114.152405

141. Takahashi M, Tada T, Nakamura T, Koyama K, Momose T. Efficacy and Limitations of rCBF-SPECT in the Diagnosis of Alzheimer's Disease With Amyloid-PET. *Am J Alzheimers Dis Other Demen.* Aug 2019;34(5):314-321. doi:10.1177/1533317519841192
142. Michels L, Warnock G, Buck A, et al. Arterial spin labeling imaging reveals widespread and Aβ-independent reductions in cerebral blood flow in elderly apolipoprotein ε4 carriers. *J Cereb Blood Flow Metab.* Mar 2016;36(3):581-95. doi:10.1177/0271678X15605847
143. Gomez-Isla T, Hollister R, West H, et al. Neuronal loss correlates with but exceeds neurofibrillary tangles in Alzheimer's disease. *Ann Neurol.* Jan 1997;41(1):17-24. doi:10.1002/ana.410410106
144. Ashford JW, Shih WJ, Coupal J, et al. Single SPECT measures of cerebral cortical perfusion reflect time-index estimation of dementia severity in Alzheimer's disease. *J Nucl Med.* Jan 2000;41(1):57-64.
145. Raz L, Bhaskar K, Weaver J, et al. Hypoxia promotes tau hyperphosphorylation with associated neuropathology in vascular dysfunction. *Neurobiol Dis.* Jun 2019;126:124-136. doi:10.1016/j.nbd.2018.07.009
146. Zhang ZH, Fang XB, Xi GM, Li WC, Ling HY, Qu P. Calcitonin gene-related peptide enhances CREB phosphorylation and attenuates tau protein phosphorylation in rat brain during focal cerebral ischemia/reperfusion. *Biomed Pharmacother.* Jul 2010;64(6):430-6. doi:10.1016/j.biopha.2009.06.009
147. Bennett RE, Robbins AB, Hu M, et al. Tau induces blood vessel abnormalities and angiogenesis-related gene expression in P301L transgenic mice and human Alzheimer's disease. *Proc Natl Acad Sci U S A.* Feb 6 2018;115(6):E1289-E1298. doi:10.1073/pnas.1710329115
148. Jaworski T, Lechat B, Demedts D, et al. Dendritic degeneration, neurovascular defects, and inflammation precede neuronal loss in a mouse model for tau-mediated neurodegeneration. *Am J Pathol.* Oct 2011;179(4):2001-15. doi:10.1016/j.ajpath.2011.06.025
149. Lourenco CF, Ledo A, Barbosa RM, Laranjinha J. Neurovascular uncoupling in the triple transgenic model of Alzheimer's disease: Impaired cerebral blood flow response to neuronal-derived nitric oxide signaling. *Exp Neurol.* May 2017;291:36-43. doi:10.1016/j.expneurol.2017.01.013
150. Park L, Hochrainer K, Hattori Y, et al. Tau induces PSD95-neuronal NOS uncoupling and neurovascular dysfunction independent of neurodegeneration. *Nat Neurosci.* Sep 2020;23(9):1079-1089. doi:10.1038/s41593-020-0686-7
151. Okamura N, Arai H, Maruyama M, et al. Combined Analysis of CSF Tau Levels and [(123)I]Iodoamphetamine SPECT in Mild Cognitive Impairment: Implications for a Novel Predictor of Alzheimer's Disease. *Am J Psychiatry.* Mar 2002;159(3):474-6. doi:10.1176/appi.ajp.159.3.474
152. Hays CC, Zlatar ZZ, Meloy MJ, et al. Anterior Cingulate Structure and Perfusion is Associated with Cerebrospinal Fluid Tau among Cognitively Normal Older Adult APOEε4 Carriers. *J Alzheimers Dis.* 2020;73(1):87-101. doi:10.3233/JAD-190504
153. Wang J, Peng G, Liu P, Tan X, Luo B, Alzheimer's Disease Neuroimaging I. Regulating effect of CBF on memory in cognitively normal older adults with

- different ApoE genotype: the Alzheimer's Disease Neuroimaging Initiative (ADNI). *Cogn Neurodyn*. Dec 2019;13(6):513-518. doi:10.1007/s11571-019-09536-x
154. Zlatar ZZ, Bischoff-Grethe A, Hays CC, et al. Higher Brain Perfusion May Not Support Memory Functions in Cognitively Normal Carriers of the ApoE epsilon4 Allele Compared to Non-Carriers. *Front Aging Neurosci*. 2016;8:151. doi:10.3389/fnagi.2016.00151
  155. Khan W, Giampietro V, Banaschewski T, et al. A Multi-Cohort Study of ApoE varepsilon4 and Amyloid-beta Effects on the Hippocampus in Alzheimer's Disease. *J Alzheimers Dis*. 2017;56(3):1159-1174. doi:10.3233/JAD-161097
  156. Donahue JE, Johanson CE. Apolipoprotein E, amyloid-beta, and blood-brain barrier permeability in Alzheimer disease. *J Neuropathol Exp Neurol*. Apr 2008;67(4):261-70. doi:10.1097/NEN.0b013e31816a0dc8
  157. Castellano JM, Kim J, Stewart FR, et al. Human apoE isoforms differentially regulate brain amyloid-beta peptide clearance. *Sci Transl Med*. Jun 29 2011;3(89):89ra57. doi:10.1126/scitranslmed.3002156
  158. Wahrle SE, Shah AR, Fagan AM, et al. Apolipoprotein E levels in cerebrospinal fluid and the effects of ABCA1 polymorphisms. *Mol Neurodegener*. Apr 12 2007;2:7. doi:10.1186/1750-1326-2-7
  159. Mahley RW, Weisgraber KH, Huang Y. Apolipoprotein E4: a causative factor and therapeutic target in neuropathology, including Alzheimer's disease. *Proc Natl Acad Sci U S A*. Apr 11 2006;103(15):5644-51. doi:10.1073/pnas.0600549103
  160. Jack CR, Wiste HJ, Weigand SD, et al. Predicting future rates of tau accumulation on PET. *Brain*. Oct 1 2020;143(10):3136-3150. doi:10.1093/brain/awaa248
  161. Ossenkoppele R, Schonhaut DR, Scholl M, et al. Tau PET patterns mirror clinical and neuroanatomical variability in Alzheimer's disease. *Brain*. May 2016;139(Pt 5):1551-67. doi:10.1093/brain/aww027
  162. Alosco ML, Gunstad J, Jerskey BA, et al. The adverse effects of reduced cerebral perfusion on cognition and brain structure in older adults with cardiovascular disease. *Brain Behav*. Nov 2013;3(6):626-36. doi:10.1002/brb3.171
  163. Toth P, Tarantini S, Csiszar A, Ungvari Z. Functional vascular contributions to cognitive impairment and dementia: mechanisms and consequences of cerebral autoregulatory dysfunction, endothelial impairment, and neurovascular uncoupling in aging. *Am J Physiol Heart Circ Physiol*. Jan 1 2017;312(1):H1-H20. doi:10.1152/ajpheart.00581.2016
  164. Lennon MJ, Koncz R, Sachdev PS. Hypertension and Alzheimer's disease: is the picture any clearer? *Curr Opin Psychiatry*. Mar 1 2021;34(2):142-148. doi:10.1097/YCO.0000000000000684
  165. Dickstein DL, Walsh J, Brautigam H, Stockton SD, Jr., Gandy S, Hof PR. Role of vascular risk factors and vascular dysfunction in Alzheimer's disease. *Mt Sinai J Med*. Jan-Feb 2010;77(1):82-102. doi:10.1002/msj.20155
  166. Alzheimer's Association 2017 Alzheimer's disease facts and figures. *Alzheimers Dement*. 2017;13:325-373
  167. Sperling RA, Aisen PS, Beckett LA, et al. Toward defining the preclinical stages of Alzheimer's disease: recommendations from the National Institute on Aging-Alzheimer's Association workgroups on diagnostic guidelines for Alzheimer's disease. *Alzheimers Dement*. May 2011;7(3):280-92. doi:10.1016/j.jalz.2011.03.003

168. Reisberg B, Shulman MB, Torossian C, Leng L, Zhu W. Outcome over seven years of healthy adults with and without subjective cognitive impairment. *Alzheimers Dement*. Jan 2010;6(1):11-24. doi:10.1016/j.jalz.2009.10.002
169. Gifford KA, Liu D, Lu Z, et al. The source of cognitive complaints predicts diagnostic conversion differentially among nondemented older adults. *Alzheimers Dement*. May 2014;10(3):319-27. doi:10.1016/j.jalz.2013.02.007
170. Glodzik-Sobanska L, Reisberg B, De Santi S, et al. Subjective memory complaints: presence, severity and future outcome in normal older subjects. *Dement Geriatr Cogn Disord*. 2007;24(3):177-84. doi:10.1159/000105604
171. Hohman TJ, Beason-Held LL, Resnick SM. Cognitive complaints, depressive symptoms, and cognitive impairment: are they related? *J Am Geriatr Soc*. Oct 2011;59(10):1908-12. doi:10.1111/j.1532-5415.2011.03589.x
172. Jessen F, Wiese B, Bachmann C, et al. Prediction of dementia by subjective memory impairment: effects of severity and temporal association with cognitive impairment. *Arch Gen Psychiatry*. Apr 2010;67(4):414-22. doi:10.1001/archgenpsychiatry.2010.30
173. Kielb S, Rogalski E, Weintraub S, Rademaker A. Objective features of subjective cognitive decline in a United States national database. *Alzheimers Dement*. Dec 2017;13(12):1337-1344. doi:10.1016/j.jalz.2017.04.008
174. Edmonds EC, Delano-Wood L, Galasko DR, Salmon DP, Bondi MW, Alzheimer's Disease Neuroimaging I. Subjective cognitive complaints contribute to misdiagnosis of mild cognitive impairment. *J Int Neuropsychol Soc*. Sep 2014;20(8):836-47. doi:10.1017/S135561771400068X
175. Balash Y, Mordechovich M, Shabtai H, Giladi N, Gurevich T, Korczyn AD. Subjective memory complaints in elders: depression, anxiety, or cognitive decline? *Acta Neurol Scand*. May 2013;127(5):344-50. doi:10.1111/ane.12038
176. Carr DB, Gray S, Baty J, Morris JC. The value of informant versus individual's complaints of memory impairment in early dementia. *Neurology*. Dec 12 2000;55(11):1724-6. doi:10.1212/wnl.55.11.1724
177. Salem LC, Vogel A, Ebstrup J, Linneberg A, Waldemar G. Subjective cognitive complaints included in diagnostic evaluation of dementia helps accurate diagnosis in a mixed memory clinic cohort. *Int J Geriatr Psychiatry*. Dec 2015;30(12):1177-85. doi:10.1002/gps.4272
178. Buckley R, Saling M, Ellis K, et al. Self and informant memory concerns align in healthy memory complainers and in early stages of mild cognitive impairment but separate with increasing cognitive impairment. *Age Ageing*. Nov 2015;44(6):1012-9. doi:10.1093/ageing/afv136
179. Silva MR, Moser D, Pfluger M, et al. Self-reported and informant-reported memory functioning and awareness in patients with mild cognitive impairment and Alzheimer's disease. *Neuropsychiatr*. Jun 2016;30(2):103-12. Subjektive Gedächtnisbeschwerden und Awareness bei Patienten mit leichter kognitiver Beeinträchtigung und Patienten mit Alzheimer Demenz. doi:10.1007/s40211-016-0185-y
180. Nunes T, Fragata I, Ribeiro F, et al. The outcome of elderly patients with cognitive complaints but normal neuropsychological tests. *J Alzheimers Dis*. 2010;19(1):137-45. doi:10.3233/JAD-2010-1210

181. Chao LL, Mueller SG, Buckley ST, et al. Evidence of neurodegeneration in brains of older adults who do not yet fulfill MCI criteria. *Neurobiol Aging*. Mar 2010;31(3):368-77. doi:10.1016/j.neurobiolaging.2008.05.004
182. Barnes LL, Schneider JA, Boyle PA, Bienias JL, Bennett DA. Memory complaints are related to Alzheimer disease pathology in older persons. *Neurology*. Nov 14 2006;67(9):1581-5. doi:10.1212/01.wnl.0000242734.16663.09
183. Visser PJ, Verhey F, Knol DL, et al. Prevalence and prognostic value of CSF markers of Alzheimer's disease pathology in patients with subjective cognitive impairment or mild cognitive impairment in the DESCRIPA study: a prospective cohort study. *Lancet Neurol*. Jul 2009;8(7):619-27. doi:10.1016/S1474-4422(09)70139-5
184. Colijn MA, Grossberg GT. Amyloid and Tau Biomarkers in Subjective Cognitive Impairment. *J Alzheimers Dis*. 2015;47(1):1-8. doi:10.3233/JAD-150180
185. Donohue MC, Sperling RA, Petersen R, et al. Association Between Elevated Brain Amyloid and Subsequent Cognitive Decline Among Cognitively Normal Persons. *JAMA*. Jun 13 2017;317(22):2305-2316. doi:10.1001/jama.2017.6669
186. Arriagada PV, Growdon JH, Hedley-Whyte ET, Hyman BT. Neurofibrillary tangles but not senile plaques parallel duration and severity of Alzheimer's disease. *Neurology*. Mar 1992;42(3 Pt 1):631-9. doi:10.1212/wnl.42.3.631
187. Giannakopoulos P, Herrmann FR, Bussiere T, et al. Tangle and neuron numbers, but not amyloid load, predict cognitive status in Alzheimer's disease. *Neurology*. May 13 2003;60(9):1495-500. doi:10.1212/01.wnl.0000063311.58879.01
188. Hall B, Mak E, Cervenka S, Aigbirhio FI, Rowe JB, O'Brien JT. In vivo tau PET imaging in dementia: Pathophysiology, radiotracer quantification, and a systematic review of clinical findings. *Ageing Res Rev*. Jul 2017;36:50-63. doi:10.1016/j.arr.2017.03.002
189. Brier MR, Gordon B, Friedrichsen K, et al. Tau and Abeta imaging, CSF measures, and cognition in Alzheimer's disease. *Sci Transl Med*. May 11 2016;8(338):338ra66. doi:10.1126/scitranslmed.aaf2362
190. Farias ST, Mungas D, Reed BR, et al. The measurement of everyday cognition (ECog): scale development and psychometric properties. *Neuropsychology*. Jul 2008;22(4):531-44. doi:10.1037/0894-4105.22.4.531
191. Risacher SL, Kim S, Nho K, et al. APOE effect on Alzheimer's disease biomarkers in older adults with significant memory concern. *Alzheimers Dement*. Dec 2015;11(12):1417-1429. doi:10.1016/j.jalz.2015.03.003
192. Rattanabannakit C, Risacher SL, Gao S, et al. The Cognitive Change Index as a Measure of Self and Informant Perception of Cognitive Decline: Relation to Neuropsychological Tests. *J Alzheimers Dis*. 2016;51(4):1145-55. doi:10.3233/JAD-150729
193. Landau SM, Breault C, Joshi AD, et al. Amyloid-beta imaging with Pittsburgh compound B and florbetapir: comparing radiotracers and quantification methods. *J Nucl Med*. Jan 2013;54(1):70-7. doi:10.2967/jnumed.112.109009
194. Kolling N, Behrens T, Wittmann MK, Rushworth M. Multiple signals in anterior cingulate cortex. *Curr Opin Neurobiol*. Apr 2016;37:36-43. doi:10.1016/j.conb.2015.12.007

195. Hartwigsen G, Baumgaertner A, Price CJ, Koehnke M, Ulmer S, Siebner HR. Phonological decisions require both the left and right supramarginal gyri. *Proc Natl Acad Sci U S A*. Sep 21 2010;107(38):16494-9. doi:10.1073/pnas.1008121107
196. Reid LM, MacLulich AM. Subjective memory complaints and cognitive impairment in older people. *Dement Geriatr Cogn Disord*. 2006;22(5-6):471-85. doi:10.1159/000096295
197. Bruce JM, Bhalla R, Westervelt HJ, Davis J, Williams V, Tremont G. Neuropsychological correlates of self-reported depression and self-reported cognition among patients with mild cognitive impairment. *J Geriatr Psychiatry Neurol*. Mar 2008;21(1):34-40. doi:10.1177/0891988707311032

Curriculum Vitae  
Cecily Gwinn Swinford

**Education**

Ph.D. in Medical Neuroscience, April 2022 – Indiana University  
Indianapolis, IN. Dissertation: *Characterization of Cerebral Blood Flow in Older Adults: A Potential Early Biomarker for Alzheimer's Disease*. Advisor: Andrew J. Saykin, Psy.D.

B.S. in Neuroscience and Behavior, May 2016 – University of Notre Dame  
South Bend, IN.

**Research Experience**

Dr. Andrew Saykin's Lab, 2017 - Current, Stark Neurosciences Research Institute,  
Indianapolis, IN, Neuroimaging of cerebral blood flow in Alzheimer's disease

Dr. Charles Tessier's Lab, 2014 – 2016, Indiana University School of Medicine, South  
Bend, IN, Drosophila model of Fragile X Syndrome

Dr. Srinivasan's Lab, 2015, Indiana University School of Dentistry, Indianapolis, IN,  
Diagnostic techniques for periodontitis

**Honors and Awards**

IU Graduate School Travel Fellowship Award 2019

IUPUI University Fellow 2016-2017

Indiana Clinical and Translational Sciences Institute Undergraduate Summer Internship  
2015

University of Notre Dame Dean's List 2012-2015

Lilly Endowment Community Scholarship Recipient 2012

**Conference Abstracts and Publications**

**Abstracts**

Swinford CG, et al. 2021. Hypertension and Race Affect Cerebral Blood Flow and  
Cognition in Older Adults without Dementia. Alzheimer's Association International  
Conference.

Swinford CG, et al. 2020. Plasma Tau is Negatively Correlated with Frontal Lobe CBF in  
Hypertensive Adults on the AD Spectrum. Alzheimer's Association International  
Conference.

Swinford CG, et al. 2019. Regional Association of Cerebral Blood Flow with Amyloid and Tau in Alzheimer's Disease. Alzheimer's Association International Conference, Los Angeles, CA.

Swinford CG, et al. 2019. Regional Associations of Cerebral Blood Flow with Amyloid, Tau and NfL in Alzheimer's Disease. Society for Neuroscience, Indianapolis, IN.

Alzheimer Disease Tau PET Subtypes in the ADNI Sample. 2018. Alzheimer's Association International Conference, Chicago, IL.

#### Published Manuscripts

Swinford CG, Risacher SL, Charil A, Schwarz AJ, and AJ Saykin. Memory concerns in the early Alzheimer's disease prodrome: Regional association with tau deposition. *Alzheimers Dement (Amst)* 2018; 10: 322-331.

Wang A, Swinford C, Zhao A, Ramos E, Gregory R, and Srinivasan M. 2016. A case-control study to determine prognostic features of salivary epithelial cells in periodontitis. *JDR Clinical and Translational Research*. 1(3): 256-265.

#### Manuscripts in Preparation

Altered cerebral blood flow in older adults with Alzheimer's disease: a systematic review

Regional cerebral blood flow is related to hypertensive status and self-identified race

Amyloid and tau pathology are associated with cerebral blood flow in nondemented older adults with and without genetic and vascular risk factors

Cerebral blood flow and cognition in the Thinking & Living with Cancer study